SDO 5540
APRIL 1980

Final Report

LOW-COST FLYWHEEL DEMONSTRATION PROGRAM

(1 OCTOBER 1977–31 DECEMBER 1979)

D. W. RABENHORST,
T. R. SMALL, and
W. O. WILKINSON

THE JOHNS HOPKINS UNIVERSITY ■ APPLIED PHYSICS LABORATORY
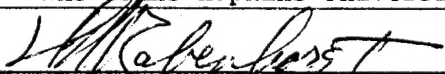
DTIC QUALITY INSPECTED 1

19960313 023

NOTICE

ERRATA SHEET -- APL REPORT NO. SDO-5540

Page 9 - Last sentence in first paragraph should be
changed to read, "Figure 9 is a photograph
from a TV sequence illustrating a flywheel
shaft whip problem, which resulted in sub-
sequent failure."

Page 64 - Second sentence from the end, delete "as
shown in Fig. 47."

*See Instructions on Reverse

1. ERDA Report No. **DOE/EC/15085**	3. Title **LOW COST FLYWHEEL DEMONSTRATION PROGRAM**
2. Subject Category No. **UC94B**	**Contract No. EC-77-C-01-5085**

4. Type of Document ("X" one)

- [X] a. Scientific and Technical Report
- [ ] b. Conference paper:

    Title of conference _____
    Date of conference _____
    Exact location of conference _____

- [ ] c. Other *(Specify, Thesis, Translation, etc.)** _____

5. Copies Transmitted ("X" one or more)

- [X] a. Copies being transmitted for standard distribution by ERDA-TIC. **per distribution category UC94B**
- [ ] b. Copies being transmitted for special distribution per attached complete address list.*
- [ ] c. Two completely legible, reproducible copies being transmitted to ERDA-TIC.

6. Recommended Distribution ("X" one)

- [X] a. Normal handling (after Patent clearance): no restraints on distribution except as may be required by the security classification.
- [ ] b. Make available only to U.S. Government agencies and their contractors.
- [ ] c. Make available only within ERDA and to ERDA contractors.
- [ ] d. Make available only within ERDA.
- [ ] e. Make available only to those listed in item 12 below.
- [ ] f. Other *(Specify)** _____

7. Recommended Announcement ("X" one)

- [X] a. Normal procedure may be followed.*
- [ ] b. Recommend following announcement limitations: _____

8. Reason for Restrictions Recommended in 6 or 7 above.

- [ ] a. Preliminary information.
- [ ] b. Prepared primarily for internal use.
- [ ] c. Other *(Explain)* _____

9. Patent Clearance ("X" one)   (Additional Info. under Item 12 below)

- [ ] a. ERDA patent clearance has been granted by responsible ERDA patent group.
- [X] b. Document is being sent to responsible ERDA patent group for clearance.

10. National Security Information *(For classified document only; "X" one)*

- [ ] a. Document does contain national security information other than restricted data.
- [X] b. Document does not contain national security information other than restricted data.

11. Copy Reproduction and Distribution

- a. Total number of copies reproduced ___250___
- b. Number of copies distributed outside originating organization ___200___

12. Additional Information or Remarks *(Continue on separate sheet, if necessary)*

Does this information product disclose any new equipment, process or material?   Yes

Has an invention disclosure been submitted to DOE covering any aspect of this information product? If so, identify the DOE (or other) disclosure number and to whom the disclosure was submitted.   Yes - Office of Counsel, DOE
Disclosure Nos. S-53,991, S-53,992, S-53,993 and S-53,994.

Are there any patent related objections to the release of this information product? No

13. Submitted by *(Name and Position) (Please print or type)**
David W. Rabenhorst, Program Manager

14. Organization   Applied Physics Laboratory
The Johns Hopkins University

15. Signature	16. Date **3-31-80**

SDO 5540
APRIL 1980

LOW-COST FLYWHEEL DEMONSTRATION PROGRAM

(1 OCTOBER 1977—31 DECEMBER 1979)

D. W. RABENHORST,
T. R. SMALL, and
W. O. WILKINSON

ABSTRACT

The Applied Physics Laboratory/Department of Energy Low Cost
Flywheel Demonstration Program was initiated on 1 October 1977 and
was successfully concluded on 31 December 1979. The total cost of
this program was $355,190. All primary objectives were successfully
achieved as follows: demonstration of a full-size, 1-kWh flywheel
having an estimated cost in large-volume production of approximate-
ly $50/kWh; development of a ball-bearing system having losses com-
parable to the losses in a totally magnetic suspension system; suc-
cessful and repeated demonstration of the low-cost flywheel in a
complete flywheel energy-storage system based on the use of ordinary
house voltage and frequency; and application of the experience
gained in the hardware program to project the system design into a
complete, full-scale, 30-kWh home-type flywheel energy-storage system.

FOREWORD

This report is the final documentation of a program conducted under the Department of Energy contract EC-77-C-01-5085 during the period 1 October 1977 to 31 December 1979. The total cost of this contract was $355,190. The work was performed under the direction of Dr. Roger Derby and Dr. George Chang, in the Mechanical Storage Branch of the Energy Storage Division of the Department of Energy, Dr. George Pezdirtz, Director.

EXECUTIVE SUMMARY

Dry-wound, selectively bonded flywheel configurations using a number of candidate low-cost materials including filaments, wires, and wide tapes were demonstrated.

A 1-kWh low-cost flywheel was evaluated in a complete energy-storage system utilizing 115-V, 60-Hz power.

Low-cost, load-relieved ball-bearing systems having measured losses comparable to all-magnetic bearing systems were developed.

Low-cost flywheel conceptual design projections ranged from 30 kWh to 160 MWh.

Using demonstrated flywheel configurations and available near-term materials, it is believed that a production flywheel cost of less than $50/kWh can be achieved.

CONTENTS

THE JOHNS HOPKINS UNIVERSITY
APPLIED PHYSICS LABORATORY
LAUREL, MARYLAND

ILLUSTRATIONS

THE JOHNS HOPKINS UNIVERSITY
APPLIED PHYSICS LABORATORY
LAUREL, MARYLAND

TABLES

1. INTRODUCTION

The availability of a variety of filamentary materials having a high strength-to-weight ratio has resulted in significant recent advancements in flywheel energy-storage technology. As a result, flywheel energy-storage systems are currently being investigated for a large and increasing number of applications both in the United States and abroad. Applications range from small, hybrid, automotive systems to large, stationary energy-storage systems. As new flywheel energy-storage systems are developed, it has become evident that for many of these systems low cost rather than low weight or low volume is the dominant requirement.

An example of the low cost requirement is in the individual home, where there are a number of important flywheel energy-storage applications that cannot be satisfied as effectively by any other known means. An increasing number of utility companies are offering nighttime energy on an experimental basis for as low as 25% of the daytime rates. Under these circumstances, a home equipped with a suitable energy-storage system could store energy at the nighttime rates for subsequent daytime use. With such a system, the rate-structure differential would be sufficient to pay for the cost of the flywheel storage system in a reasonable number of years, after which the customer would be able to receive energy at the nighttime rate, which could be as much as 75% lower than daytime rates.

Also, a suitably configured home storage system could make stand-alone home solar photovoltaic and wind energy systems practical by enabling them to deliver stored energy during obvious cyclic operation periods when the energy would not otherwise be available. Such homes would also have emergency power when it is needed.

An equally attractive home energy-storage application is one that would eliminate the daytime load peaks caused by home airconditioning systems. This application would have the advantage of eliminating one of the most costly summertime diurnal peaking problems faced by the utility companies. In this application, the flywheel energy-storage system would be charged at night, when demand is low, and connected directly to the airconditioner compressor in the daytime by means of a mechanical clutch, thereby allowing the stored mechanical energy in the flywheel to be transferred directly to the airconditioner compressor, rather than by electrical conversion. The components required for this type of operation are quite similar to those used in automotive airconditioning systems.

In contrast to the mobile energy-storage system, the stationary systems such as the home storage system have no requirement

for minimizing weight or system volume, except to the degree that
weight or volume affects system cost. However the flywheel system
cost over the lifetime of the system involves the operating cost
in addition to the initial cost and general maintenance costs.
In the case of the flywheel system (exclusive of energy transfer
equipment), the capital cost is dominated by the cost of the fly-
wheel, whereas the operating cost is dominated by the bearing
and aerodynamic losses. If seals are required, their losses will
be comparable to the aerodynamic and bearing losses. The aero-
dynamic losses can be minimized in the stationary system by an
effective vacuum pump, but the energy to drive this pump must be
considered in the system losses. The importance of the flywheel
bearing losses and aerodynamic losses is illustrated by the fact
that they are contributing to the system losses whenever the sys-
tem is operating — and most importantly during extensive coasting
periods when no energy is (intentionally) being transferred into
or out of the system.

It can be seen from the foregoing discussion that two of the
most important factors affecting the overall cost of a flywheel
energy-storage system are the cost of the flywheel and its con-
tainment structure and the losses in its bearing system. Accord-
ingly, the two main objectives of this program are the optimiza-
tion of these two factors.

The specific principal objectives of the program were as
follows:

1. Demonstrate the feasibility of mass-producing flywheels
   at a cost near $50/kWh.

2. Investigate low-loss, long-life bearing systems for sta-
   tionary flywheel energy-storage systems.

3. Demonstrate the low-cost flywheel in a complete energy-
   storage system operating at typical home voltage and
   frequency.

4. Provide a basic design projection of a full-size 30-kWh
   home storage flywheel, and describe the applicability
   of the low-cost flywheel technology to large stationary
   storage systems.

The principal objectives of the program could be most econom-
ically achieved by a flywheel energy-storage system having operat-
ing flywheel characteristics that were the same as those for the
flywheel in a full-scale home storage system, in all respects ex-
cept total energy. Thus the demonstration flywheel system would
operate at the recommmended voltage, frequency, operating rota-

tional speed, and at essentially the same power level, but at a flywheel mass equivalent to only 1 kWh (as opposed to 30 or 40 kWh).

There is at present a significant research and development effort aimed at developing second generation batteries to satisfy the needs of the home storage, utility storage, and vehicle storage applications. However, the flywheel may have certain intrinsic advantages over the batteries including those listed in Table 1. If these potential advantages can be realized, the low-cost flywheel may have an important role to play in many future energy-storage applications.

Table 1

Potential advantages of flywheels in comparison with batteries for stationary storage applications

1. Can be designed for a 30-year lifetime.

2. Can be used in 100% parallel hook-up for maximum reliability on 115 VAC, 60-Hz power.

3. Lifetime cost may be much lower.

4. System efficiency can be much higher.

5. Environmental control is simpler and less critical.

6. Can easily handle at least a 94% depth of discharge.

7. No gaseous emissions.

- 3 -

2. FLYWHEEL TESTING LABORATORY

The APL Flywheel Fabrication and Testing Laboratory is described in Ref. 1. This facility consists of a complex of four spin-test chambers and has a separate area for the fabrication, assembly, and spin balancing of the flywheels. The general arrangement of the Flywheel Testing Laboratory (FTL) is illustrated in Figs. 1 and 2. Test chamber 1 is shown in Fig. 3 and chamber 2 is shown in Fig. 4. The control console is illustrated in Fig. 5.

One of the important accomplishments during the course of the low-cost flywheel demonstration program was the development of a universal flywheel suspension system, which eventually permitted the spin-testing of a large variety of flywheels having different masses and different rotational speeds without encountering potentially damaging resonant conditions. A prinicpal element of this universal flywheel suspension system is the flexible turbine mount illustrated in Fig. 6. The damping characteristics of the special elastomer used in the installation, together with a carefully designed geometry, enabled this system to damp out quite effectively the forward and retrograde whirl vibrations that otherwise would have been encountered at the various critical speeds of the flywheel and its suspension system during the spin-test. This principal of operation was also carried through to the final demonstration systems, which were subsequently installed for evaluation in test chamber 4, which is illustrated in Fig. 7. In this installation the elastomer damping material was located between the electric motor/generator housing and the flywheel support and vacuum chamber.

The APL facility is equipped with a Dynafax camera and high-speed strobe lights allowing photos to be taken at rates of up to 25,000 frames per second. A typical high-speed photo sequence is shown in Fig. 8.

One difficulty with the high-speed photography system is that the photographic recording is initiated by the failure of the flywheel, a situation that precludes the possibility of obtaining pictures of the failure itself. For example, it can be seen in Fig. 8 that the failed pieces of the flywheel have already traveled a considerable distance by the time the first picture is recorded.

A television recording eliminates the basic problem of optical coverage at the point of the flywheel failure. The picture frame rate limitation of the television system is not present in the high-speed camera system. The principal advantage of the
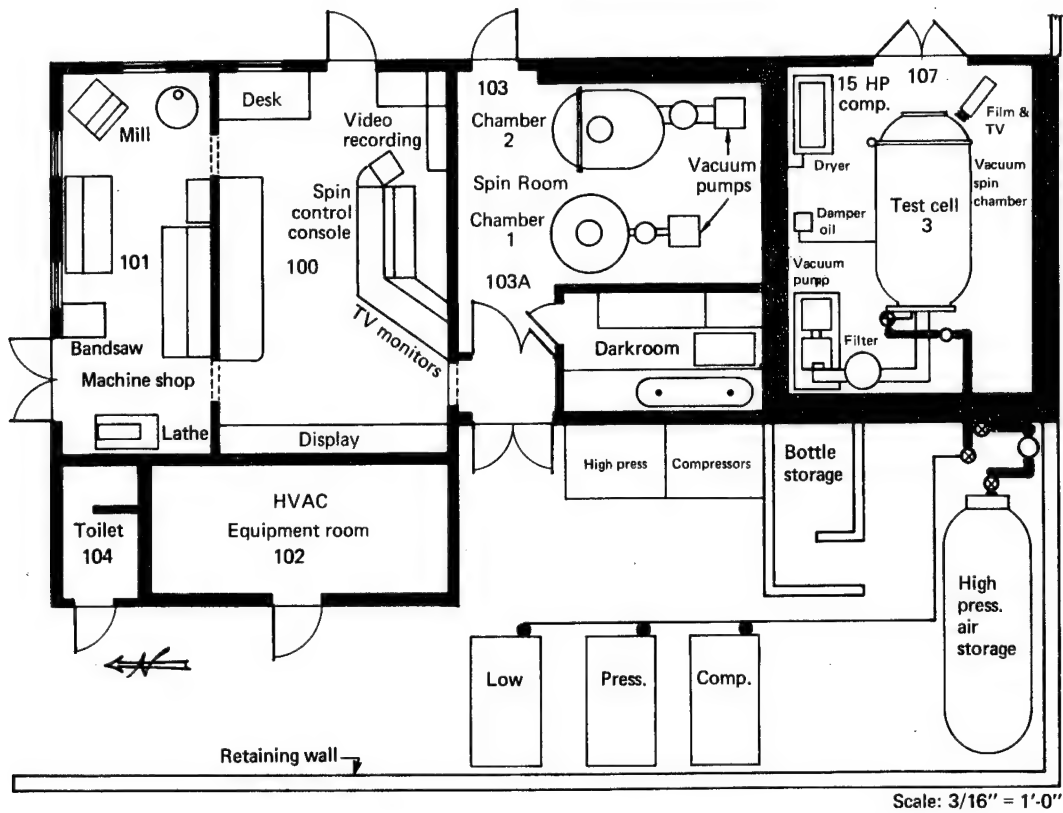
Fig. 1   Layout of the flywheel testing laboratory.
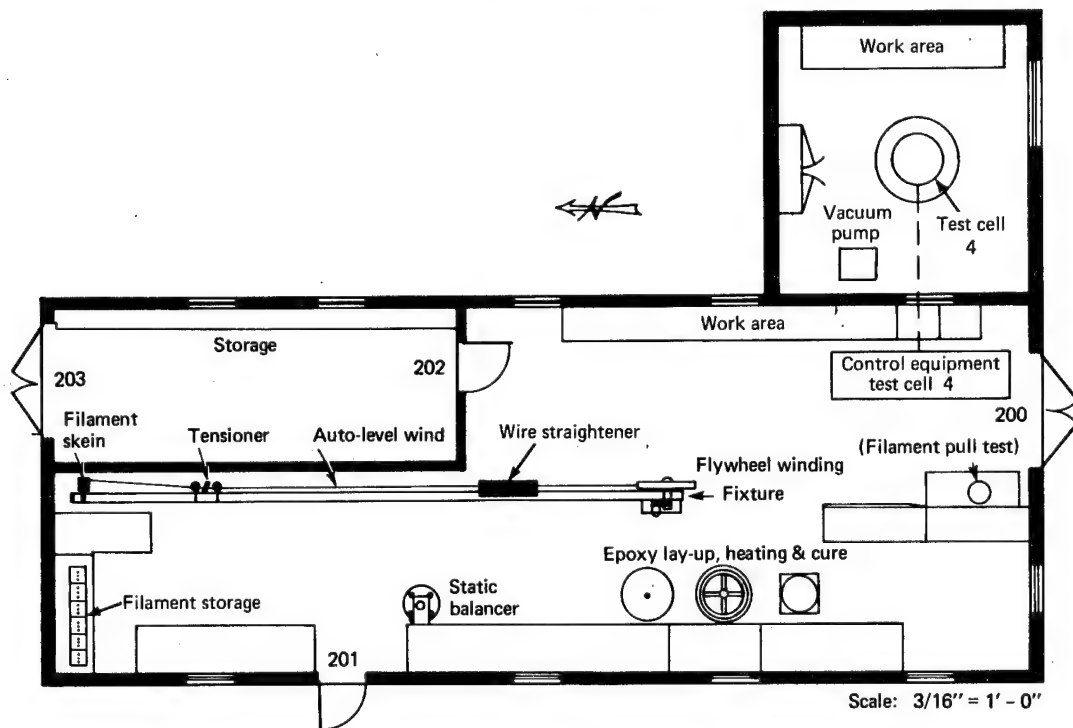
Fig. 2   Layout of the flywheel fabrication and test annex.
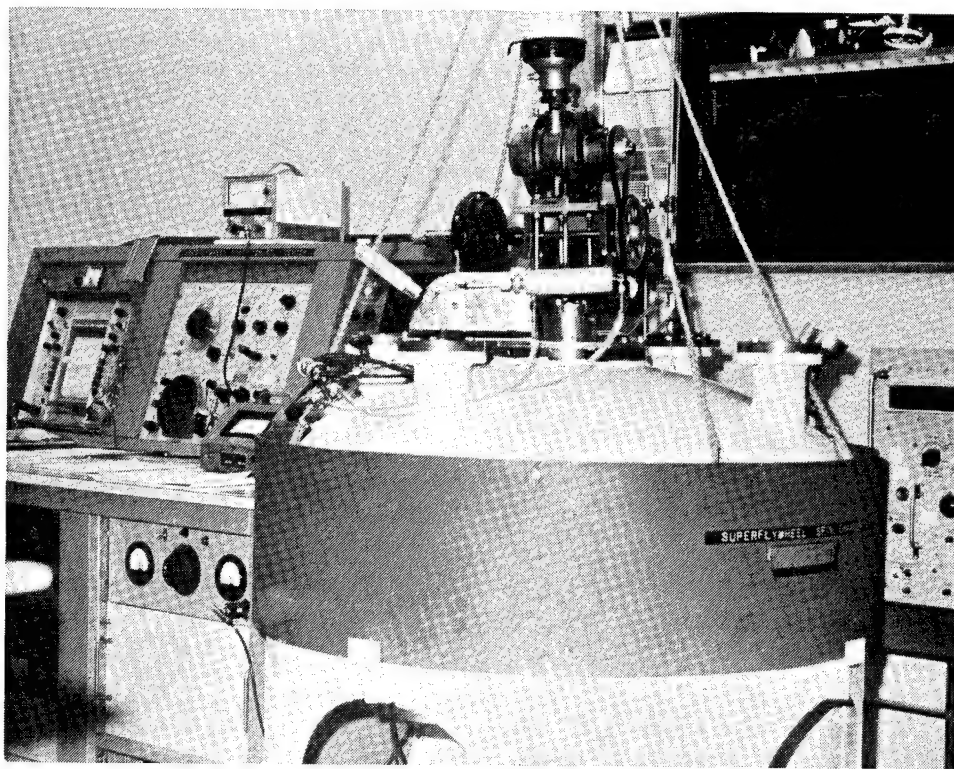
Fig. 3   Test cell 1 installation.
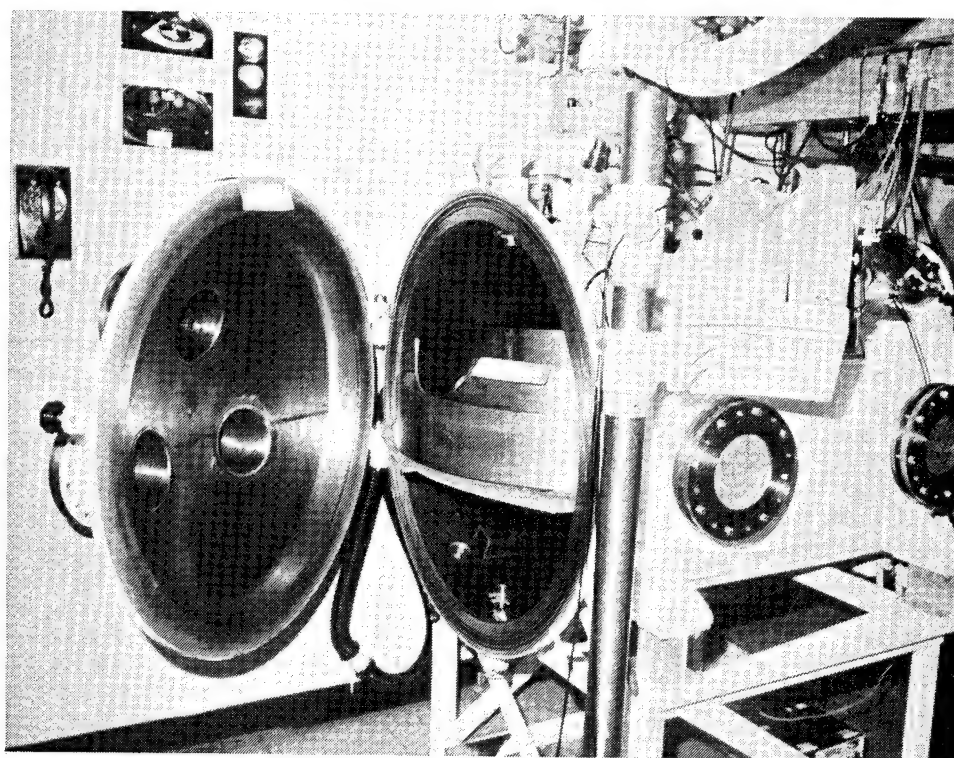
Fig. 4   Test cell 2 installation.

Fig. 5   New control console.
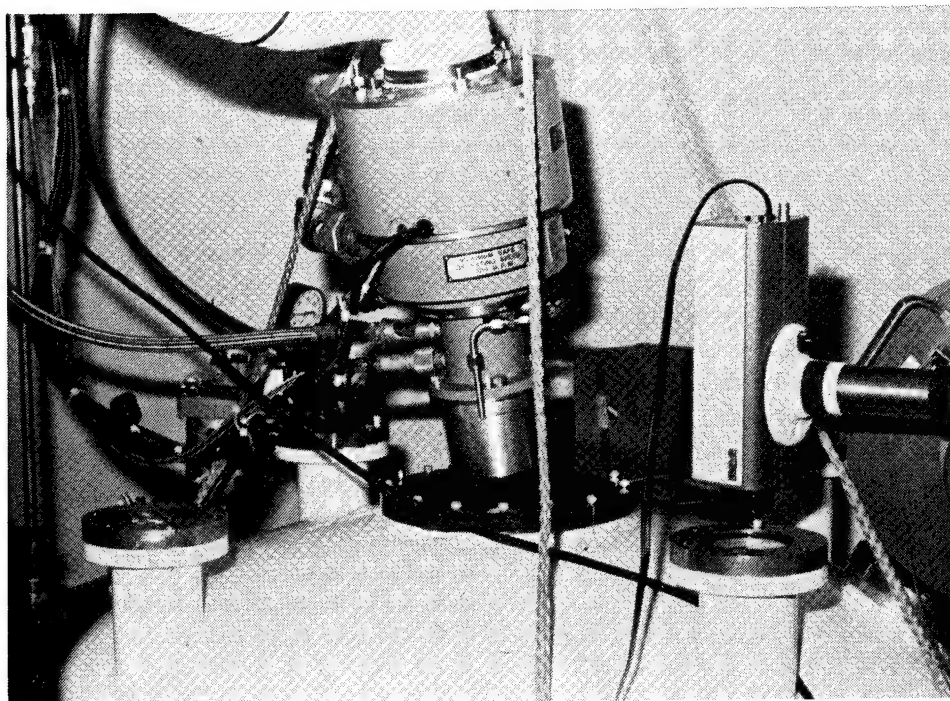
Fig. 6   Flexible turbine mount installation.
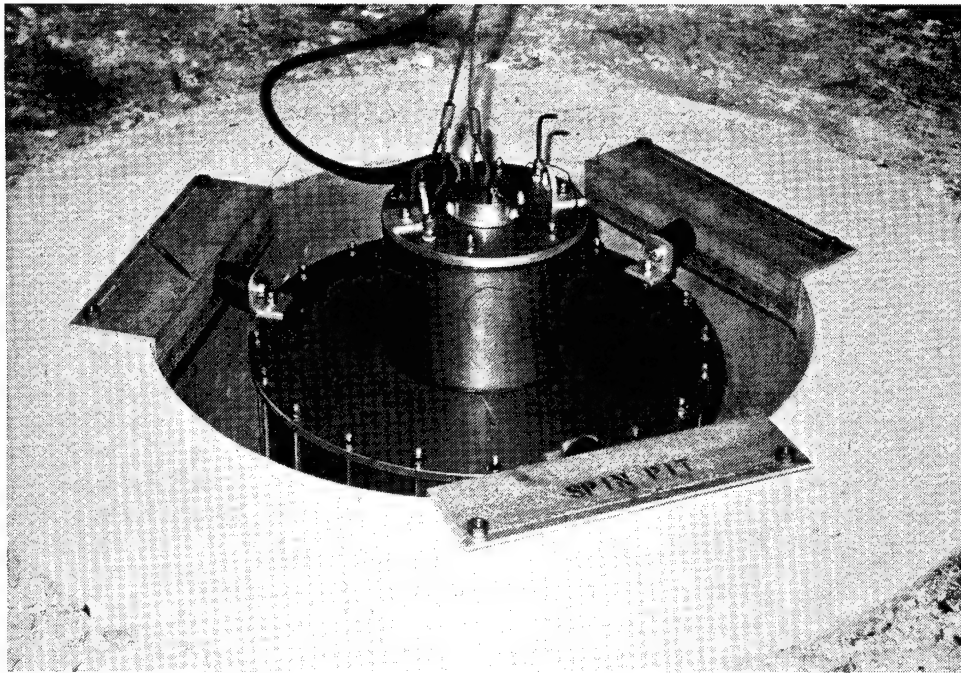
Fig. 7   Test cell 4 installation.

television system is that the picture is available for viewing
at all times up to and including the time of the flywheel failure.
Nominally speaking, this allows the actual failure to be viewed by
the test conductor. However, since the frame rate of the present
APL television camera is limited to thirty frames per second,
there is a high probability that the flywheel failure could occur
during the many flywheel revolutions between TV pictures. It is
evident that the development of a high-speed television record-
ing system would provide improved coverage having the advantages
of both systems. Figure 9 is a photograph from a TV sequence
illustrating a crack developing in the intermediate flywheel hub
at 14,000 rpm.

An air turbine capable of 60,000 rpm was installed in the
test facility. This air turbine has been used as a main drive
motor for all flywheel testing at APL, with the exception of the
final demonstration units, which were powered by an electric
motor/generator system. The turbine, which was made by Barbour
Stockwell, has given excellent service, and after several hundred
spin tests, still contains the original bearings. The compressed
air for driving the turbine was provided by three surplus truck-
mounted air compressors powered by internal combustion engines.

- 9 -
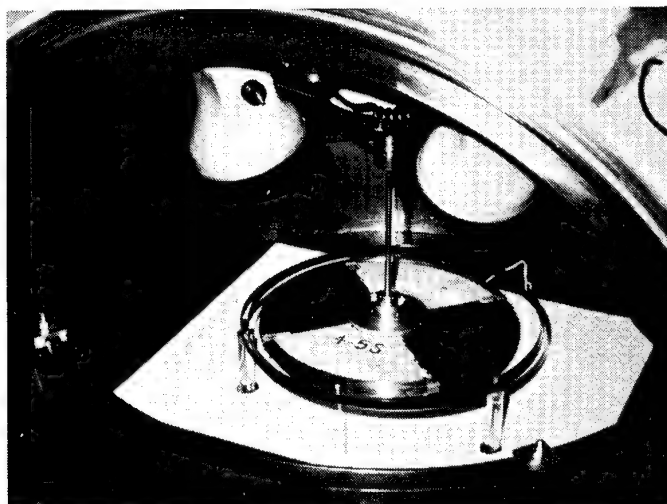
Fig. 8   Typical high-speed photo sequence.
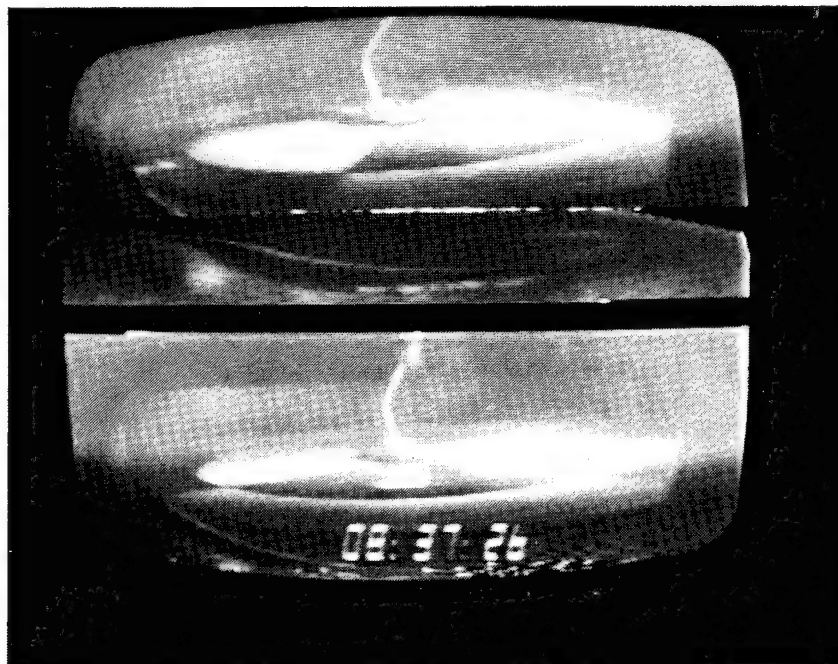
Fig. 9   An example of the value of TV video recording.

Table 2 lists the characteristics of the various APL spin-test chambers in the APL FTL.

Table 2

Characteristics of the flywheel test cells

Item	Cell 1	Cell 2	Cell 4
Approximate flywheel diameter (in.)	32	32	24
Spin motor	Air motor/ synch. belts	Air turbine	Electric motor/generator
Maximum rpm	35,000	60,000	15,000
Approximate horsepower	5	10	2
Vacuum performance (Torr)	$<10^{-4}$	$<10^{-4}$	10^{-2} (nominal)

3. DISCUSSION OF LOW-COST FLYWHEEL MATERIALS

A principal component of the flywheel cost is the material from which it is made. In order to be low cost, the strength-to-weight ratio per unit cost of the material must be high since this value would translate into a high energy per unit cost. However, it is equally important that the flywheel be configured to minimize the manufacturing cost.

A material having a high strength-to-weight ratio per unit cost does not necessarily have high strength per se. As a matter of fact, from the standpoint of energy-to-cost ratio the optimum materials in a flywheel configuration appeared to be those having relatively low strength and an even lower relative cost. Three of these materials were evaluated in the present program: (a) vinyl-impregnated glass strands, (b) steel wire, and (c) Metglas* amorphous ribbon.

The following general criteria were used in the selection of the low-cost materials for the present program. First, the material had to have an acceptable strength-to-weight ratio per unit cost. Second, in consideration of the potential applications, which could eventually require enormous amounts of this material, the adequacy of supply was determined. Third, the materials also must be capable of operating effectively and competitively in the anticipated flywheel environment; therefore, the materials must be capable of maintaining their performance in a vacuum and have a predicted performance over long periods of time (ten years or more) under the static and cyclic load conditions expected to be encountered. Finally, it was necessary that the material have reasonable handling characteristics, including the capability of being bonded reliably. The vinyl-impregnated glass, steel wire, and Metglas ribbon materials were selected on the basis that they would apparently meet these general requirements. The individual capabilities of the selected materials are described in the following discussion.

VINYL-IMPREGNATED GLASS

A process has been developed by PPG Industries of Pittsburgh, Pennsylvania, for impregnating strands of glass filaments with various polymers such as vinyl. The vinyl impregnant reduces abrasion between the glass filaments and provides some protection from exposure to water vapor. The performance characteristics

---

* Metglas ribbon is a proprietary material developed by the Allied Chemical Corporation of Morristown, New Jersey.

of vinyl-impregnated glass, together with some of the other materials considered, are listed in Table 3. The strength of the vinyl-impregnated glass was determined at first through pull tests, which were extended over a relatively long time, compared to the usual time for tensile tests of materials in this category. Over a load application period lasting several minutes, the ultimate tensile strength of the vinyl-impregnated glass was measured to be 264,000 psi — a considerably higher tensile strength than would be provided by the virgin glass material without the vinyl impregnant. It should be noted, however, that although the long-term strength of the vinyl impregnated glass was relatively high compared to the tensile strength of the virgin strands, the allowable strength used throughout this program was 50% of the ultimate measured tensile strength.

Table 3

Assumed cost factors for wound flywheel structures

Materials Used in Current Program	(1) Usable Energy Density Wh/lb	(2) Material Cost $/lb	(3) Set-up Cost $/lb	(4) Winding Cost $/lb	(5) Wound Structure Cost Factor* $/kWh
50/50 vinyl-glass	15	0.50	0.025	0.075	40
0.0125-in. steel wire	13	0.63	0.025	0.075	56
0.5-in. Metglas metal ribbon	14	1.0	0.025	0.0015	70
Possible Near Term Materials (1985)					
10/90 polymer-glass	24	0.50	0.025	0.075	25
Super paper	8	0.12	0.025	0.00015	18
Crystalline polyethylene @ 175,000 psi (0.25-in. tape)	28	0.50	0.025	0.003	19
Bamboo Tulda	20	0.10	0.125	0.003	11

*Wound structure cost factor, $(5) = \dfrac{1000\ [(2) + (3) + (4)]}{(1)}$

It will be noted in Table 3 that there are two types (first and fourth items) of vinyl-glass. The first item in Table 3 is the material that was available for experimentation during the course of the program. This material consisted of approximately 50% vinyl and 50% glass. Since the energy density of a given material is a function of its usable strength divided by its density, it follows that the usable energy density of the 50/50 vinyl-glass would be considerably inhibited by the presence of the vinyl, which in comparison to the glass has no useful strength in this situation. In the flywheel application, it would be highly desirable to reduce the vinyl to an absolute minimum to obtain the maximum strength-to-weight ratio. The manufacturer agreed that it would be possible to produce the vinyl-glass material in a configuration having 10% vinyl and 90% glass. This potential material is the fourth item listed in Table 3 as a future material. Although the tensile strength remains the same, the 10/90 material has an intrinsic energy density of 44 Wh/lb, compared to 32 Wh/lb for the 50/50 material. This condition obviously translates into comparable advantages in material costs and hence flywheel costs.

In addition to its relatively high performance in a flywheel, in terms of energy per unit weight, the vinyl-impregnated glass material appeared to have excellent handling characteristics. It was found that the tackiness of the outer surface of the strands resulted in stability of the strand after it was wound into the flywheel configuration. Also, the material had excellent failure characteristics.

All tests were conducted with the 50/50 vinyl-glass material. Although it would have been desirable to conduct a number of tests with the 10/90 material, this material was not available during the program.

It was also noted that there was a lack of performance data on the polymer-impregnated glass-strand material, such as measured tensile strength, static and cyclic fatigue, creep, and allowable stress over long-term conditions. During later stages of the program, the vinyl-impregnated glass became unavailable in any form, making further development with this material during the program impossible. However, a second source of polymer-impregnated glass-strand material was found after the program was concluded, and samples containing less than 10% polyurethane were obtained. The new source for the material is Engineered Yarns, Inc., Coventry, Rhode Island.

STEEL WIRE

The second low-cost flywheel material selected for evaluation was steel wire, similar to that which is used in the manufacture of steel-belted tires and in the manufacture of reinforced high-pressure hoses. It is also similar to the type of steel wire currently used for rotor blade retention straps in helicopters. In this last application, a bundle of several thousand steel wires is applied as a tension strap to accommodate the centrifugal force of the helicopter rotor blade, while torsional pitch change of the rotor blade is allowed during the normal rotation. Here, the cyclic stress pattern of the steel wire is probably more severe than the corresponding cyclic stress pattern in a flywheel application, inasmuch as the cyclic stress rate is about 400 cycles per minute in the helicopter, as opposed to approximately 400 cycles per year in a home storage flywheel. Also, in the helicopter application, the stress in all of the wires is essentially equal, whereas the stress in the wound flywheel wire varies as the square of the wound radius. Since this varying stress prohibits the possibility of simultaneous failure of all of the wires in the flywheel, it is generally accepted (Ref. 2) that the design stress for the flywheel wire can be a higher proportion of the ultimate tensile strength than that of the helicopter wire. A level of 70% has been used in the present program, compared with about 40% for the helicopter application.

A principal virtue of the steel wire used in these evaluations is that it is a mature material having well documented physical and cost characteristics. The steel wire is available in the form and in the potential quantities that would ultimately be required, and it exhibits reasonably good failure characteristics in the flywheel configuration, as described in Section 4.

Two difficulties that were encountered in the work with the steel-wire flywheels were its static instability and the "wire cast" problem. In this connotation the static stability refers to the fact that the slickness of the wire tends to make it slide out of place once it has been wound into its desired configuration. The eventual solution to the slickness problem was to tie the wound wire in a considerably larger number of places than was necessary with the other materials.

The wire cast problem eventually required the procurement of a wire straightening machine, to ensure that all the wire going into the fabrication of the flywheel was acceptably straight. Figure 10 is a good illustration of the problems that can result from wire cast. As it comes from the manufacturer the coil of wire formed directly from the spool is badly warped, but a second coil of wire that has been properly straightened has good flat stability.

- 16 -
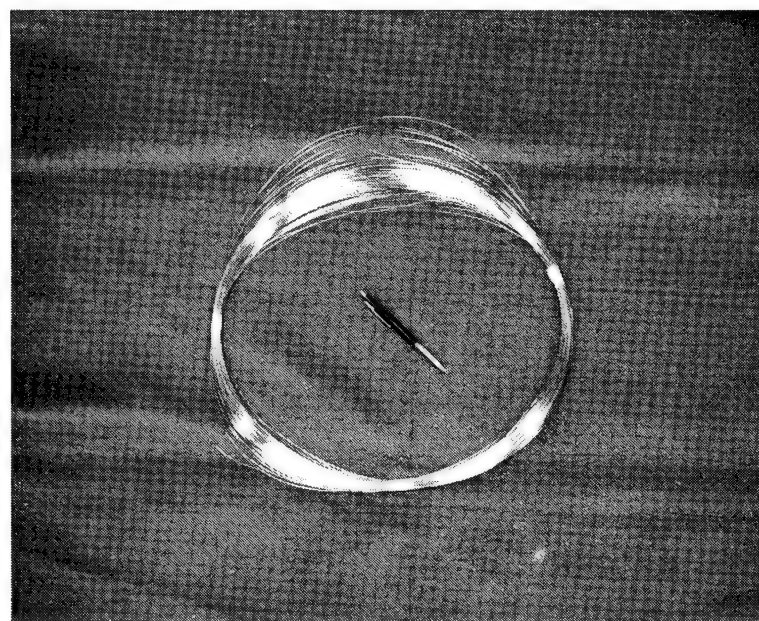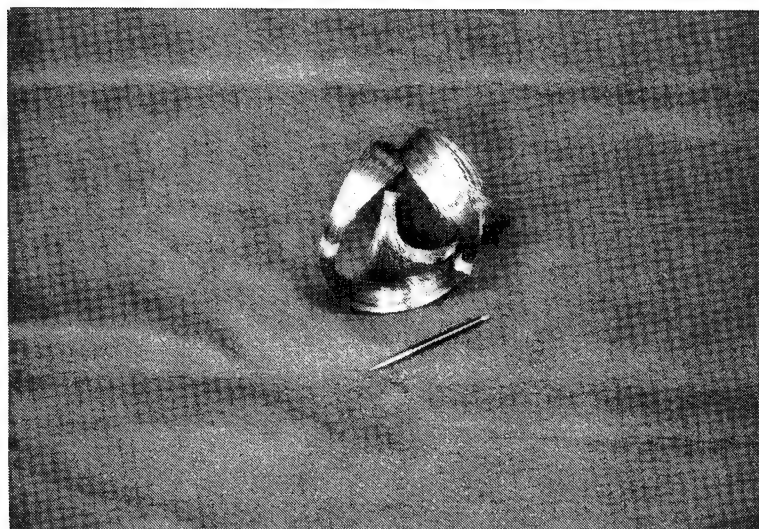
Fig. 10   An example of the "wire cast" problem.

Figure 11 illustrates the wire straightening machine that was introduced into the flywheel fabrication process and provided good results. This machine is fabricated by the Sjogren Company of Brynmawr, Pennsylvania. It is a relatively simple device consisting of a number of orthogonally located rollers with grooves matched to the outer surface of the wire. The rollers are adjustable so that they gently bend the wire back and forth as it is drawn through the machine. The presence of the Sjogren wire straightener in the fabrication process involving the steel wire has consistently alleviated the wire cast problem. It should also be noted that the Sjogren wire straightener is a relatively standard piece of equipment in the wire industry.

METGLAS AMORPHOUS METAL RIBBON

The Metglas amorphous metal ribbon has a number of unique characteristics that make it especially suitable for flywheels, especially for those flywheels requiring cost optimization or volume optimization. The material has a strength-to-density ratio that is slightly higher than the best available steel but with a potential cost comparable to the steel. However, unlike the steel wire, the Metglas material is available in strip form, which
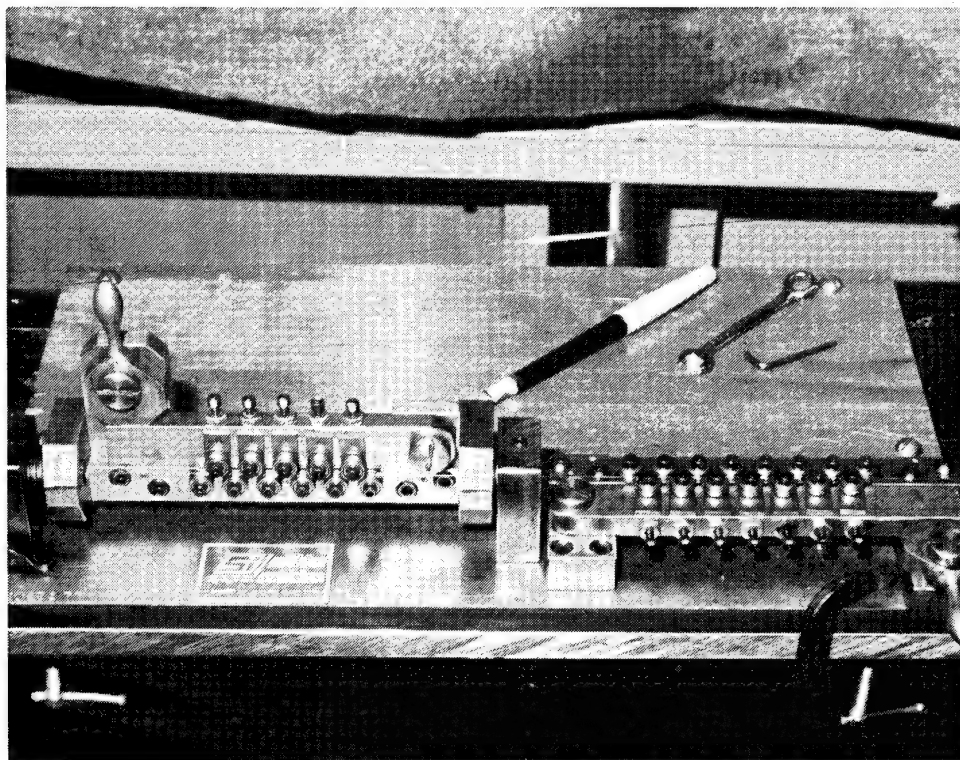
Fig. 11   Sjogren wire straightener.

- 18 -

greatly reduces flywheel fabrication cost. The Metglas material
is several times more corrosion resistant than the best stainless
steel, and has a magnetic permeability that is several times that
of the best silicon iron. For the latter reason, a major effort
is under way to develop Metglas ribbon to be used in place of
silicon iron in the manufacture of electrical transformers. An
objective of a current Metglas ribbon program sponsored by the
Electric Power Research Institute at the Allied Chemical Corpora-
tion has been stated to be the achievement of a production cost
of $2/lb by 1985. On the basis of this objective it has been
assumed that the eventual costs in million pound lots may be from
60 cents to one dollar per pound.

In addition to its good strength-to-weight ratio per unit
cost, the amorphous quality of this material gives it some rather
unusual physical characteristics. It has virtually no creep with-
in its own limits of operation and fatigue is nearly nonexistent.
Yield strength is always a very high proportion of the ultimate
strength. Thus, the usable strength can be a relatively high
percentage of its breaking strength compared to that of the other
materials evaluated.

The nominal tensile strength of the experimental Metglas rib-
bon used in the program was about 365,000 psi. However, one prob-
lem encountered was that the strength at one end of a reel of
ribbon was typically about 20% lower than that at the other end.
This problem was accommodated by winding the flywheel with the
highest strength material on the outside, where the anticipated
stresses during rotation would be higher. By the conclusion of
the program, the Metglas ribbon received from the Allied Chemical
Corporation had a tensile strength of 439,000 psi, and the ratio
of maximum to minimum strength was improved. Further improvement
in tensile strength is expected as refinements in the fabrica-
tion process are developed to polish the edges of the ribbon. In
the "as-cast" condition this material has minute cracks along the
edge that represent stress concentration, reducing the strength
of the material. The projected production material will employ
suitable means such as electro polishing or mechanical slitting
to eliminate the cracked edges. At the end of the present pro-
gram the manufacturer reported significant progress in this area,
and Metglas ribbons with greater consistency and greater tensile
strength than were available for the fabrication of flywheels
during the course of the program are now in production.

Future projections for Metglas ribbons appear to make it even more attractive for the flywheel application, principally in terms of the flywheel fabrication cost and the energy per unit volume. An obvious advantage of the Metglas ribbon is its excellent packaging efficiency. Its rectangular cross section, coupled with the fact that it comes in various widths, means that often a single flat winding of this ribbon material will constitute the entire flywheel. For example, at the present time the Metglas ribbon is available in widths ranging from 1 mm to 1/2 in. The material used in the present program was primarily of the 1/2-in. variety (Fig. 12). The manufacturer advises that within the next six months the material will become available in 1-in. widths, within
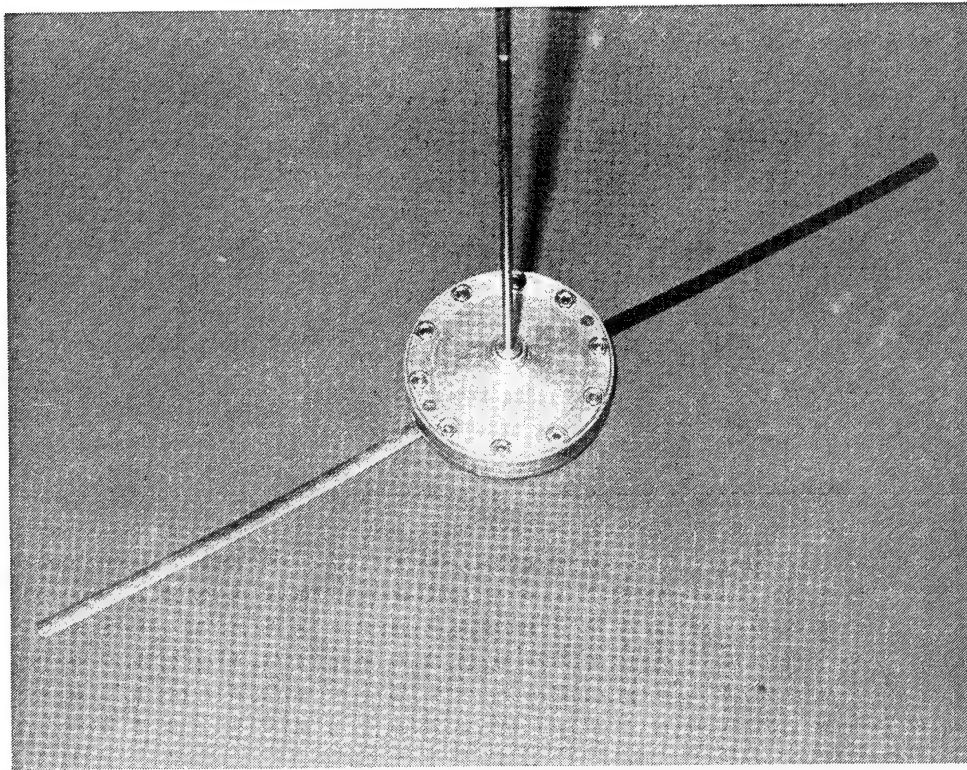
Fig. 12   Spin test of Metglas ribbon.

- 20 -

18 months in 2-in. widths, and within about two years it will be available in 4-in. widths. The 4-in. width is a direct outgrowth of the development of this material for the electric transformer program.

One problem encountered was the difficulty in establishing acceptable bonds with the Metglas ribbon. Conventional epoxy resins are relatively ineffective. Various contact cements, although they yield somewhat better results, were still unacceptable. During the course of the program the bonding problem was apparently solved at the United Technology Center in East Hartford, Connecticut (Ref. 3). Table 4 lists some of the resins that yielded exceptional results in the bonding of Metglas ribbons.

Table 4

Bonding agents for 2826 MB Metglas amorphous ribbon
(from Ref. 2)

Material	Basic Type	Supplier	Cure Cycle (hours)	Bond (MPa)	Strength (psi)
PR 286	Epoxy liquid	3M Co.	4 @ 180°C	2.9	415
Epon 828	Epoxy liquid	Shell Oil Co.	2 @ 100°C 2 @ 150°C 2 @ 180°C	3.0	430
FR 7015	Epoxy liquid	Fiber Resin Corp.	48 @ 25°C	7.5	1090
FM 300µ	Epoxy/nylon film	American Cyanamid	1 @ 180°C	30.8	4470
FM 1000	Epoxy/nylon film	American Cyanamid	1 @ 180°C	32.5	4710
FM 1046	Epoxy/nylon film	American Cyanamid	1 @ 180°C	29.6	4300
AF-42	Epoxy/nylon film	3M Co.	1 @ 180°C	28.4	4120
EA 9649R	Epoxy/Novalac film	Hysol	1 @ 180°C	13.4	1940

In summary it should be stated that Metglas amorphous metal ribbon, in view of its high potential energy per unit cost and high energy per unit volume, may be one of the best near-term materials for the flywheel application.

OTHER MATERIALS CONSIDERED

A number of additional materials was investigated for possible use in the low-cost flywheel. A material generally referred to in the literature as crystalline polyethylene has been mentioned by previous authors as a potential flywheel material. Reference 4 states that crystalline polyethylene has been produced in the laboratory in kilometer lengths having a strength-to-weight ratio that is approximately double that of Kevlar*. It also has an alleged projected cost that is comparable to the base material, which means that the crystalline polyethylene could possibly compete both with the lowest cost materials in future flywheels and with the highest performance materials, if its strength-to-weight ratio is anywhere near the value predicted. Although it was not possible to obtain this particular material for testing, two different types of crystalline polyethylene obtained through the Pirelli Company, S.p.A., in Milan, Italy, were evaluated. Measured strengths (see Fig. 13) ranged as high as 175,000 psi at densities of about 0.04 lb/in^3. The resulting performance as a low-cost flywheel is covered in Table 3.
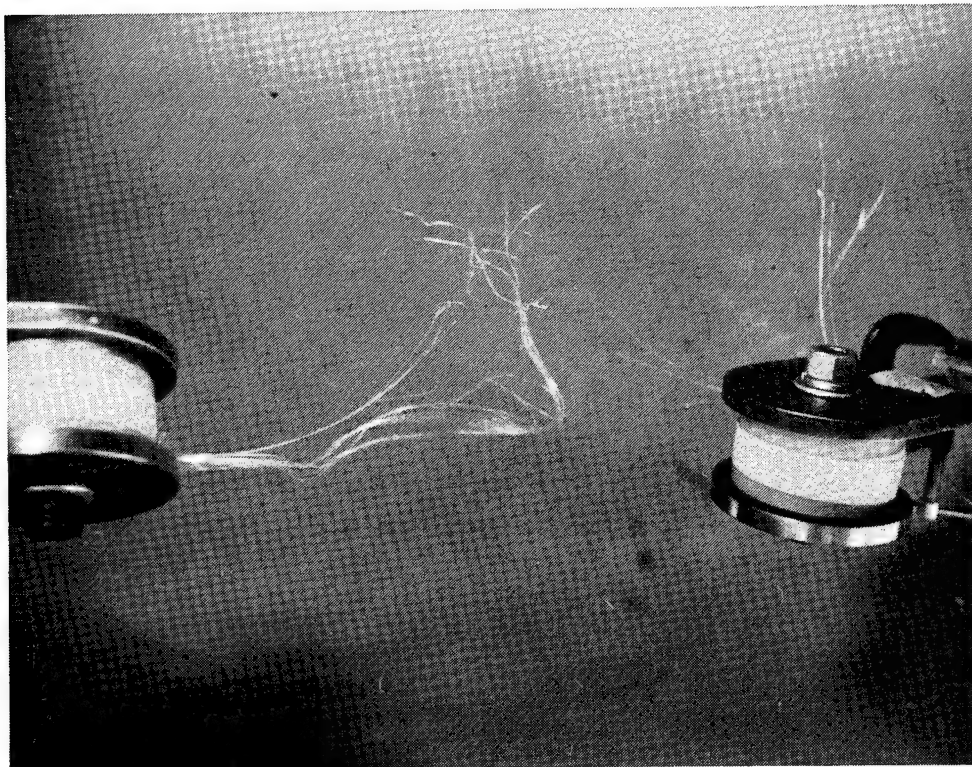
Fig. 13   Pull test of crystalline polyethylene.

* Kevlar is a registered trademark of the DuPont Company.

Previous studies at APL had indicated that a variety of cellulosic materials may be applicable to flywheel technology (Ref. 5). Accordingly, an extensive evaluation of wood and wood products and their possible application to the low-cost flywheel was initiated at the University of Minnesota. The final report from that evaluation (Ref. 6) indicated that some cellulosic products may be applicable to the low-cost flywheel technology. For example, while conventional plywood does not appear to be competitive with other low-cost materials for the flywheel itself, it may eventually prove to be an excellent low-cost intermediate hub material. (In fact, it was used for this application in many of the flywheels in the present program (Fig. 14).) As might be expected, the principal difficulty with using plywood in this manner was the relative inconsistency of the plywoods. It was difficult to identify defects before the defect showed up as a flywheel hub failure during the spin-test period (as indicated in Fig. 15). In the future, ultrasonic test procedures could be used to identify defects.
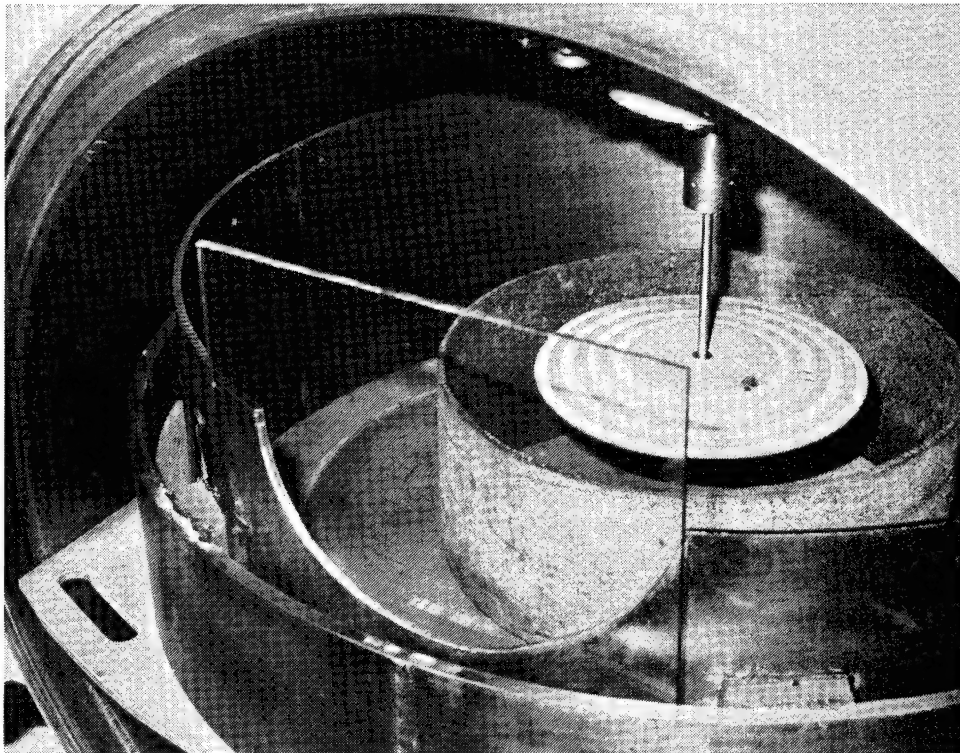
Fig. 14   Spin test of birch plywood.

In view of the extremely low cost of the cellulosic materials in general (10 to 16 cents per pound), the conclusion was drawn

- 23 -

a. 0 s: Crack begins
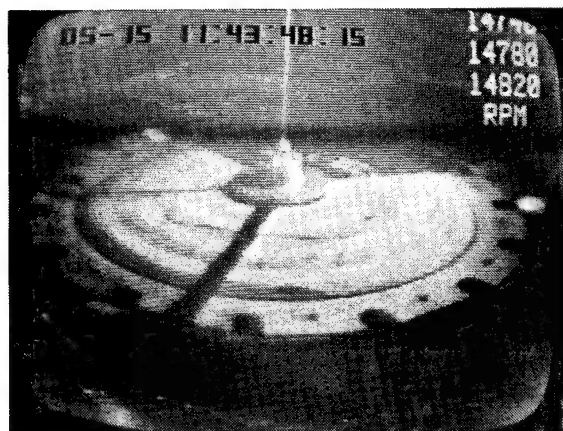
b. 26.26 s: Crack all around

c. 31.45 s: Flywheel falls away

Fig. 15   Failure of plywood interlaminar bond.

from the University of Minnesota study that the next most important thing in the minimization of the flywheel cost was to minimize the fabrication cost. Pure wood scarfed into a continuous length and wound into a flywheel shape in very thin layers may provide higher flywheel performance in terms of energy per unit weight (hence per unit cost), since its fibers would be more nearly in line with stresses.

The study of cellulosic materials indicated clearly that paper products appeared to be the best for potential low-cost flywheels. Ordinary kraft paper comes close to competing with the other low-cost materials tested. This is especially true because the kraft paper could possibly be used virtually right off the spool, as supplied by the manufacturer. Methods have been developed (described later in this report) by which the paper can be wound on a mandrel so shaped that the final wound structure would maintain its structural integrity and stability during the cyclic stress cycles of flywheel operation.

One potential cellulosic product that appeared to be clearly superior to the others is a proposed material called "super paper". The production of super paper involves known methods of orienting the cellulosic fibers to form a unidirectional material having a much greater strength than what is available in conventional paper products. In the University of Minnesota study, it was conservatively estimated that paper having a tensile strength of 48,700 psi could be manufactured by this process. It appears that flywheels made of super paper would be competitive in the low-cost field, even in consideration of conservative handicaps applied for long-term static-fatigue and cyclic-fatigue stresses, as well as for operation within the vacuum in the flywheel container.

One area that needs additional research is the cost of the flywheel container. Generally speaking, the cellulosic materials will occupy considerably more volume for a given energy than do the other low-cost materials of competitors. There are a number of ways to alleviate this problem. For example, in view of the extremely low cost of the cellulosic material, it is practical to consider winding it in flywheels having a much lower inside radius than is practical with the other materials because of the higher cost. Obviously, a flywheel wound in a thick ring can store more energy than a flywheel wound in a thin ring, even considering the fact that the specific energy is lower for the former case. In an actual comparison, the container volume for a super-paper flywheel was really only 2.5 times as large as the comparable container for a steel-wire flywheel, even though the specific performance of the super-paper flywheel was only one sixth that of the steel wire in terms of energy-to-weight ratio.

- 25 -

It was clear from the University of Minnesota report that the potential future impact of cellulosic materials in the field of low-cost flywheels justifies a vigorous pursuit of this technology.

MATERIALS SUMMARY

Vinyl-impregnated fiberglass, steel wire, and Metglas amorphous metal ribbon were evaluated in spin tests of wound structures designed for minimum fabrication cost. The estimated costs for mass production of these structures were, respectively, $40, $50, and $70 per kWh. On the assumption that a flywheel hub and attachment structure would cost an additional 25%, the estimated cost of the mass-produced flywheels would be, respectively, $50, $70, and $88 per kWh. Additional near-term materials that might permit the mass-production cost of the flywheel to be reduced to the range of $14 to $31 per kWh were identified. It would appear from these data that the production of flywheels at a cost of less than $50 per kWh is feasible.

4. FLYWHEEL CONFIGURATIONS

The pseudo-isotropic (P-I) disc and bare-filament wound-ring flywheel configurations, because of their apparent low fabrication cost, appeared to be the best ones available for the low-cost flywheel.

PSEUDO-ISOTROPIC DISC FLYWHEEL

The principal features of the P-I disc flywheel configuration are illustrated in Fig. 16 and described in Refs. 7 and 8. It can be seen that the disc is comprised of layers of unidirectional filamentary material orientated so that the fibers in one layer are at an exact predetermined angle with the fibers in the adjacent layer. It has been found that a composite material fabricated in this way has strength characteristics that are nearly isotropic when the flywheel is rotated in the plane of the fibers. Fabrication of such a composite material is relatively simple in comparison with the conventional wound composites. Flywheels made in the P-I configuration generally exhibit good performance in terms of energy per unit weight and especially in terms of energy per unit volume. However, on a cost basis, no combination of P-I materials and configurations was found to be competitive with the bare-filament wound configurations described in the following discussion. For example, according to the 3M Company, P-I fiberglass/epoxy material costs $4.50 to $9.00 per pound.

Typical P-I flywheels are illustrated in Fig. 17. During the testing of the P-I flywheels (previous APL program), a number of additional disadvantages of the configuration were encountered. One of these disadvantages (discussed at length in Ref. 8) was with the method of attaching the flywheel to its support shaft. Generally speaking, the methods developed do not necessarily apply to flywheels weighing more than a few pounds. The alternate available method was to attach the flywheel to its shaft by means of a series of through bolts. However, this method generally results in flywheel performance being much lower than if the bolt holes were not present (Refs. 9 and 10).

In addition to the higher cost and the hub attachment problem, another difficulty that was encountered is illustrated in Fig. 18. This picture shows two mild-steel rings, used as containment structures during typical flywheel tests. The ring in the foreground was completely destroyed by a single test of a P-I flywheel that had an energy of only 300 Wh at failure. The ring in the background, which suffered very little damage, was used as a containment structure for approximately 50 spin tests to destruction of bare-filament wound flywheels, some of which had greater energy and greater density at failure. By design intent, the stress in

- 27 -
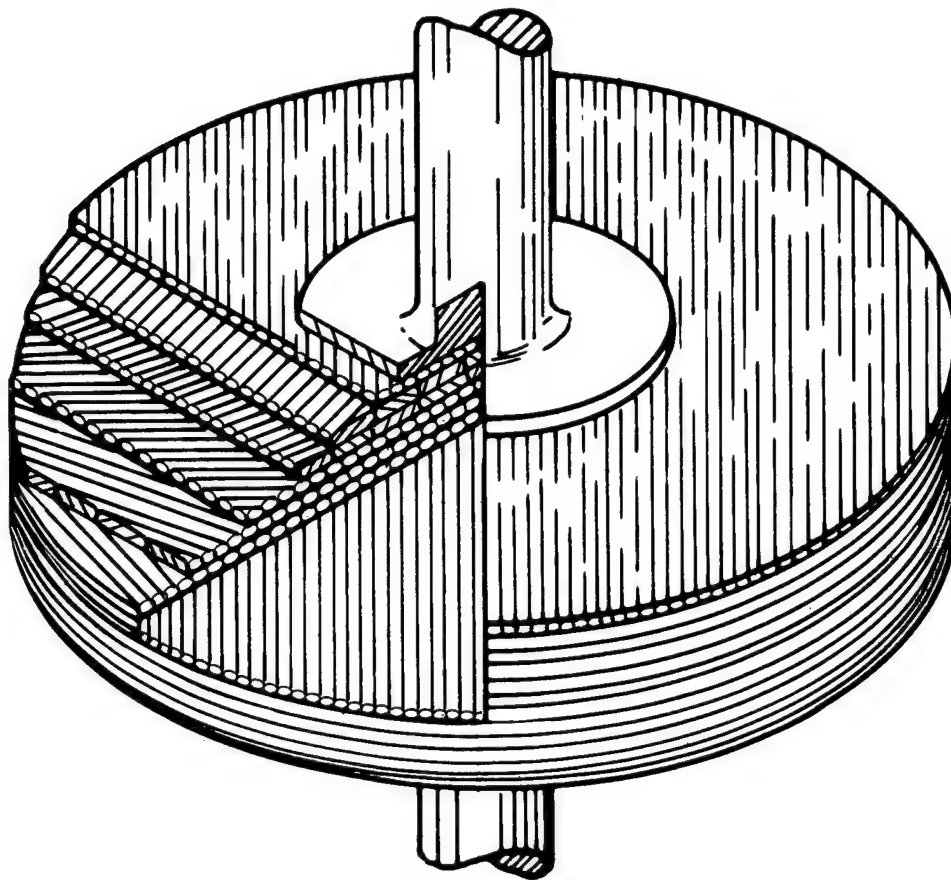
Fig. 16   Concept of the pseudo-isotropic (P-I) bond.
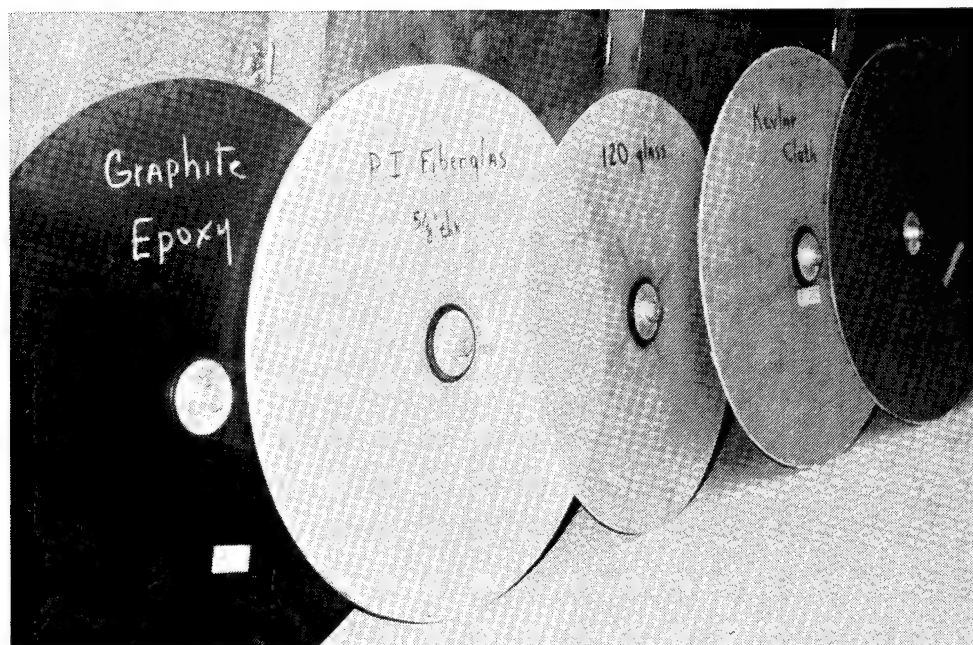
Fig. 17   Typical P-I disc flywheels.

the P-I flywheel is nearly the same at all locations throughout the flywheel. For this reason when the flywheel fails from overspeed, it fails catastrophically. In contrast, the wound flywheel stress varies as the square of the radius from the center of rotation. Thus, in a flywheel whose inside radius is half its outside radius, the stress on the inner filaments is only one-fourth of the stress on the filaments at the outer edge.
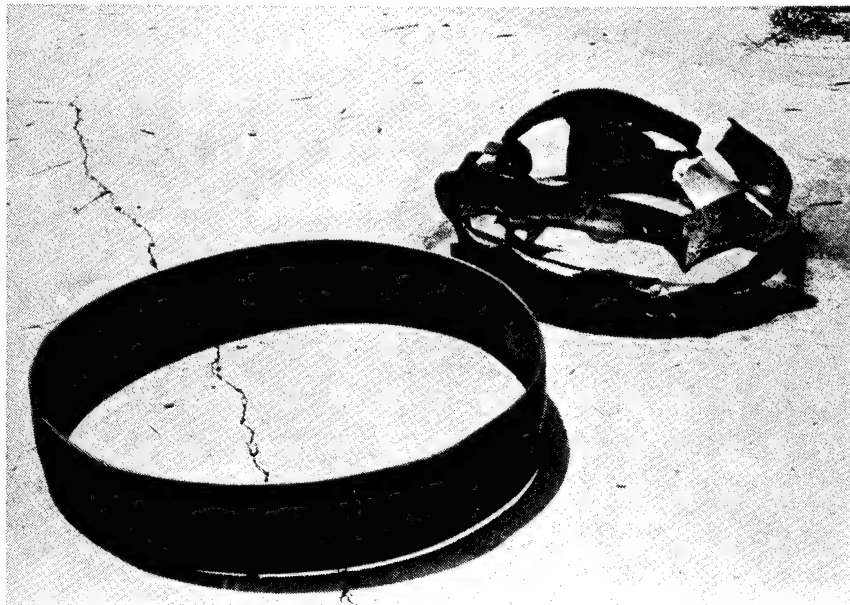
Fig. 18   Containment comparison between P-I disc and wound bare-filament flywheels.

Although the P-I disc did not prove to be cost-competitive with the wound flywheel configuration, it was found nevertheless that this material is excellent for intermediate hubs.

THE BARE-FILAMENT WOUND-RING FLYWHEEL

The APL bare-filament wound-ring flywheel concept is illustrated in Fig. 19 and is described in detail in Ref. 8. The principal feature of this flywheel configuration, other than the fact that it is a wound structure of filamentary or ribbon materials, is that the wound filaments are held together by a minimum of resin to form a stable structure. Since the performance of the flywheel is a function of the strength-to-weight ratio of its construction material, it follows that the flywheel's performance will be greater if the weight of the resin used in its construction

- 29 -

is held to an absolute minimum. It will be noted in the discussion
that follows that there are some bare-filament flywheel configura-
tions in which the resin is not used at all.
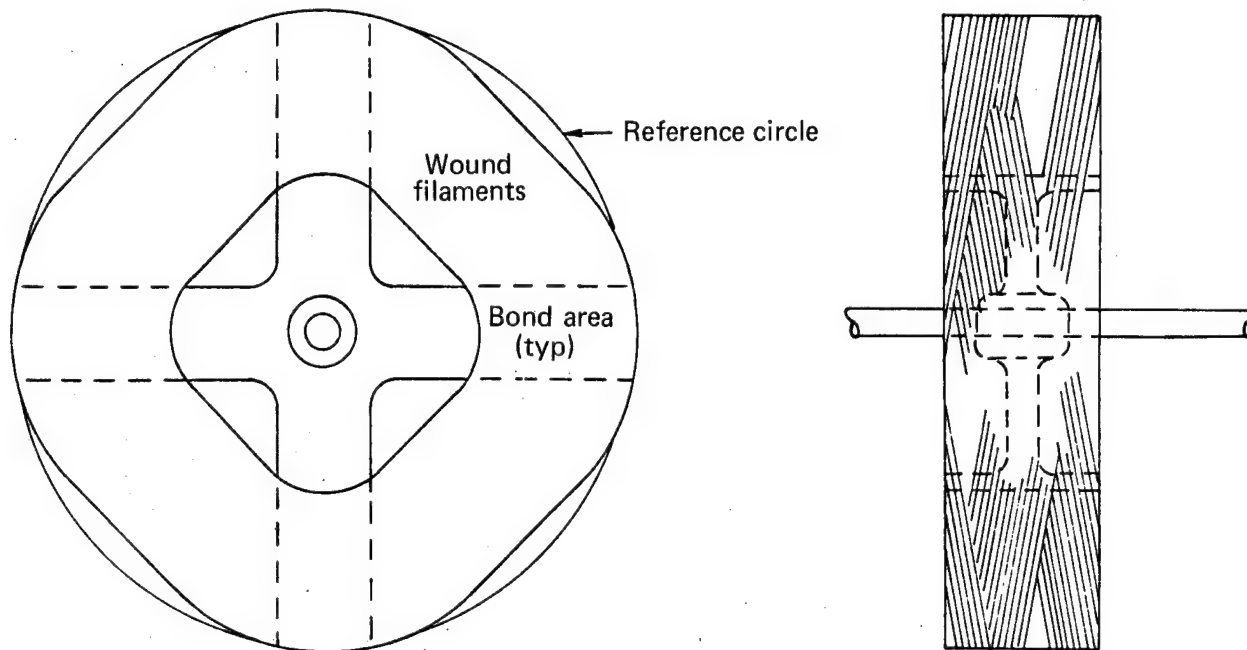
Fig. 19   Concept of the APL bare-filament flywheel.

The various performance parameters of the wound bare-filament
flywheel are illustrated in Fig. 20. The figure shows that the
energy per unit weight is proportional to the inside radius, where-
as the energy per unit volume is inversely proportional to the
inside radius. These important relationships are used to determine
the basic flywheel configuration in consideration of the material
costs and the estimated fabrication costs. In those cases where
the material cost is relatively high, it is advantageous for the
flywheel configuration to have a maximum inside radius consistent
with the size and volume requirements of the flywheel system. For
example, flywheels made of cellulosic materials at around ten
cents per pound compared with metallic substances such as steel
wire and Metglas ribbon at about a dollar per pound demonstrates
that the metallic materials are most cost-effective when the in-
side radius of the flywheel is a high percentage of the outside,
such as around 85%. In contrast, the cellulosic materials, which
cost one-tenth as much, were found to be more effective in the
overall flywheel cost argument if the inside radius was much less,
such as 50%. Generally speaking, the lower cost materials provide
much lower intrinsic performance than the moderate cost materials,
and for these lower cost materials the cost of the flywheel's

- 30 -

container becomes predominant, necessitating a minimization of flywheel volume.

Notes:

1. At maximum value the M-R E/W is 50% higher than the brush $(0.5\lambda$ vs. $0.33\lambda)$

2. The Ref. A line indicates the R_i at which the volume is the same as the brush (15% of a solid disc)

3. At Ref. B the E/W is equal to the brush E/W $(0.5 \times 0.667 = 0.333)$, while volume is 4.47 times better.

4. The use of certain bare filaments, rather than composite form could effectively double all E/W and E/V values, compared with the brush which requires composite rods.

Fig. 20   Performance parameters of the wound flywheel.

BARE-FILAMENT FLYWHEEL

Typical bare-filament flywheel-fabrication processes are described in the following paragraphs. Small, half-scale flywheels were used for development testing. For these units the filamentary material was wound directly on the flywheel hub, which generally consisted of a piece of half-inch thick plywood that had been machined to the desired shape and diameter. The plywood hub was held securely between two heavy side plates that served as axial winding limits during the flywheel fabrication.

The winding material was transferred from its shipping spool to the flywheel by means of an adjustable-helix winding fixture (Fig. 21), developed for this purpose at APL. Using this helix winding device, the optimum helix angle was determined experimentally for each of the flywheel materials.

Once the initial end of the winding material had been se-
cured to the plywood hub, the flywheel was wound automatically to
the desired radial thickness by means of the helix winding device.
When the winding was complete, the end of the material was
terminated by securing it under one of the radial wraps with
epoxy. The half-scale rotors generally had four radial wraps made
from Kevlar filaments. The radial wraps were soaked with epoxy
while the flywheel was horizontal and still on the winding form.
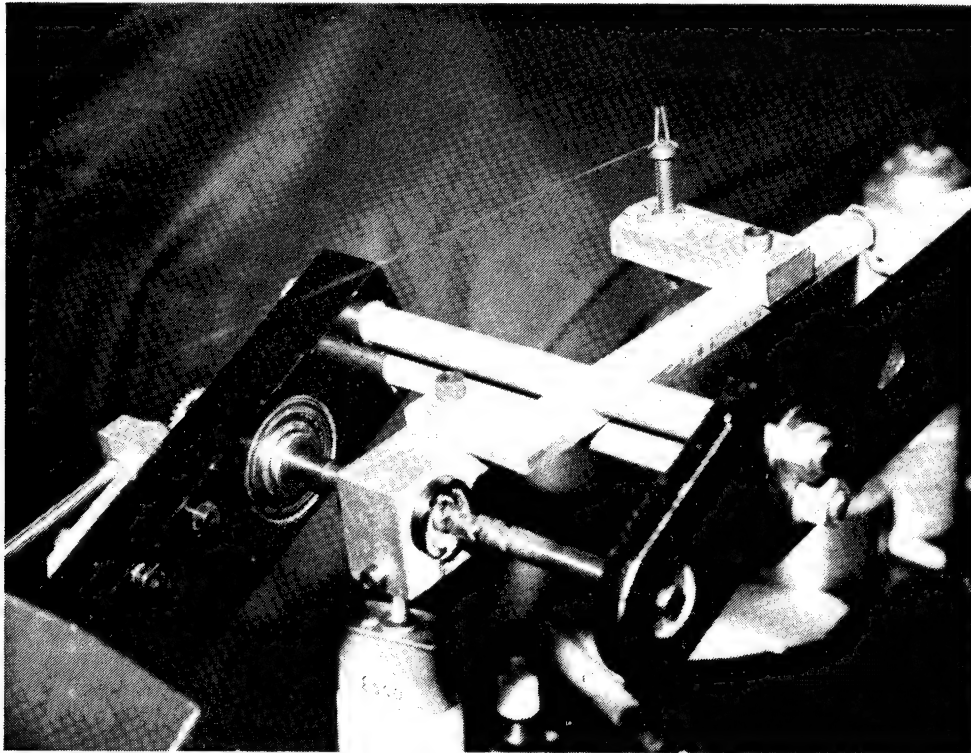
Fig. 21   Adjustable-helix winding fixture.

In the case of subcircular developmental flywheels, the radial
wrap positions were coincident with the four points of the fly-
wheel's maximum diameter. When the radial wraps had been completed
and the resin applied, the complete flywheel (and winding fixture)
assembly was cured at the desired temperature. After curing, the
flywheel was removed from the winding fixture, and the excess
epoxy flashing was trimmed. At this stage the flywheel was ready
for balancing.

Fabrication of the full-scale flywheels was similar to the
fabrication of the half-scale flywheel, except for the initial
winding process. Because most of the full-scale flywheels fabri-
cated employed a plywood or fiberglass intermediate hub structure
that was only a fraction of the axial thickness of the flywheel
itself, it was necessary to provide an additional structure

- 32 -

extending the full axial width, to permit winding the flywheel.
This structure was fabricated from the winding material by wet-
winding the filaments in epoxy so that, upon curing, a thin
solid ring was formed from the winding material. The special
mandrel on which this filament/epoxy ring was wound is illustrated
in Fig. 22. This ring acted as a compression ring on which the
remainder of the bare filaments were wound until the flywheel was
completed to the desired radial thickness. The winding mandrel
for the inner ring was made of two pieces of solid aluminum,
clamped to either side of the intermediate hub structure. The
aluminum pieces had appropriate axial taper angles and were
painted with a mold-release agent to permit removal after the
wet-wound filamentary structure had been cured and the flywheel
completed.
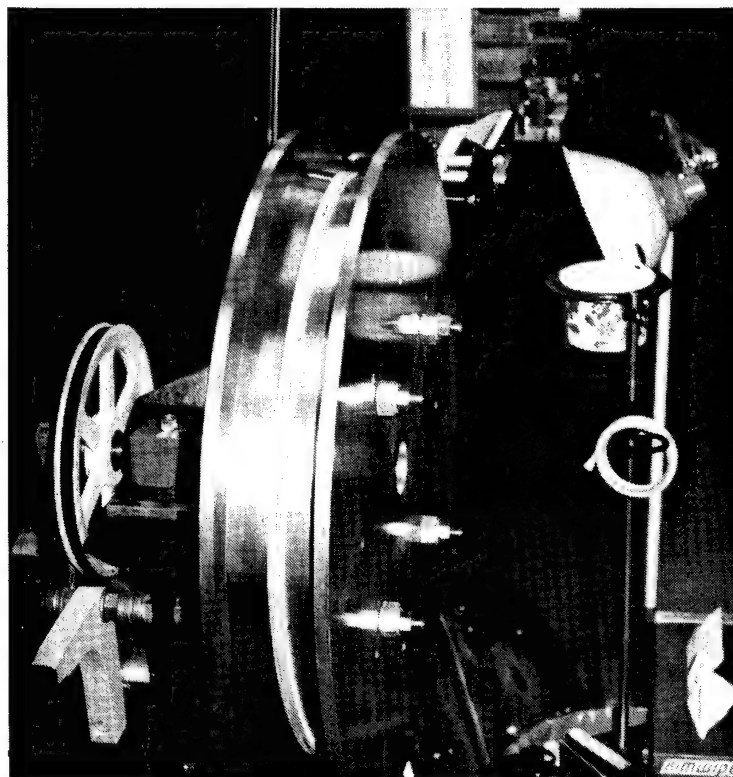
Fig. 22   Special winding mandrel for full-size flywheels.

One minor problem associated with the wound flywheel is
that static-spin balancing is a more complex operation than bal-
ancing the P-I disc, because the removal or addition of mass any-
where on the wound structure would cause undesirable stress con-
centrations. This problem was resolved by shifting the flywheel
center of geometry to be coincident with the center of mass. The
basic concept for doing this (first described in Ref. 8) involves

the use of a radially adjustable ring in the center of the flywheel
hub. This ring, which fits the flywheel support shaft, was posi-
tioned radially by four set screws on the main hub assembly. Dur-
ing balancing, the set screws were readjusted after each successive
balance run to move the center of the shaft in the direction of
the imbalance.

The gross magnitude and direction of the flywheel imbalance
was determined by spinning the flywheel on its flexible quill
shaft and measuring the runout of this shaft during rotation. The
runout was measured by moving a grease pencil radially inward
towards the spinning shaft until it barely touched the shaft,
leaving a mark on the shaft (Fig. 23). On successive spin-
balance runs, the inner ring was adjusted until the grease pencil

Fig. 23   Typical flywheel balance methods.

left a mark completely around the shaft. Using this method, it
was believed that the flywheel center of mass was located within
one to three thousandths of an inch from the center of rotation.
The method used appeared to be adequate for balancing flywheels
mounted on flexible quill shafts.

- 34 -

5. FLYWHEEL TEST RESULTS

Approximately 60 flywheel spin tests were conducted during the program. The principal objectives of these tests were to develop an optimum flywheel fabrication procedure that would demonstrate a high material-use factor and acceptable flywheel-failure characteristics, while permitting low-cost fabrication. Details of the test articles are listed in the appendixes.

To save time and money, most of the spin tests were conducted at about half scale with respect to flywheel diameter and about one-tenth to one-twentieth scale with respect to flywheel mass. It is believed that during spin testing the half-size flywheel would demonstrate essentially all of the physical and geometric characteristics of the ultimate full-scale flywheel. It was also believed that the much lower mass of the test flywheel would in no way inhibit or otherwise modify the empirical data that would be obtained from the spin tests. The typical flywheel spin tests during the program followed the general procedures outlined in the following paragraphs.

A detailed design was established on the basis of the information obtained from the previous spin tests. Appropriate fabrication tooling was obtained, and the flywheel was wound in the APL facility, using one of the three materials already described. The flywheel was then installed on the APL balance fixture and was statically balanced according to the procedure that has been described.

After the flywheel is balanced it is installed in the spin-test chamber, using an expendable flexible quill shaft made from drill rod. Generally speaking, each flywheel has its own quill shaft, and each quill shaft has a specially machined groove around its periphery to permit the quill shaft to fail under severe conditions without damaging the air turbine or its bearings. This procedure has been quite successful since more than 200 spin tests have been made on the same air turbine without any need for changing the turbine bearings. Most of these spin tests were to destruction of the flywheel.

Prior to the spin test, an appropriate number of concentric containment rings is installed in the test chamber having configurations that are consistent with the mass, rotational speed, and momentum-transfer characteristics of the flywheel to be tested. The main purpose of the containment rings is to absorb the initial impact of the flywheel fragments, while minimizing the torsional shock to the test chamber itself. Concentric steel rings with elastomer spacers have proven to be quite successful during the course of the program.

- 35 -

After the flywheel is installed, the test chamber is secured and the pressure inside is reduced to 10^{-3} Torr or below. The air compressors are started, the instrumentation is set in the operating modes, and the spin test is begun. Typically, the automatic turbine-acceleration mode is set in accordance with the pre-determined estimated maximum rotational speed of the flywheel under test. In order to prevent damaging the turbine from over-speed when the inertia of the flywheel suddenly vanishes from the rotating mass, the turbine control is arranged to cease accelera-tion of the turbine immediately when a predesignated rotational speed is reached.

A video tape recording is made of the entire test using strobe-illuminated TV cameras located on the test chamber. Rota-tion speed, time, identification, and other information is print-ed automatically on the video screen. Axial vibration, as re-ceived at a point on the turbine housing, is monitored on a spec-trum analyzer and is continuously recorded. An audio recorder makes a continuous record of all noise emanating from the test cell, with special emphasis on bearing noise. During the test, an audio alarm sounds whenever the vacuum within the test cell has degraded 10%. The acceleration of a 5-lb test flywheel from rest to a rotational speed of 30,000 rpm normally takes two or three minutes.

If the test rotor is run to destruction, the debris is care-fully examined for possible indication as to the cause of failure. In a surprising number of cases the probable cause of flywheel failure was identified from examination of the flywheel debris. This examination also included careful consideration of the con-dition of the quill shaft in terms of its final shape, as well as the nature of the fracture (that is, whether the fracture was in tension, torsion, or shear).

SUMMARY OF VINYL-IMPREGNATED GLASS FLYWHEEL TESTS

The typical vinyl-impregnated glass flywheel configuration is illustrated in Fig. 24. This flywheel has a 15-in. outside di-ameter and a 12-in. inside diameter, making the inside to outside ratio 80%. The hub is fabricated from Baltic birch plywood and has a bolted-on aluminum hub assembly. At the center of the hub is located the small positioning ring (described previously) that allows the geometric center of the flywheel to be adjusted during the flywheel balance operations. Typically the vinyl-glass fly-wheels could be configured to have a lower inside-to-outside radius ratio, since the greater strength-to-weight ratio of this material results in a higher intrinsic performance factor. The configuration has a greater overall volume occupied by the wound filaments than the steel wire or Metglas ribbon flywheels, but
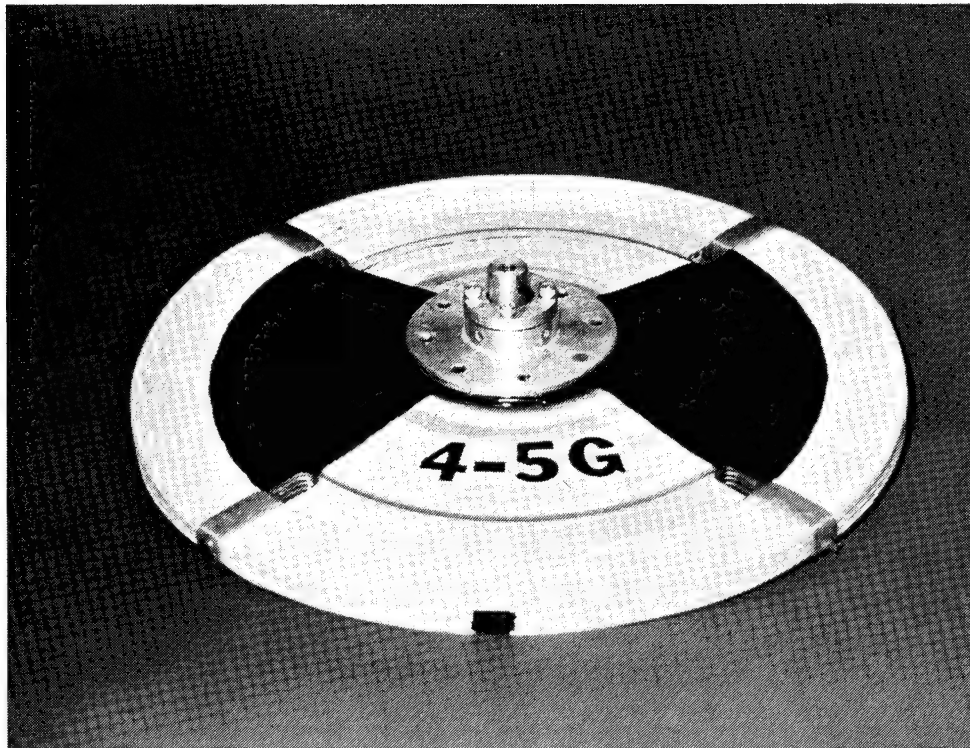
Fig. 24   Vinyl-impregnated glass-fiber flywheel.

this additional volume occupies only the area inside of the outer ex-
tremity, which means that the overall swept volume of the flywheel
is not increased. The result is that the energy per unit volume
for the vinyl-glass flywheel is generally comparable to flywheels
made from the other materials.

It will be noted that the radial wraps located in the four
quadrant positions show up as black radial bands in Fig. 24.
These bands represent the only areas on the entire flywheel where
the wound filaments are bonded to each other. In all other areas
the windings are dry-wound bare filaments. The vinyl-impregnated
glass-strand material remains in place, even after many cycles
throughout its operating speed range.

The typical failure characteristic of the vinyl-impregnated
glass flywheel is illustrated in Fig. 25. A careful examination
of the failed particles indicated that the bulk of the glass fi-
bers had not been broken, and that the plywood hub appeared to be
broken by impact, rather than from overstress during rotation.
Those fibers that had failed apparently failed in extremely small
particles. This particular flywheel failed at a rotational speed
of just under 24,000 rpm.

-37 -

Fig. 25   Typical failure mode of vinyl-glass flywheel.

The ruggedness of this vinyl-impregnated glass flywheel is illustrated in Fig. 26. Because of shaft failure this flywheel was unintentionally dropped into the test cell at full operating rotational speed three successive times before the flywheel was finally retired. On each of these occasions the flywheel bounced around inside of the test cell for a considerable period of time before eventually coming to rest. It will be noted that during this process all four of the radial wrapped areas were completely destroyed, yet the bare filament vinyl-impregnated glass remained in place until it was ground off by impact with the chamber wall.

The static stability of the wound bare-filament vinyl-impregnated fiberglass is illustrated clearly in Fig. 27, where it can be seen that even after the wound filaments are sawed loose from the hub, they remain virtually intact, even though there is no resin used in the winding process. Another extreme example of the static winding stability of the vinyl-impregnated glass is illustrated in Fig. 28. The flywheel shown in this picture has a 24-in. outside diameter ratio of 61%. Even though there is no resin used in the entire flywheel other than for termination of the initial and final strand, the flywheel remains in perfect condition even after considerable handling.

- 38 -
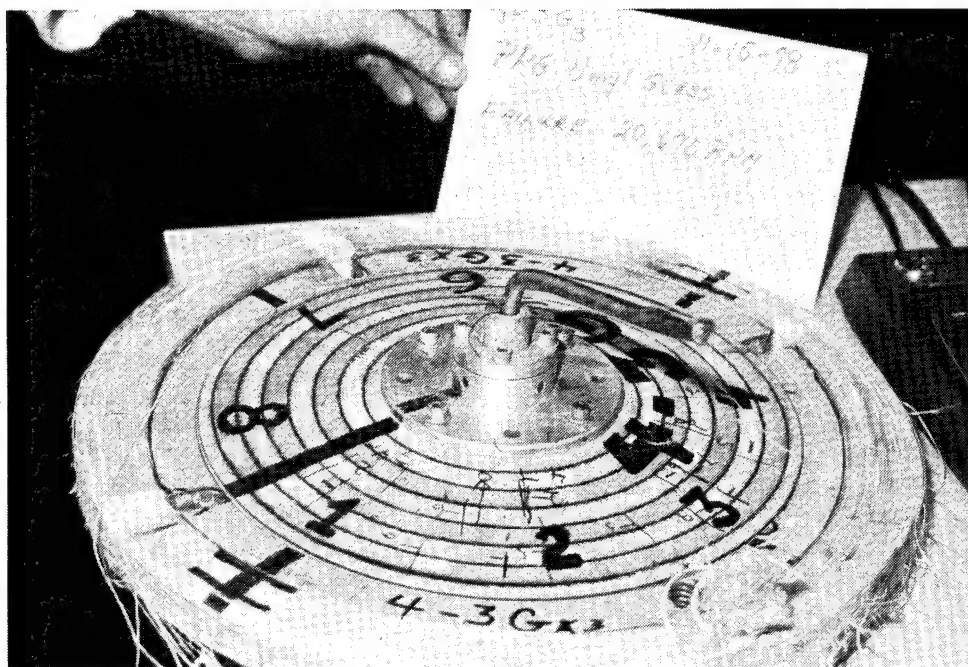
Fig. 26   Vinyl-glass flywheel after third impact.
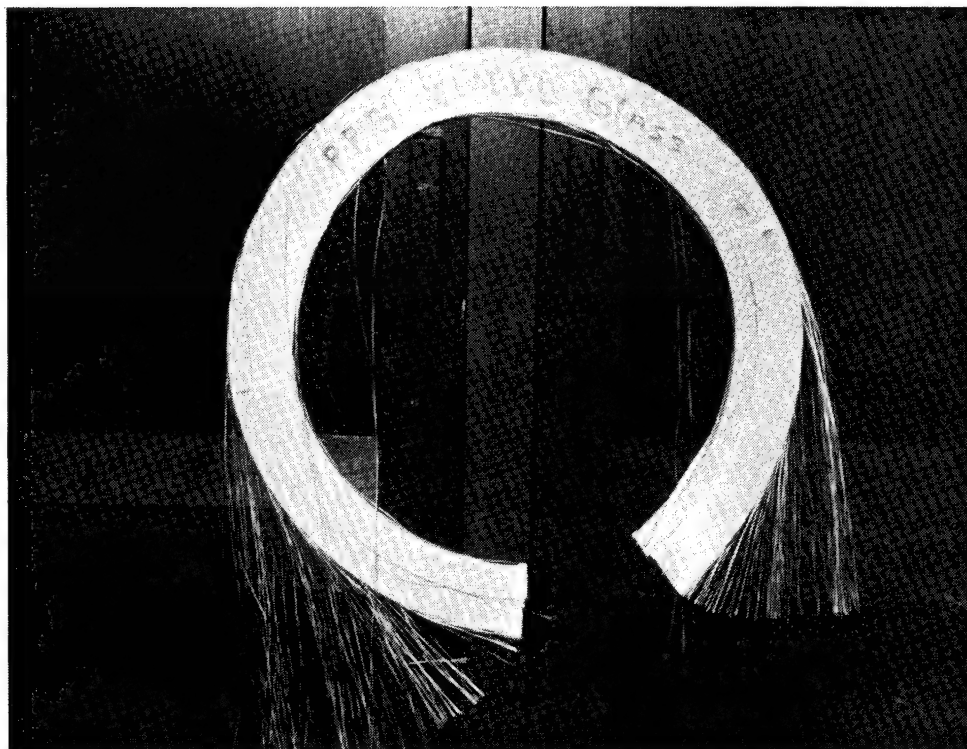
Fig. 27   Illustration of the winding stability of vinyl-glass fibers.
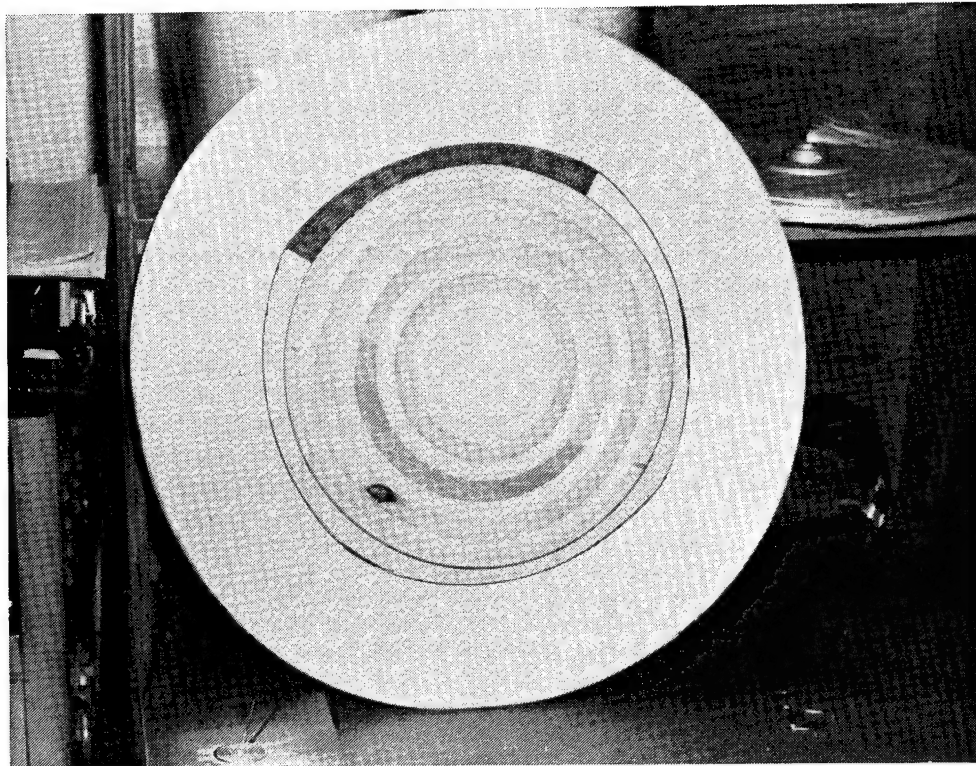
Fig. 28   Full-scale vinyl-glass flywheel.

Following are some observations based on the results of testing the vinyl-impregnated glass flywheel. A good material use factor was demonstrated, because the stress level achieved was 82 or 83% of the design stress level. The ruggedness and good failure characteristics, coupled with simplicity of fabrication, were demonstrated. The vinyl-impregnated glass flywheels appeared to have excellent dynamic stability, and balance did not change measurably during the spin tests. In view of the accumulated time on specific units, it would appear that the static fatigue of the vinyl-impregnated glass material is considerably higher than would normally be expected; however, it is recognized that more testing is required in this area.

Problem areas encountered with the vinyl-impregnated glass material are as follows: Initially, there was difficulty in finding the correct resin for terminating the ends of the vinyl. However, a vinyl-compatible resin was found in the EPON 828/Jeffamine mixture, and successful bonding using this material was achieved. Although the vinyl-glass material appears quite promising for flywheel fabrication, testing of this material had to be terminated because it was withdrawn from the market.

SUMMARY OF TESTS OF STEEL-WIRE FLYWHEELS

The basic configuration of most of the flywheels used during
the steel-wire spin-test program is illustrated in Fig. 29. Typi-
cally, the ratio of inside-to-outisde diameters was relatively
high compared to the ratios used in the vinyl-glass flywheel pre-
viously described. In the case of the steel-wire flywheels, this
ratio was typically 85 to 95% in order to permit optimization of
the performance of the flywheel in terms of energy per unit weight.
The energy per unit weight was optimized because the steel wire
used exhibited a slightly lower strength-to-weight ratio per unit
cost than the other materials. Therefore, to minimize the overall
cost of the steel-wire flywheel, it was necessary to minimize the
weight of the steel wire used in its construction.

Fig. 29   Steel-wire flywheel.

Also, the typical configuration of the steel-wire flywheel
involved a subcircular winding on a birch plywood intermediate
hub. By subcircular, it is meant that the mid-quadrant points
have a slightly smaller diameter than the quadrant points. Or,
stated in another way, the radius of curvature between the
quadrant points is greater than the radius of curvature of a cir-
cular flywheel having a radius equal to the quadrant radius. The
purpose of the subcircularity is to maintain a negative stress
factor at the quadrant points during all conditions of flywheel

- 41 -

operation. This results in an inward force tending to hold the
steel wire onto the hub at all times. The negative stress factor
is also enhanced by the steel wire being radially wrapped at the
quadrant points as illustrated in Fig. 29.

As illustrated in Fig. 30, the steel-wire flywheel generally
exhibited excellent failure characteristics, the failed particles
being small. Typically a relatively large proportion of unfailed
wire remained after flywheel destruction. Also, the steel-wire
flywheels exhibited excellent dynamic stability throughout the
tests.
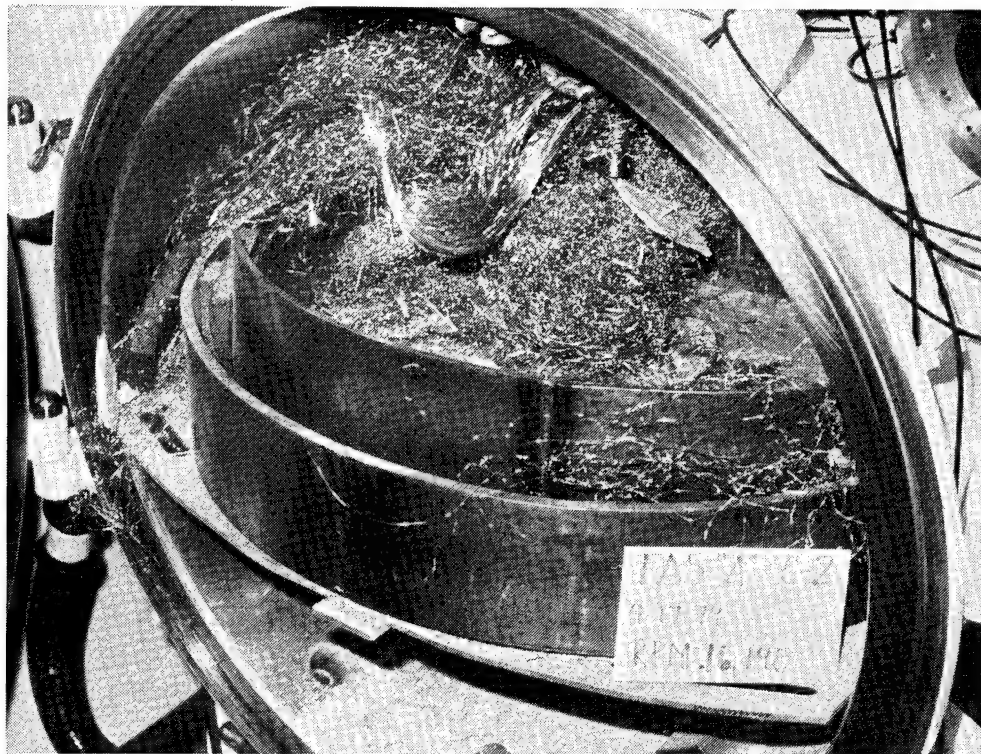
Fig. 30   Typical failure mode of steel-wire flywheel.

In addition to the conventional steel-wire flywheel config-
uration described above, there was one attempt to eliminate the
radial wraps, as illustrated in Fig. 31. Instead of radials, the
flywheel was wound subcircularly in such a manner that epoxy was
applied at the radial points during the winding process. It was
an unfortunate coincidence that this configuration was tried at
a time in the program when there was also difficulty in obtaining
adequate bonding of the steel wire. Consequently this potentially
successful configuration had to be abandoned before it was ade-
quately tested. The bonding problem was subsequently determined

- 42 -

to have been caused by inadequate removal of petroleum-based con-
taminents that had accumulated on the wire during the manufacture
and subsequent handling processes.
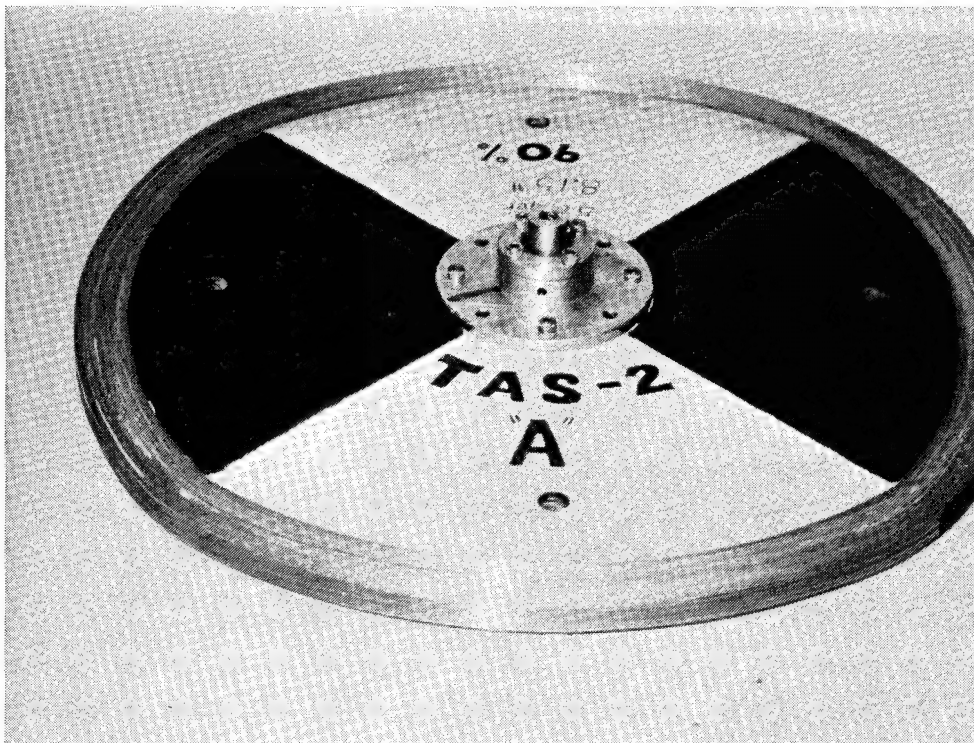
Fig. 31   Bare-filament steel-wire flywheel without radial wraps.

As stated in the preceding sections, the steel-wire flywheel
was selected as the final design; however, the decision to use the
steel wire came so late in the program that it was impossible to
provide optimum tooling for the flywheel. Nevertheless a satis-
factory 1-kWh steel-wire flywheel was designed and fabricated
using the available tooling and did subsequently meet the re-
quired test parameters. The tooling that was used was a modifi-
cation of the tooling that was originally made for a Kevlar fly-
wheel in a previous program. The Kevlar flywheel had 15 radial
wrap positions, whereas the steel-wire rotor needed only eight
radial wrap locations with 3% subcircularity between.

The principal design characteristics of the 1-kWh flywheel
are illustrated in Fig. 32. The 24-in. O.D. resulted in an axial
length on the order of 2.25 in., giving a final weight of the
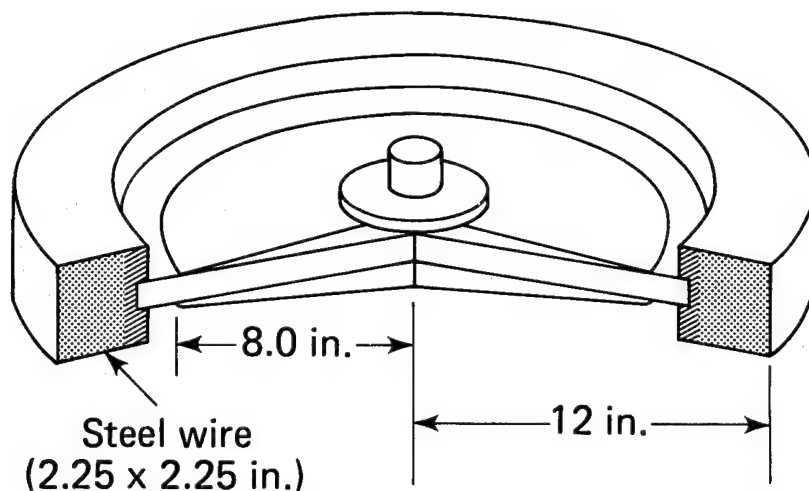
Fig. 32   Principal design characteristics of the 1-kWh steel-wire flywheel.

wound steel wire of approximately 70 lb. As indicated in Fig. 32,
the winding is conducted in such a way that the intermediate hub
material is actually captured in the initial steel-wire winding.
Also, this initial winding was conducted with steel wire wetted
with epoxy, so that the initial compression ring of the flywheel
was a solid composite material of wound steel wire and epoxy.
This compression ring is designated as the cross-hatch area in
Fig. 32 and serves as the full winding mandrel for the remainder
of the steel wire that was wound without the use of epoxy.

Two problems were encountered in the full-scale steel-wire
flywheel fabrication that had not been experienced in the fabri-
cation of the smaller flywheels tested previously. The first of
these concerns the wire "tracking" problem; that is, once the com-
pleted flywheel was removed from the winding mandrel and tooling,
the flywheel would not hold its shape because the wire tended to
slide out, causing considerable bulging at the bare-filament mid-
quadrant locations. This particular problem was precipitated by
the fact that the identical geometry was maintained for the full-
scale flywheel as had been used for the sub-scale flywheel, namely
the four-quardrant configuration. Once this problem had occurred,
it was decided that an eight-lobed configuration rather than the
four-lobed configuration would be required. However, this late in
the program, when the tooling had already been fabricated, it
was not possible to reconfigure the tooling for the eight-lobed
configuration. Consequently, it was decided that the winding tool-
ing that had been made previously for 15 radial wrapped positions

- 44 -

be used. This basic tooling, with only slight modifications, permitted fabrication of a 1-kWh steel-wire flywheel having the desired operating characteristics. This flywheel is illustrated in Fig. 33.
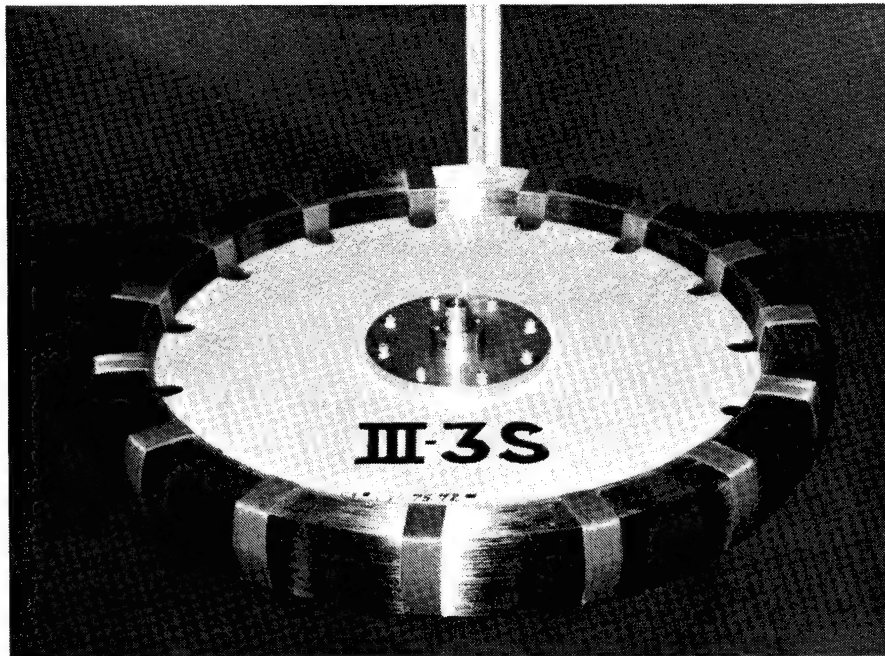
Fig. 33   1-kWh steel-wire flywheel.

It was determined early in the process of winding the 1-kWh flywheel that the winding would require considerably greater precision than was required for the earlier, smaller flywheels. A special CVT winding transmission was developed that would not only permit precision winding but would enable the winding helix angle to be changed during the winding process, while maintaining carefully controlled wire tension. The special fixture, which was fabricated to permit this precision winding, is illustrated in Fig. 21.

Another problem experienced during the full-scale flywheel program concerned the discovery of major defects in the birch plywood from which the intermediate hub had been fabricated. Late in the program, during one of the spin tests of the full-scale steel-wire flywheel, the video tape clearly illustrated gradual delamination of the birch plywood taper in the intermediate hub, immediately followed by the destruction of the flywheel at well below its design conditions. Subsequent examination of the debris clearly indicated that in the intermediate plywood hub there had been a void of several square inches where there had been no effective

bond between adjacent layers. It is believed that in the flywheel production program nondestructive techniques for materials testing could have isolated this defect before fabrication of the flywheel hub; however, for the present program it was immediately decided that a more reliable intermediate hub material be used to prevent recurrence of this problem. It will be noted in Fig. 33 that the intermediate hub material is not plywood but a quasi-isotropic composite of fiberglass epoxy, provided to the program previously by the Lord Corporation, Erie, Pennsylvania. While the strength-to-weight ratio of this fiberglass composite per unit cost was inadequate for it to be competitive in the present program as a low-cost flywheel material, this material did serve as an excellent intermediate hub material for the full-scale flywheel.

The bare-filament steel-wire flywheel technology has also been used by others. Figure 34 shows a 2.5-kWh bare-filament steel-wire
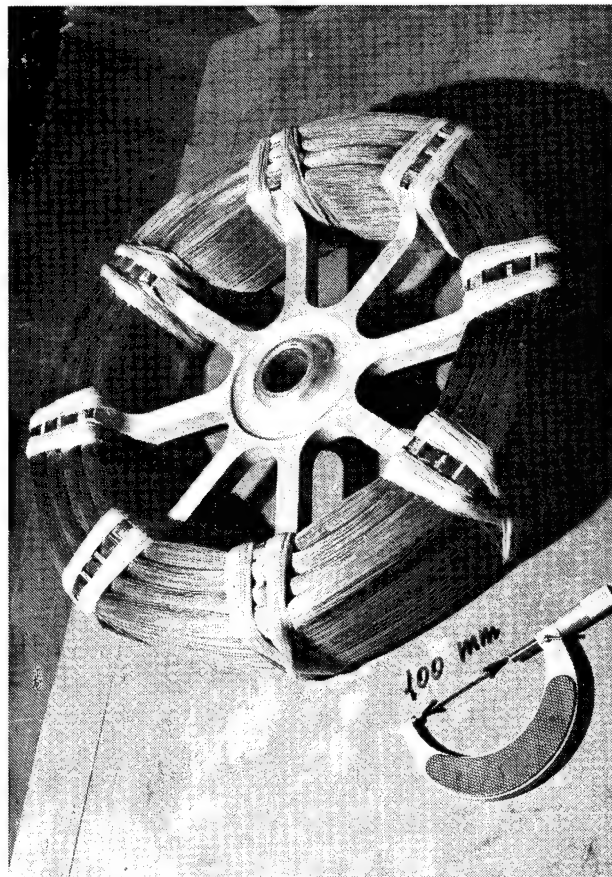
Fig. 34   Italian 2.5 kWh bare-filament steel-wire flywheel.

flywheel, which is currently being evaluated for use in the Italian flywheel hybrid bus program. The Italians, under the direction of

- 46 -

Professor Giancarlo Genta at the Institutto della Motorizizzioni,
Torino, Italy, have been experimenting with a variety of bare-
filament flywheel materials, including steel wire and Kevlar.

Following are conclusions that can be drawn from the steel-
wire flywheel tests: When the present program concluded, steel
wire was the most mature reliable material tested. The problems
encountered in the fabrication of steel-wire flywheels are all
amenable to near-term solutions. As indicated in Table 3, the
steel-wire flywheel has lower performance in terms of energy per
unit weight and energy per unit cost than the vinyl-glass flywheel.
The energy per unit weight can be improved only at the expense of
increasing the cost, because the stronger steel wire costs more.
The marginal energy per unit cost also tends to reduce the energy
per unit volume because inordinately high ratios of inside-to-
outside diameter are required to optimize weight, limiting the
amount of steel-wire material that can be used in the flywheel
structure. However, despite these marginal performance limita-
tions, the steel-wire flywheel is definitely competitive in terms
of performance in all of these same areas, compared with steel
isotropic flywheels or lead-acid batteries, as illustrated in
Table 5.

SUMMARY OF TESTS OF METGLAS AMORPHOUS RIBBON FLYWHEELS

Spin tests of the Metglas amorphous ribbon flywheel, while
considerably fewer than the tests of other types, nevertheless
demonstrated the future potential of this material for use in ve-
hicular as well as stationary flywheel applications. In terms of
energy per unit weight its performance falls between that of the
vinyl-impregnated glass flywheels and the steel-wire flywheels.
However, the energy per unit volume for this type exceeds that for
either of the other types because of the relatively high usable
strength and exceptional packaging efficiency of this material.
The somewhat higher energy-to-weight ratio also permits the use of
more effective diameter ratios, thus allowing more material to be
wound to further increase the volumetric effectiveness.

Aside from the initial bonding problems experienced early in
the Metglas-ribbon flywheel test program, this material has dem-
onstrated excellent fabrication characteristics. The brief ex-
perience in the present program indicated that future Metglas-
ribbon flywheels should present extremely low fabrication cost.

The typical Metglas-ribbon flywheel (Fig. 35) has a basic
geometry that is identical to that of the steel-wire flywheel (Fig.
29). Flywheels fabricated from Metglas amorphous metal ribbon also

- 47 -

appear to have excellent failure characteristics, as illustrated
in Fig. 36. The average failed particle size compares with a few
inches of the steel wire previously described and is therefore
relatively simple to contain in the event of flywheel failure.

Table 5

Performance of flywheels in comparison with lead-acid batteries

Application	Energy/Weight (Wh/lb)	Energy/Volume $(Wh/ft^3)*$	Design Lifetime (Years)	Relative 20-Year Cost Factor[†]
Steel flywheel in Oerlikon Bus (1948)	1.25 (Ref. 9)	<500	20	10
Steel flywheel in New York Subway (1978)	5.5 (Ref. 10)	<2000	20	3
Lead-acid battery	12	≈1000	5	5
Steel-wire flywheel	12	1500	20	1
Steel-wire flywheel	10	3000	20	1.25

* Including containment.

† Equals energy-to-weight times design lifetime relative to steel wire
at 90% inside radius.

    The main problem (mentioned previously) encountered in the
early stages of the Metglas-ribbon flywheel program was the diffi-
culty in bonding this material with conventional adhesives. This
problem manifested itself in the very first spin test of the
Metglas-ribbon flywheel, where the flywheel simply unwound at a
rotational speed considerably below its design speed. In this
particular instance it was fortunate that the flywheel did not
completely destroy itself (because of hub bonding failure, this
flywheel had been accidentally dropped at a high peripheral vel-
ocity to the floor of the test cell). After the test, careful ex-
amination of the Metglas amorphous ribbon remaining on the inter-
mediate hub revealed that the strength of the bond between adjacent
layers of Metglas ribbon was nearly zero. Also, as indicated pre-
viously, satisfactory solutions for bonding the Metglas amorphous
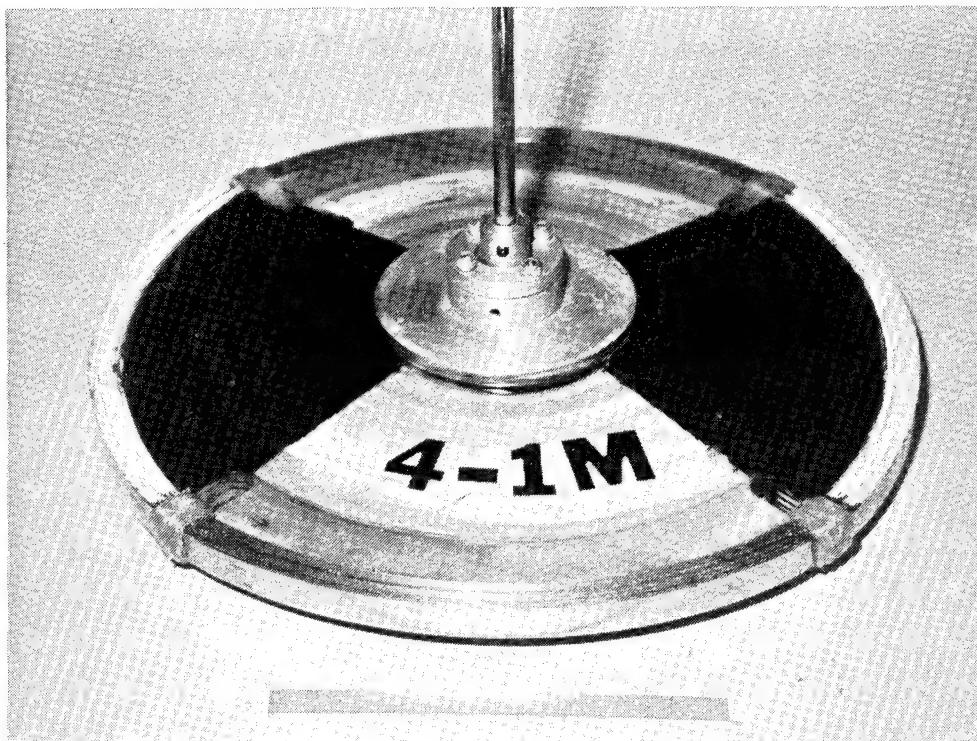
Fig. 35   Metglas amorphous ribbon flywheel.

Fig. 36   Typical failure mode of the Metglas-ribbon flywheel.

ribbon were defined before the present program was completed, as indicated in Table 4.

From the brief Metglas-ribbon flywheel tests, it appears that this material represents an excellent candidate for moderately low-cost flywheel applications, particularly for applications involving vehicles, where energy per unit volume may be a predominant requirement. The possible future availability of this material in wider widths makes it even more attractive from the standpoint of minimizing flywheel-fabrication problems. Also, from the negligible material-creep and static- and cyclic-fatigue problems, it appears that flywheels made from Metglas amorphous metal ribbon would have excellent long-term operating characteristics.

6. LOW-LOSS, LONG-LIFE BEARING DEVELOPMENT

To keep operating costs low, the home energy-storage system will require bearings that are capable of long life and minimum losses. After preliminary investigations were made of available bearing types, it was thought best to concentrate on bearing concepts that involve the use of conventional rolling contact bearings.

The preliminary studies had indicated that magnetic suspension would not be applicable to the low-cost system at the present state of-the-art, even though the intrinsically low-loss and long-life characteristics of magnetic suspension would be attractive. Also, an analysis of a variety of fluid-bearing concepts resulted in the conclusion that, while these bearings offered the prospect of low cost and long life, the bearing losses would preclude their operation in any very low-cost flywheel system.

The preliminary bearing-evaluation study revealed that there are a few promising concepts that could result in considerable improvement in the loss characteristics of conventional rolling contact bearings. In order to evaluate the candidate systems, a special bearing test fixture (Fig. 37) that allowed direct comparison of bearing losses at design rotational speeds and vacuum conditions was designed and fabricated. This piece of equipment allowed simultaneous testing of four separate bearing assemblies at identical rotational speeds and vacuum conditions.

The test equipment was designed to simulate as closely as practicable the actual bearing conditions in the energy-storage system. That is to say, the radial loads on the bearings during testing were close to zero, while the axial loads for the respective bearings were intentionally varied over a predetermined range of axial preload conditions. Typical preload conditions were 2, 4, 8, and 16 pounds, respectively, on each of four bearings simultaneously. The test bearings were Bardon 100H, which were vapor decreased and lubricated with three or four drops of Mobile 1 oil for the test. It had been previously determined through evaluation testing that the synthetic Mobile 1 oil provided excellent lubrication under the normal flywheel vacuum conditions of the energy-storage system. Mobile 1 is, in fact, used for the lubrication of all bearings in the APL flywheel test operations.

The four sets of preloaded baseline test bearings were operated continuously at 10,000 rpm for 10^8 revolutions (1000 hours) with no obvious problems. One drop of oil was applied to each bearing each day during the testing period. On alternate days the rotational speed was set at 1800, 7500, 13,200, and 17,000 rpm to measure the drag torque of each bearing pair. Drag variation with rotational speed was very slight. The average drag at the respec-

- 51 -

tive preload values was recorded from a torque watch and is indicated in Table 6. The recorded values indicate that the losses in the 100H bearings at essentially zero radial load and at minimum nominal axial preload are very low. It can be concluded that if these bearings could be arranged in a final energy-storage system so as to operate at or near these test conditions, the total losses in the bearing in the energy-storage system would be comparably low.
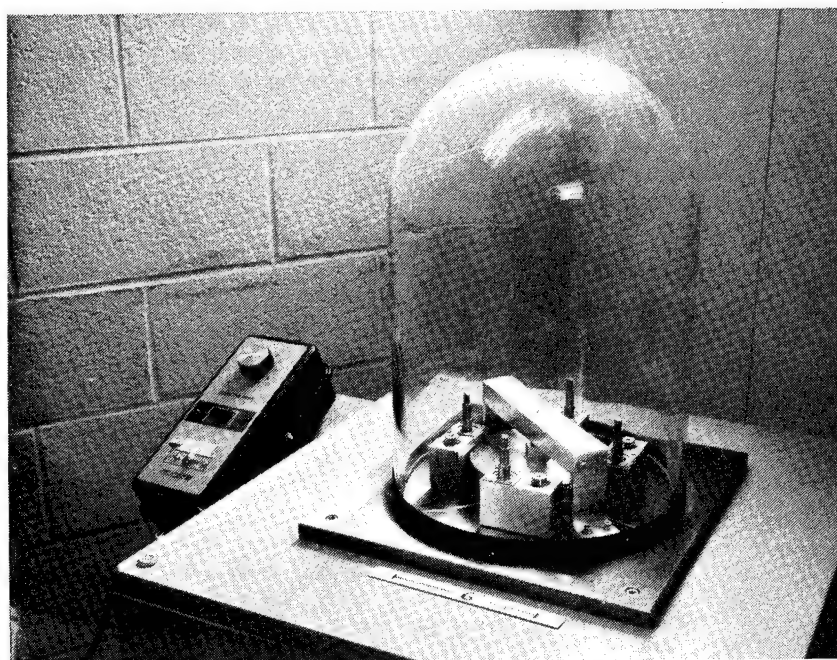
Fig. 37   Fixture for bearing spin test.

As described in Refs. 11, 12, and 13, facts concerning the four well-known generalized bearing parameters are that (a) the bearing losses increase with increased rotational speed, (b) the allowable load decreases with increased rotational speed, (c) the loss increases with the size of the bearing for a given condition, and (d) the load increases with the size of the bearing for a given condition. From the generalized bearing operating parameters the the following assumptions can be made: (a) by reducing the effective rotational speed of the bearing, not only are the bearing losses reduced, but the allowable load on the bearing is increased; (b) since the allowable load varies with size, the size of the bearing can be reduced; (c) the reduction in size causes a further reduction in losses; and (d) additional load relief, such as by means

of passive magnets, permits a further reduction in size, hence a
further reduction in bearing loss.

Table 6

Losses* in 100H bearings after 10^8 revolutions

Bearing Pair	Preload (1b)	Torque (in.-oz)	Losses (W)
1. Baseline, #1	2	0.18	1.3
2. Baseline, #2	4	0.19	1.4
3. Baseline, #3	8	†	†
4. Baseline, #4	16	0.29	2.1
5. APL Series‡	2	≈0.045	≈0.37

* All data taken at 10,000 rpm; however, occasional measurements
  were taken at 1800, 7500, 13,200, and 17,000 rpm, with little
  change noted in bearing torques.

† No data were recorded on item 3 because torques were erratic
  (for no apparent reason).

‡ The geometry of the series bearing pair is such that each pair
  is essentially the equivalent of <u>one</u> conventional bearing.

It was pointed out previously that the stationary flywheel
system readily permits the use of a quill-mounted flywheel, essen-
tially eliminating the radial bearing losses. It was also clear
that the axial or vertical loads could be reduced considerably by
using a passive magnet system. For the development of this system,
APL initiated a small subcontract to the Jobmaster Corporation in
Randallstown, Maryland. A number of alternate means of obtaining
the magnetic load relief for the bearings was discussed with this
organizaiton. Originally it had been contemplated that a re-
pulsive magnet system be used. In this system, two magnets are
placed in opposition to one another so as to create a vertical
thrust in the flywheel suspension system. Such a system would
have a number of apparent advantages, among which is the advantage
that the repulsive forces between the two magnets will increase as
the distance between the two magnets decreases, resulting in a
system having static stability. A disadvantage of such a system,

however, is that it requires two magnets, as opposed to a single-magnet system operating in the attractive mode. Also, considering the nature of the magnetic materials involved and the magnetic circuit in which they would be used, it was apparent that more magnetic material would be required in a system using two repulsive magnets than would be used in a system using a single attractive magnet. In consideration of the basic objective of the overall program, the least expensive (attractive magnets) system was chosen and was subsequently fabricated by the Jobmaster Corporation. The detailed analysis and designs for this system are contained in Ref. 14.

The magnetic load-release system produced by the Jobmaster Corporation for the flywheel energy-storage system is illustrated in Fig. 38, and its performance characteristics are shown in Fig. 39. It was subsequently determined that the performance of this unit could be nearly doubled by increasing the pole piece thickness 50% and reducing the operating gap 25%. The magnetic material selected was one that would be optimized for minimum axial thickness, round shape, high coercivity, aging stability, low cost, and ready availability. These requirements were easily met by a ring-shaped barium ferrite magnet such as those commonly used in the loudspeaker industry.

The production cost of the magnetic load-relief unit in quantities exceeding 10,000 units is estimated by the Jobmaster Corporation to be $2 to $3. This cost includes the magnetic material, fabrication, and assembly of the unit, including magnetization.

Since the radial bearing loads were effectively reduced by the flexible quill shaft, and the axial bearing loads were effectively reduced by the magnetic unloading system, attention was turned to the various possible concepts for reducing the effective rotational speed of the bearing. Two such concepts to be evaluated were the series bearing concept and the slow roller bearing concept. The physical characteristics of the series bearing concept are illustrated in Fig. 40, and Fig. 41 is a photograph of the series bearing test components. As the name implies, the series bearing consists of two conventional bearings operating in series; i.e., functionally, the bearings operate concentrically, although, as indicated in Fig. 41, they both actually have the same diameter. While operating one bearing inside of the other, each bearing rotates at approximately half the initial rotational speed, and at half the rotational speed there is a corresponding reduction in the bearing losses.

The series bearing test unit was run on the bearing test fixture at conditions that were identical to those used for the baseline test bearings, and the results are compared in Table 6. The measured drag of the series bearing at 10,000 rpm is approximately

- 54 -
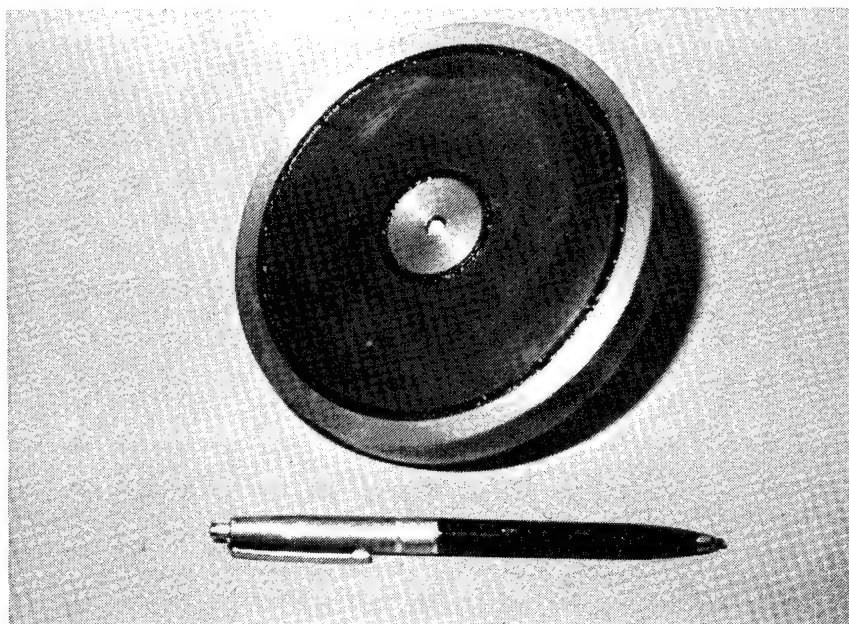
Fig. 38   Magnetic load-relief unit.
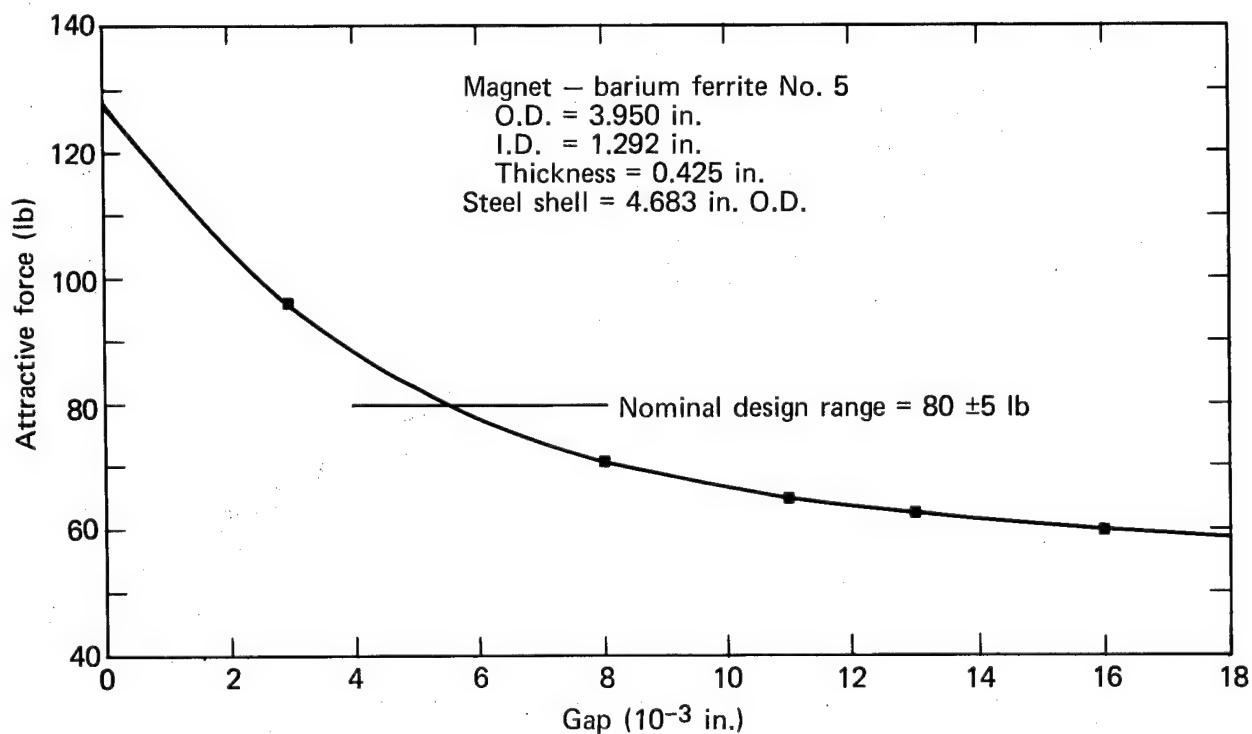
Fig. 39   Performance of magnetic load-relief unit.
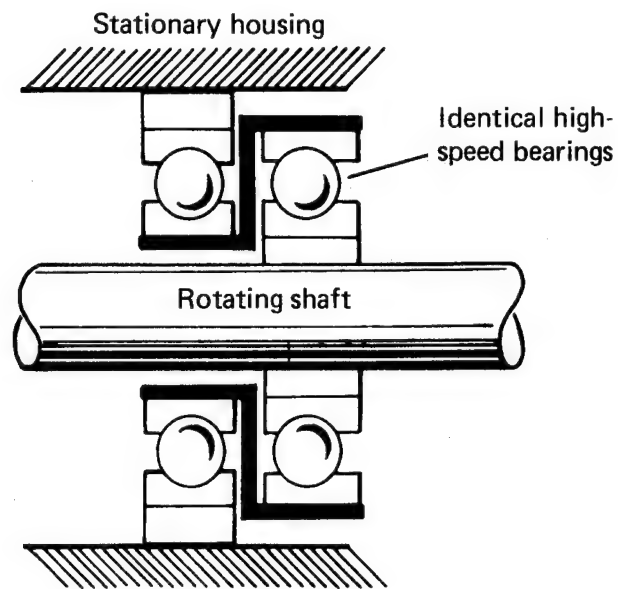
Fig. 40   Series-bearing concept.
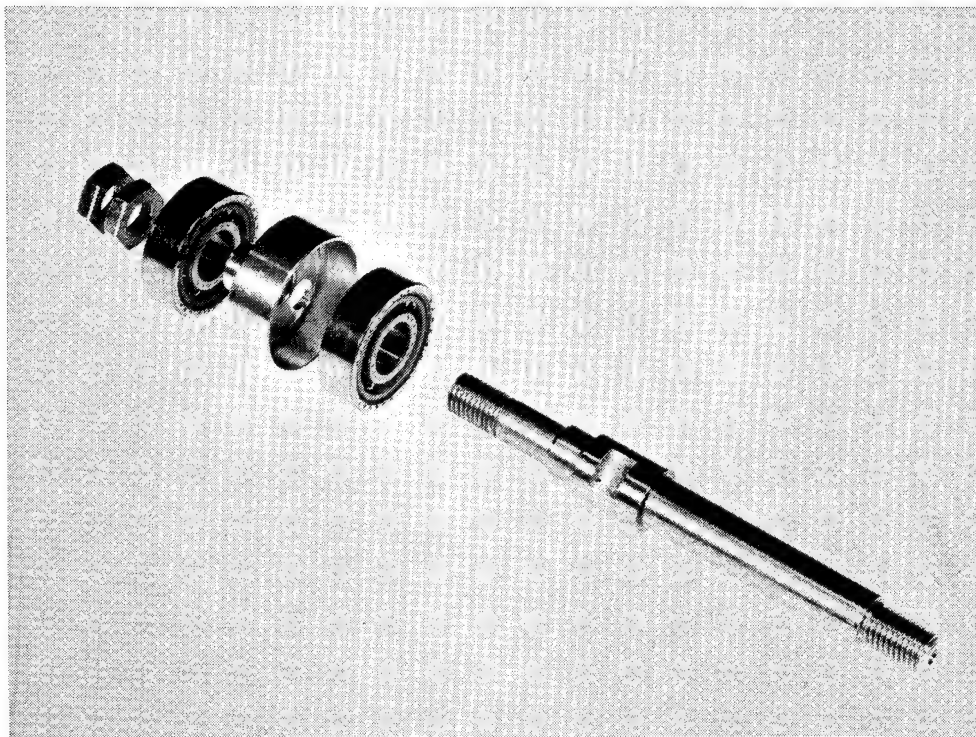
Fig. 41   Series-bearing components.

0.37 W, or 28% of the drag of the baseline test bearings (to which they were otherwise identical). Note that the series bearing unit constitutes a single operating bearing, even though two 100H bearings are used; therefore, in order to be directly comparable to the baseline bearing pair, the drag of the series bearing would have to be doubled (i.e., 0.74 W). Thus, the series bearing presents a final drag that is 56% of the drag of identical conventional bearings. It should also be noted that the predicted life of the series bearing unit at half the nominal rotational speed is considerably longer than that of the conventional bearing and may be longer by as much as an order of magnitude (Ref. 11).

The second concept for reducing the effective rotational speed of the flywheel bearing is illustrated in Fig. 42. Using this configuration instead of the two-to-one rotational speed reduction of the series bearing, the slow-roller concept can produce rpm reduction by as much as an order of magnitude. Again, the reduction in the rotational speed of the bearing permits a greater load carrying capacity, which in turn permits a reduction in the bearing size. The net effect is an additional reduction in bearing loss.
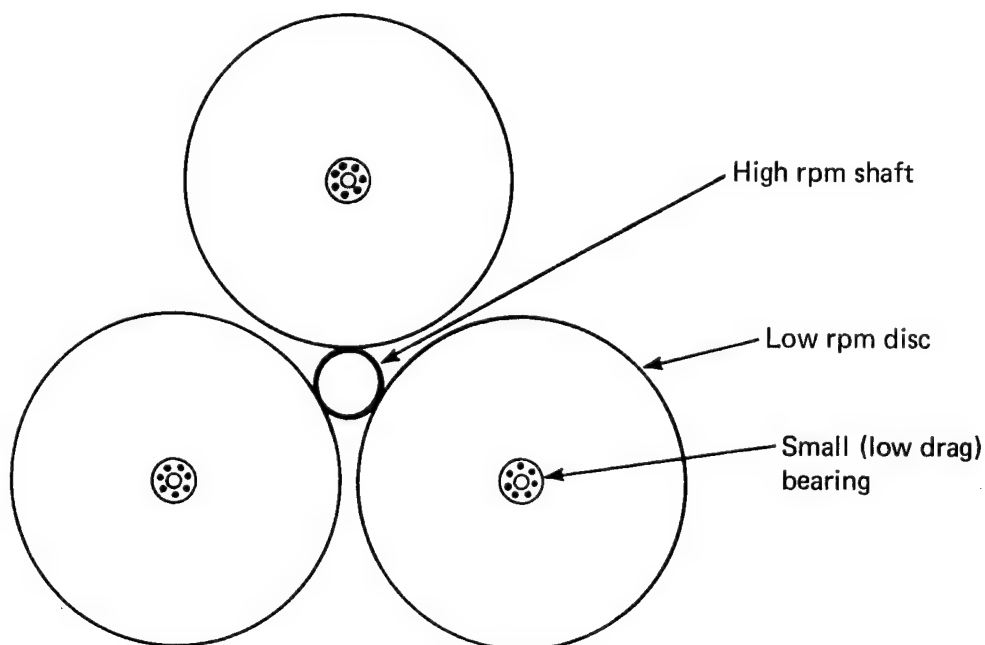
Fig. 42   APL slow roller-bearing concept.

Table 7 provides an interesting comparison between the various magnetically unloaded bearing concepts and conventional bearings. Here the losses of bearings designed to support comparable flywheel weights are listed side by side. The data in column 1 are taken from Ref. 12 and indicate that the bearing losses (corrected

to 10,000 rpm) are 25 W. The data in column 2 reflect the results of reducing the conventional bearing size by radial and axial load relief. The measured bearing losses in this condition are 1.4 W, or only 5.6% of the losses in conventional bearings in the unloaded condition. It will be noted that the bearing bore for the column 2 condition is only 1/3 that required for the column 1 condition.

Table 7

Comparison of bearing performance

Parameter	(1)	(2)	(3)	(4)
		Bearing Type		
	Conventional*	Plain, Unloaded	Series, Unloaded	Slow Roller, Unloaded†
Flywheel rotating weight	97	85	85	85
Bearing type	206H	100H	100H	36H
Bearing bore (mm)	30	10	10	6
Bearing losses @ 10,000 rpm (W)	25	1.4	0.74	≈0.30
Loss comparison (%)	100	5.6	3.0	≈1

* Date from Ref. 12

† Slow roller bearing characteristics are estimated from known relationships of the smaller bearings and lower rotational speeds (Ref. 12); all others are actual measurements.

The data in column 3 indicate the further reduction in measured losses resulting from the introduction of the series bearing to the unloaded case of column 2. The introduction of the series bearing results in a loss reduction to 0.74 W, or 3% of that for conventional bearings.

And finally in column 4 the predicted characteristics of the slow-roller unloaded bearing are indicated. This column reflects a further reduction in bearing size to a 6 mm bore, with a corresponding bearing loss (estimated from Ref. 9) at less than 0.25 W. This results in the estimated drag of the unloaded slow roller bearing as less than 1% of the drag of the original conventional bearing. By further improving the magnetic load-relief unit (as

described above) the flywheel weight can be doubled, without the need for changing the bearing configuration.

It is apparent from the foregoing discussion that flywheels can utilize rolling contact bearings having total losses on the order of 1 W per 100 lb of flywheel. Projected lifetimes may be orders of magnitude greater than that of conventional bearings because the loads and rotational speeds are greatly reduced. This potential hundredfold improvement in bearing losses appears to justify the modest complexity of these bearing concepts, especially in consideration of the complexity of alternate systems such as magnetic suspension. The APL studies further implied that these concepts appeared to be applicable (to a degree) to vehicular as well as to stationary flywheel systems.

7. ENERGY-STORAGE SYSTEMS

An objective of the current program is to demonstrate the flywheel in a complete energy-storage system. The design criteria established for the system were:

1. Both the charge and discharge cycles for the flywheel unit were to be performed electrically with the input and output being 120 V, 60 cycle AC.

2. The electrical components were to be purchased comercially.

It was recognized that the second criterion would require a compromise in the overall efficiency of the system compared to a design that optimized the power equipment. However, since such design is within the state of the art, it was felt that the compromise warranted the savings in time and expense.

Figure 43 is a block diagram of the motor/generator control system. The system consisted of a 3-hp, 2-pole, 3-phase squirrel-cage induction motor (purchased from Copeland Electric Co.), which was controlled by a unit (Fig. 44) provided by Volkman Electric Drives Co. The control unit was modified to permit operation of the motor as a generator.
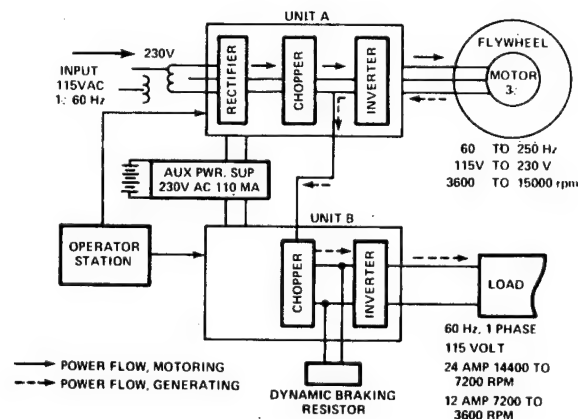
Fig. 43   Block diagram of the energy-storage system.
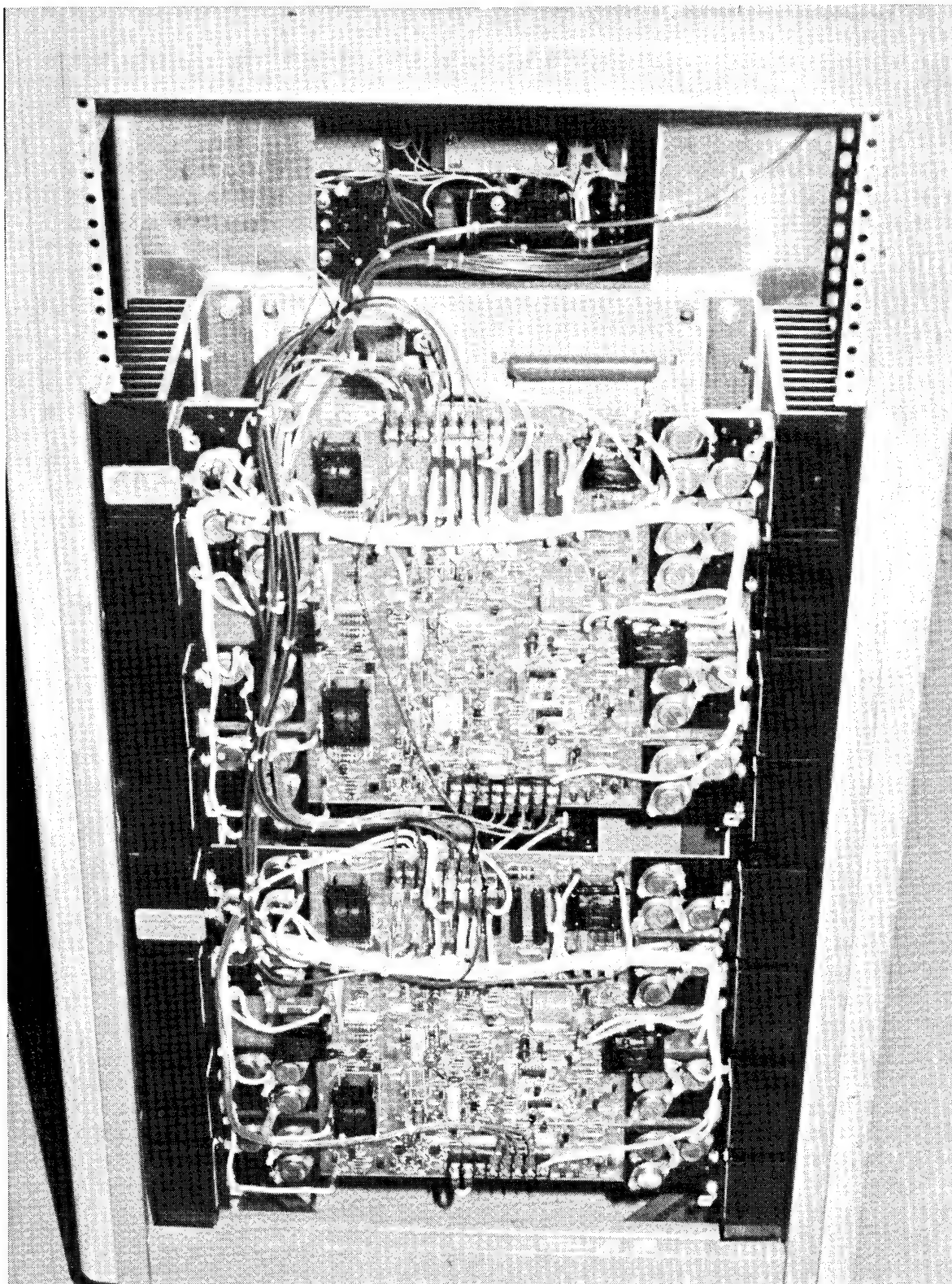
Fig. 44   Control components of the energy-storage system.

The complete system was designed to operate essentially automatically to convert electric energy from a conventional wall receptacle to be stored as kinetic energy in the flywheel, and, subsequently, to permit this kinetic energy in the flywheel to be transferred essentially automatically to a variety of electrical loads. The types of loads used for the demonstration were incandescent lamps and universal AC-DC motors.

Three motor/generators and two sets of electronic control equipment were obtained for the program. Only one of the electronic control systems was completely built, permitting the remaining components to be utilized as necessary for spares. Two motor/generators were assembled.

The principal characteristics of energy-storage system 1 (ESS-1) are shown in Table 8. The principal components of this system are illustrated in Fig. 45, where it can be seen that the flywheel is an isotropic aluminum slab construction. It is comprised of six 1/2-in.-thick slabs. The induction motor/generator components are shown in Fig. 46.

As illustrated in Fig. 44, the motor/flywheel combination are accelerated from rest by the action of unit A, which receives 115-volt, single-phase, 60-Hz input power, rectifies it to a controlled level DC voltage, and inverts it to a controlled frequency three-phase AC voltage. Voltage level and frequency are controlled in accordance with the curve shown in Fig. 47. Current is limited by a servo that monitors current drawn by the motor and controls the voltage level and frequency to the motor. By maintaining constant current per phase, the motor produces a constant torque up to the point where the line voltage reaches 230 VAC at 120 Hz (7200 rpm). At this point the motor is providing more than four horsepower. The frequency of the excitation is controlled from 120 to 240 Hz to continue to maintain constant current to the motor, even though the voltage is held constant at 230 V.

At 240 Hz the motor (flywheel) rotational speed should be slightly less than 14,400 rpm. Because the flywheel is fully charged at this speed input power is disconnected and the flywheel is allowed to coast until electrical power is required.

When all input power removed and the flywheel motor/generator is commanded to generate electricity, an auxiliary power supply powered by two small-lead-acid batteries is activated to power the control relays and provide excitation to the inverter of unit A in the following manner.

The inverter of unit A supplies three-phase excitation to the motor at low voltage and at a frequency that is ramped down from

Table 8

Characteristics of energy-storage system 1

Purpose:	1. Evaluate flywheel suspension dynamics.
	2. Evaluate and refine electronic control equipment.
	3. Validate satisfactory operation of motor/ generator and cooling system in a vacuum environment.
	4. Conduct preliminary flywheel life-cycle tests*.
Flywheel:	100-lb laminated aluminum disc, 20.5-in. diameter, approximately 500 Wh stored evergy.
Bearings:	Size 77R16, 1-in. bore; shielded; lubrication, grease.
Motor/generator:	2-pole, induction type, 3 hp, water cooled, in vacuum housing.
Operational rotational speed:	14,400 rpm maximum, 3600 rpm minimum
Vacuum:	10^{-2} Torr. Sealing accomplished with flat elastomer gaskets.

* Conducted with final flywheel design, at end of program.

250 Hz until it matches the frequency corresponding to the present rpm of the flywheel. The motor then becomes an induction generator and is fully excited. When the proper current is produced by the generator, the servo controlled frequency changer mantains the excitation frequency at the proper value, which is a few hertz below the synchronous speed of the motor/generator. Output from unit A is supplied as DC to the chopper/inverter section of unit B, where it is converted to 115-V, single-phase, 60 Hz power and made available to an external load. As shown in Fig. 47, an external load can draw up to 24 A for flywheel speeds from 14,400 rpm down to 7200 rpm. This load must be reduced to 12 A between 7200 rpm and 3600 rpm as one of the concessions resulting from the use of available hardware.
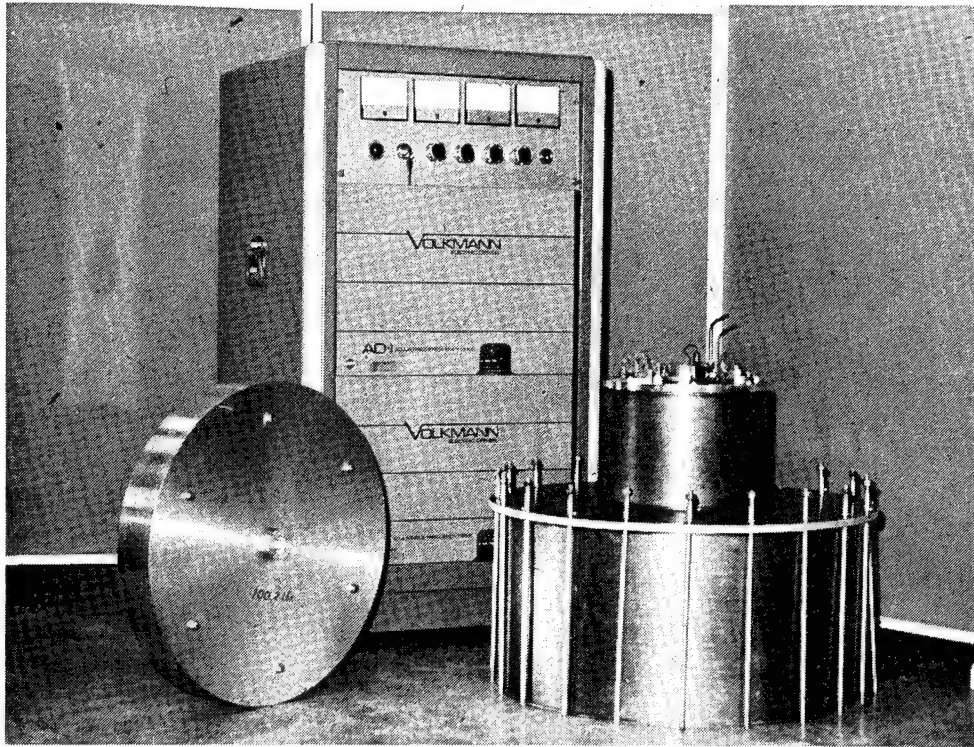
Fig. 45   Components of energy-storage system 1.
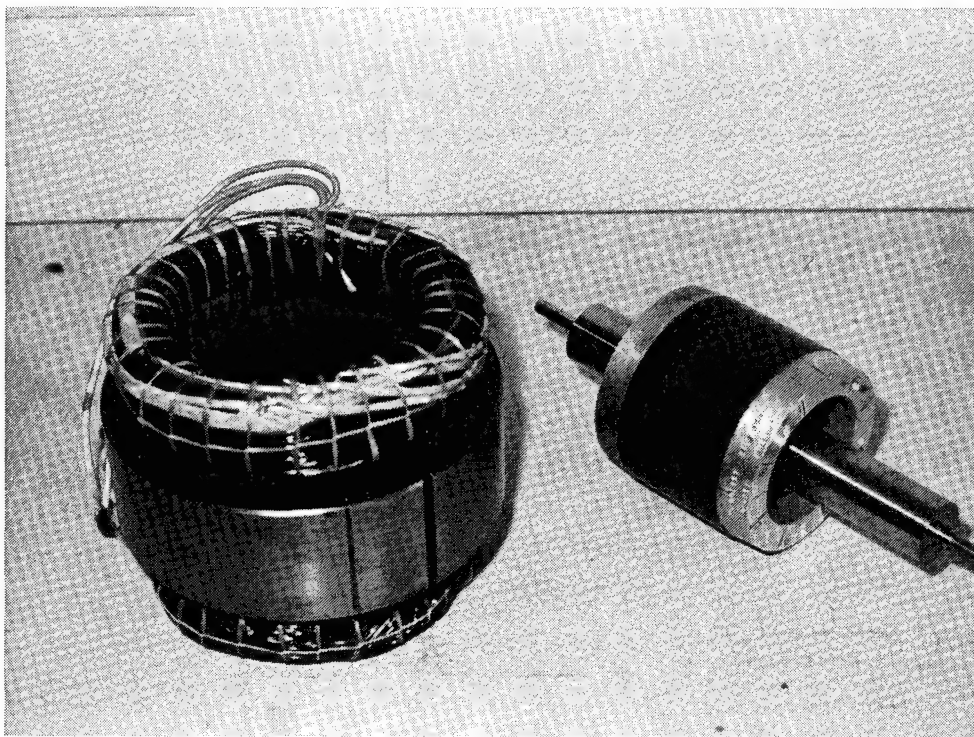
Fig. 46   Components of the induction motor/generator.
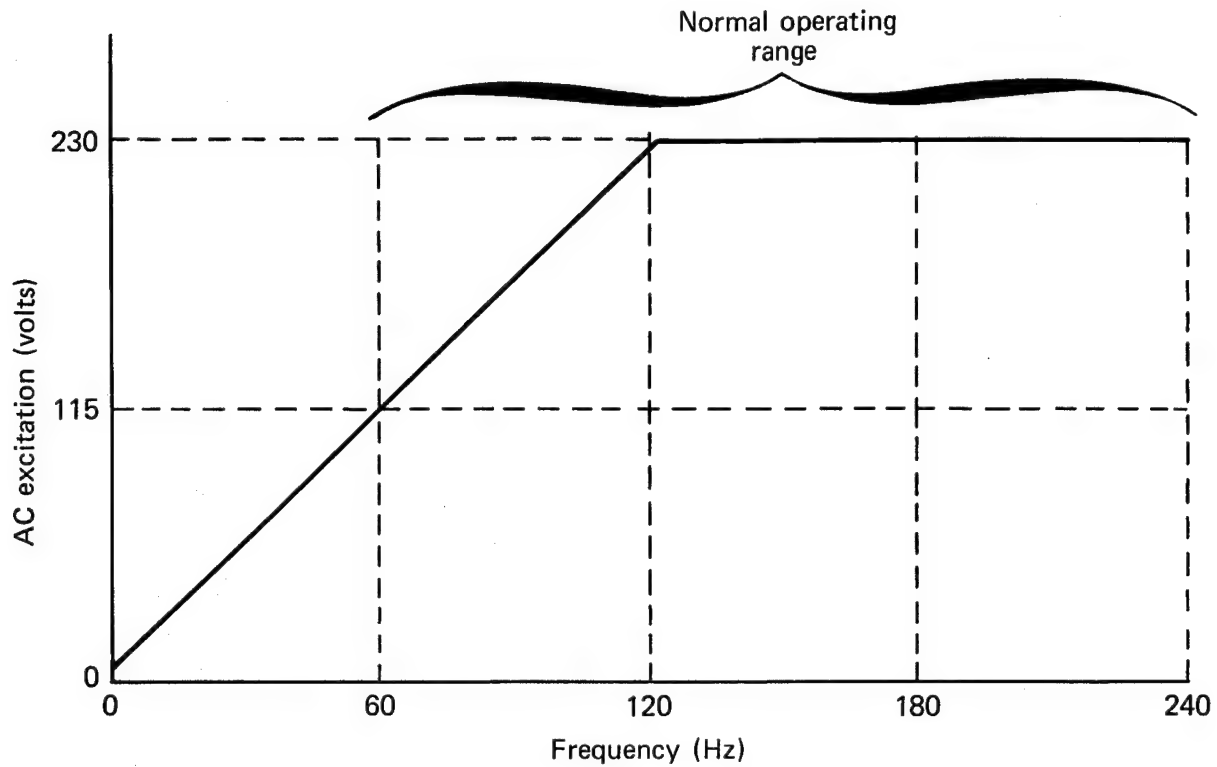
Fig. 47   Operating characteristics of the motor/generator.

Normally the minimum rotational speed of the flywheel is 3600 rpm, at which speed the flywheel energy content is down to 1/16th of the original storage level. Dynamic braking resistors are also included, to allow the rotating machinery to be safely and promptly slowed from any operational speed down to approximately 800 rpm, where an external DC source is applied to one phase of the motor to bring it to full stop.

Operation of ESS-1 allowed a number of electronic control problems to be solved quickly and allowed the flywheel suspension system, which utilizes only the two bearings required for the motor/ generator unit, to be demonstrated.

As indicated in Table 9, energy-storage system 2 (ESS-2) was intended to be the final demonstration system, and utilized the 1-kWh wound steel-wire flywheel and the magnetically relieved low-loss bearing system. In addition to the items indicated, ESS-2 was eventually equipped with a 2-in., 250-W oil diffusion pump further lowering housing pressure so as to permit aerodynamic losses to be minimized.

For ESS-2 using a 76-lb., 24-in. bare-wire flywheel, the energy stored is given by the relation:

$$E(Wh) = (3.9 \times 10^{-6})(rpm)^2 \tag{1}$$

so that 1 kWh is stored at about 16,000 rpm. The predicted limit for the rotor was 18,500 rpm or about 1.33 kWh, based on ultimate stress of the steel wire. However, because of limitations imposed by tooling and safety, speeds were limited to 14,400 rpm or 0.81 kWh.

ESS-2 was operated over more than 25 charge/discharge cycles, both for test and demonstration. During the test cycles, the charge and discharge energy was measured as a function of flywheel rpm. The efficiencies were computed from the equation:

$$\eta_{C,D} = \frac{E(rpm_2) - E(rpm_1)}{\displaystyle\int_{t_1}^{t_2} P\,dt} \tag{2}$$

where $E(rpm)$ represented the energy stored in the flywheel as computed from Eq. 1 and P is the power supplied or received from the flywheel over the time interval $(t_2 - t_1)$. The charge efficiencies, η_C, were found to be 50 ±5%, independent of flywheel speed. The discharge efficiencies varied linearly from 62% at 6000 rpm to 88% at 13,000 rpm. The value of η_D dropped rapidly below 6000 rpm to about 30% at 3600 rpm.

As noted earlier, the performance of the electrical machinery was compromised so that available equipment could be used; therefore, the measured efficiencies are not typical of values that could be obtained with equipment designed specifically for this application. It is believed that charge and discharge efficiencies on the order of 90% or better should be possible, and that this level should be used for system cost estimates.

The coasting losses of the rotating system were determined from changes in rotational speed measured as a function of time. The coasting losses include flywheel aerodynamic losses, bearing losses, and motor/generator coasting losses. The total coasting loss as a function of rotational speed is shown in Fig. 48. Although it was not possible to make independent measurements of the three loss types, it was possible to indicate the contribution of the bearings to the total coasting from the previous measurements described in detail in Section 6. The measured bearing loss is also shown in Fig. 48. A comparison of the bearing loss with the curve of total losses shows that the aerodynamic and motor coasting losses are orders of magnitude greater than the bearing losses.

Table 9

Characteristics of energy-storage system 2

Purpose:	1. Demonstrate satisfactory operation of a suspension system tailored to final flywheel.
	2. Demonstrate low-cost flywheel.
	3. Demonstrate low-loss bearings and one-drop-per-day oiling system.
	4. Evaluate system energy losses.
	5. Complete flywheel life-cycle tests.
Flywheel:	1000 Wh; 31,500 turns of steel wire forming the rim with pseudo-isotropic fiberglass epoxy hub; 76 lb.; 24-in. outside diameter.
Bearings:	Size 100H, 10 mm bore; unshielded; one-drop-per-day oiling.
Motor/generator and cooling:	Same as system 1.
Electronic controls:	Same as system 1.
Vacuum:	Less than 10^{-3} Torr (using 0.8 cfm fore pump and 2-in. oil diffusion pump). Sealing by elastomer "O" rings.

Of the total flywheel energy loss per hour, the coasting losses range from about 1.5% at the low end of the operating rotational speed range to about 12% at the high end. The aerodynamic losses relative to total flywheel energy should diminish as the size of the flywheel is increased to the full-size home storage unit because the losses are related to the flywheel surface, whereas the energy is related to flywheel weight, hence, volume. Nevertheless, the aerodynamic loss will still be a significant factor in flywheel energy storage systems until suitable means for reducing it are available. One solution may be to use a lighter gas (such as hydrogen) in the flywheel container but still at the same pressure (10^{-3} Torr).

It may be possible to run additional loss measurement tests in the future at a lower container pressure such as 10^{-4} Torr.
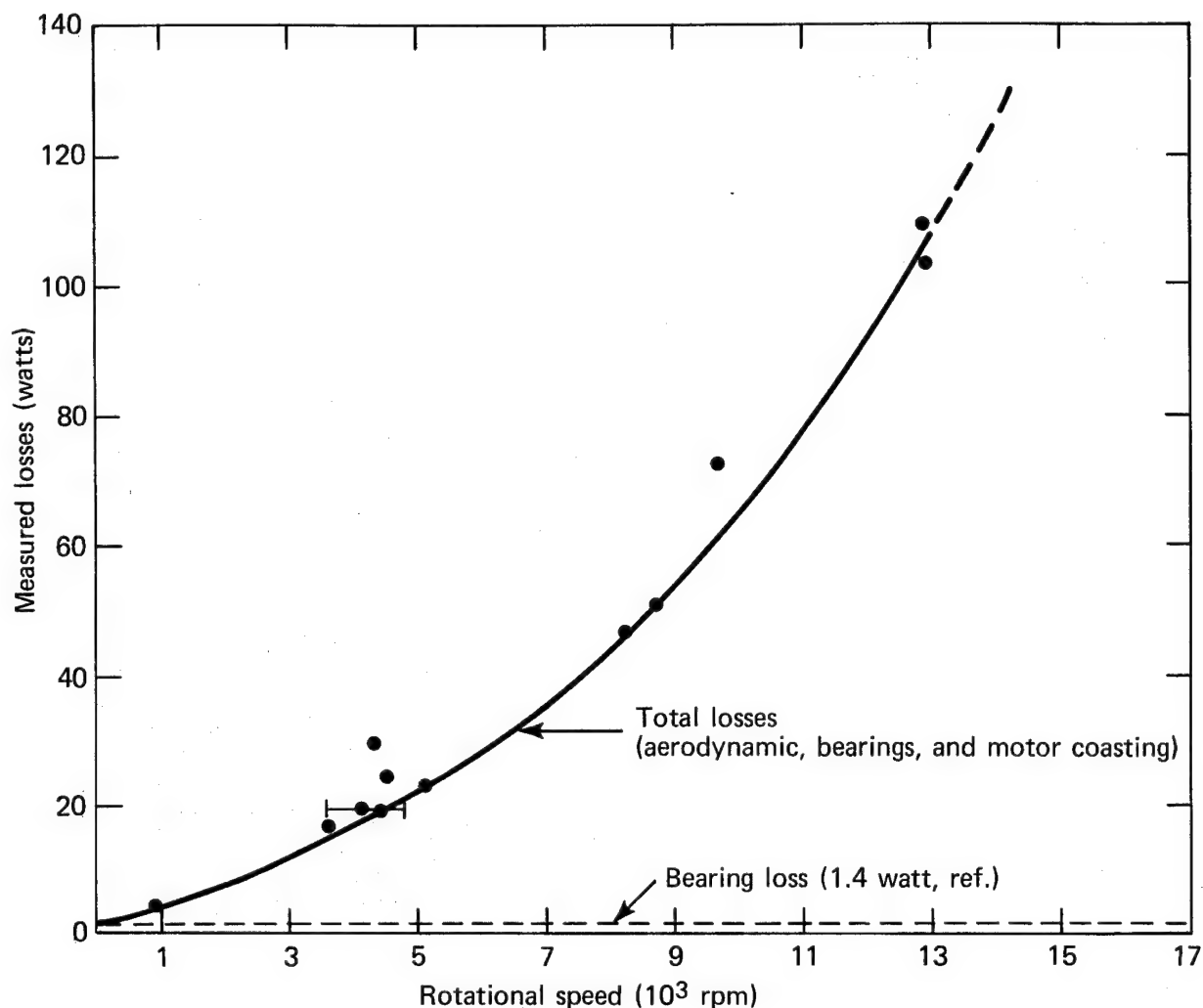
Fig. 48　Coasting losses in system 2; TAS III-3 flywheel; vacuum = 10^{-3} Torr.

The lower container pressure used in conjunction with the hydrogen
could reduce the aerodynamic losses by about two orders of magni-
tude.　However, since the increased vacuum pump losses at the
lower container pressure must be charged to the flywheel system,
it is not obvious that lowering the pressure would reduce the
overall losses.　Clearly, more work is required to optimize the
vacuum system.

The ESS-2 assembly is shown in Fig. 49, and its final test
installation in test cell 4 is shown in Fig. 50.

Fig. 49   Energy-storage system 2 with final flywheel.
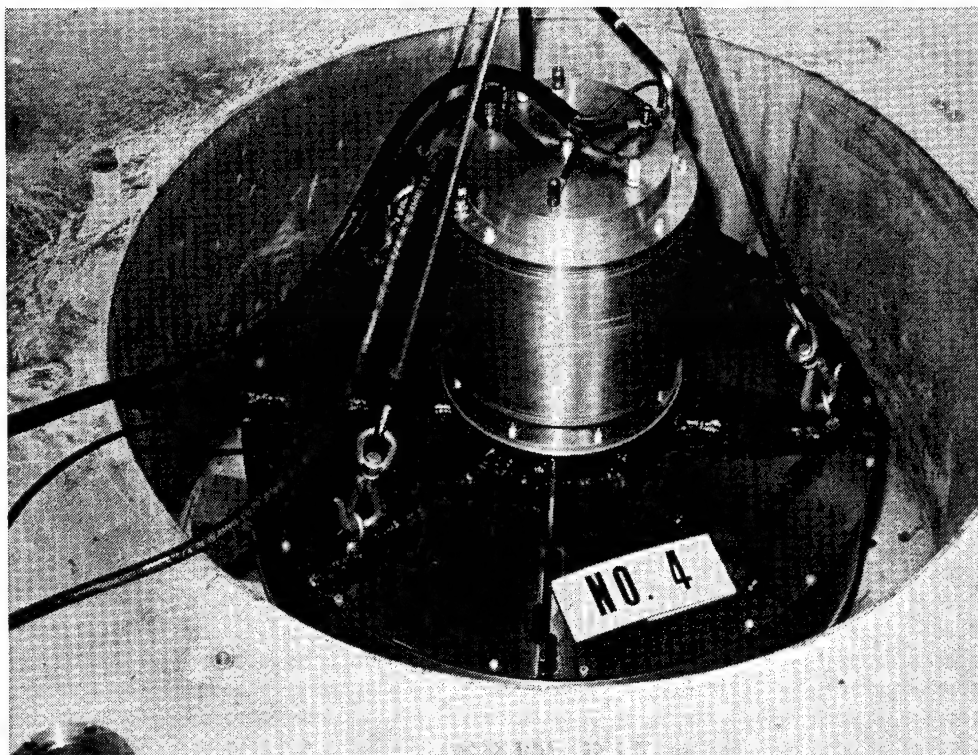
Fig. 50   Energy-storage system 2 in the test cell.

8. FLYWHEEL PROJECTIONS

In accordance with one of the stated objectives of the program, the final 1-kWh flywheel design was projected into a full-scale 30-kWh flywheel for a home storage system. The study included consideration of two separate flywheel configurations, one of them having a minimum-weight rotation speed, and the other a minimum overall size. The characteristics of the two full-scale flywheels are listed in Table 10. The type A configuration, having an outside

Table 10

Typical characteristics of 30-kWh flywheels

Parameter	Type A Configuration (minimum weight)	Type B Configuration (minimum size)
Outside diameter (in.)	36	32
Inside diameter (in.)	30 (83% O.D.)	22 (69% O.D.)
Axial length per segment (in.)	3.375	3.8
Total axial length (in.)	35	28
Number of segments	10	7
Weights (lb):		
Steel-wire rings	2080	2235
Fiberglass hub (3/8-in. thick)	19.6	10.5
Aluminum hub and spacer	2.2	2.2
Steel tie-bolt shaft	8.2	6.7
Total weight	2110	2254.4
Weight of one segment	211	322
Energy in steel-wire rings (kWh)	30.3	30.2
Flywheel cost factor	100%	107%
Container cost factor	100%	70%
Maximum rotational speed (rpm)	9600	10,800

diameter of 36 in., is essentially a scaled up version of the fly-
wheel developed in this program. The principal difference, other
than the scaled features, is that the type A configuration is com-
prised of 10 separate segments arranged as shown in Fig. 51. The
basic characteristics of the flywheel segment are illustrated in
Fig. 52, while the aluminum hub features are illustrated in Fig. 53.

The basic geometry is similar to the 1-kWh flywheel, with the
wound bare steel wire outer ring integrally attached to a fiber-
glass P-I disc serving as the intermediate hub that, in turn, has
an aluminum-hub attachment assembly. The two principal geometric
differences between the type A configuration and the 1-kWh fly-
wheel are the subcircular configuration (as recommended in the
previous flywheel discussion) and the aluminum hub with a large
hole in the center to permit tying the respective flywheel seg-
ments together into a single rotating unit.

The type B flywheel configuration (Table 10) has a smaller
outside diameter than the type A, and has an additional ring in-
board of the outside ring, making the inside-to-outside diameter
ratio 69% (compared to 83% in type A). The net result is a slight
reduction in the energy-to-weight ratio of the flywheel, hence a
slight increase in the fabrication cost. However, it will be
noted that the considerably smaller size of the type B configura-
tion results in a corresponding decrease in the container cost
factor — sufficient that the overall flywheel system cost would be
comparable for the two types.

The second flywheel design projection involved a brief summary
of the possible characteristics of the flywheel system sized for
utility-peaking operations. The basic hypothesis is that the in-
dividual flywheels for this system would not be appreciably larger
in dimensions than those that were tested in the present program.
By limiting the diameter to 48 in., compared with 24 in. for the
1-kWh flywheel, it is believed that the design projection can be
made with reasonable confidence. As with the 30-kWh flywheel, the
utility baseline unit is comprised of a small number of discrete
rings similar to the flywheels developed in the program in basic
configuration and construction. The general characteristics of
this flywheel are illustrated in Fig. 54, while the physical char-
acteristics are listed in Table 11.

After a number of iterations, it was concluded that a favor-
able packing configuration for the utility flywheel modules would
be to locate them in circular rings of five modules each, with a
common central bay for maintenance and repair and/or removal of
the flywheels. It was further reasoned that an economical arrange-
ment would be to store the units in silos comprised of eight floors,
for a total of 40 flywheel modules per silo. The general arrange-

Single ring configuration
10 segments

Double ring configuration
7 segments
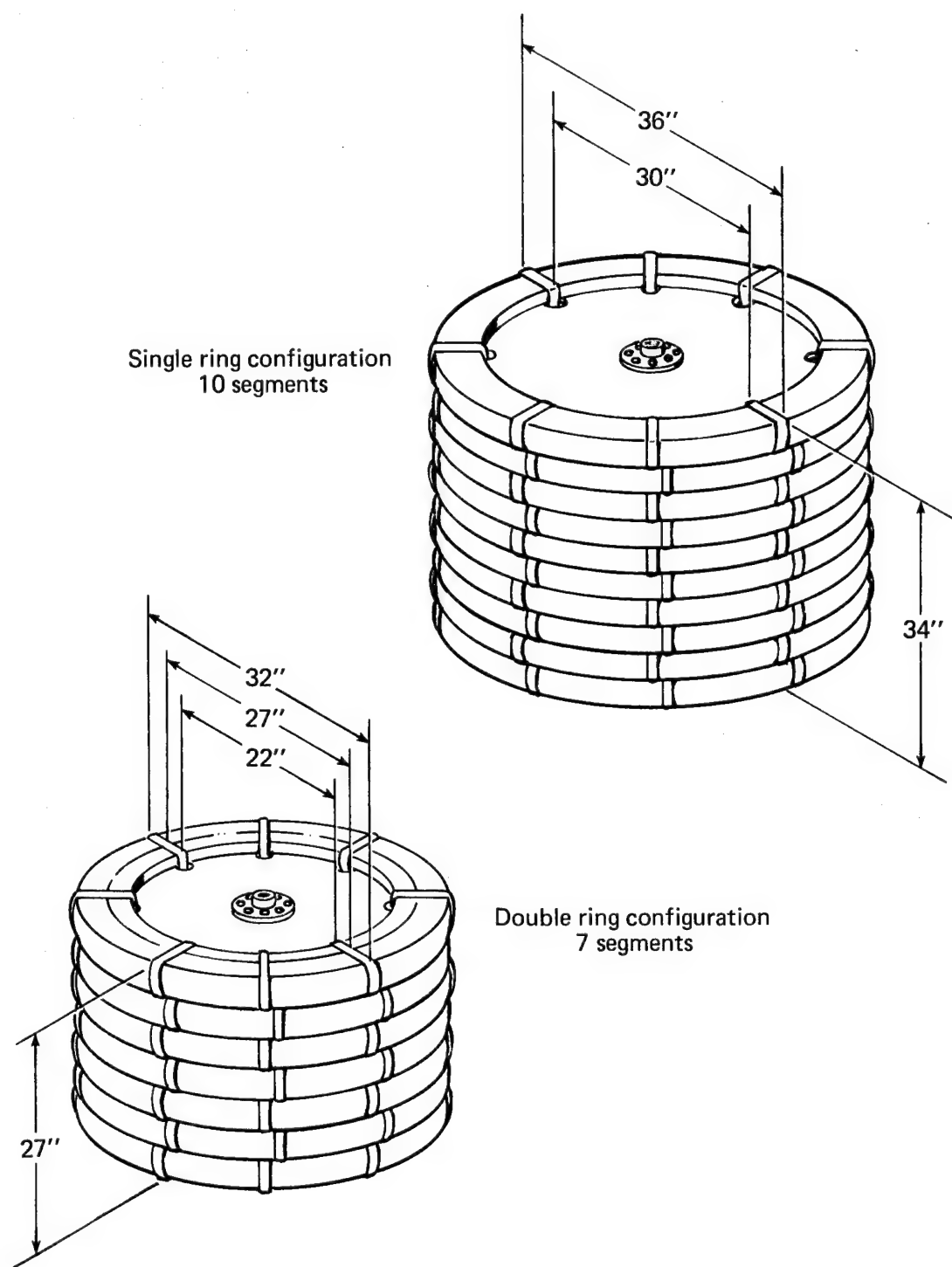
Fig. 51   General arrangement for the 30-kWh flywheel.
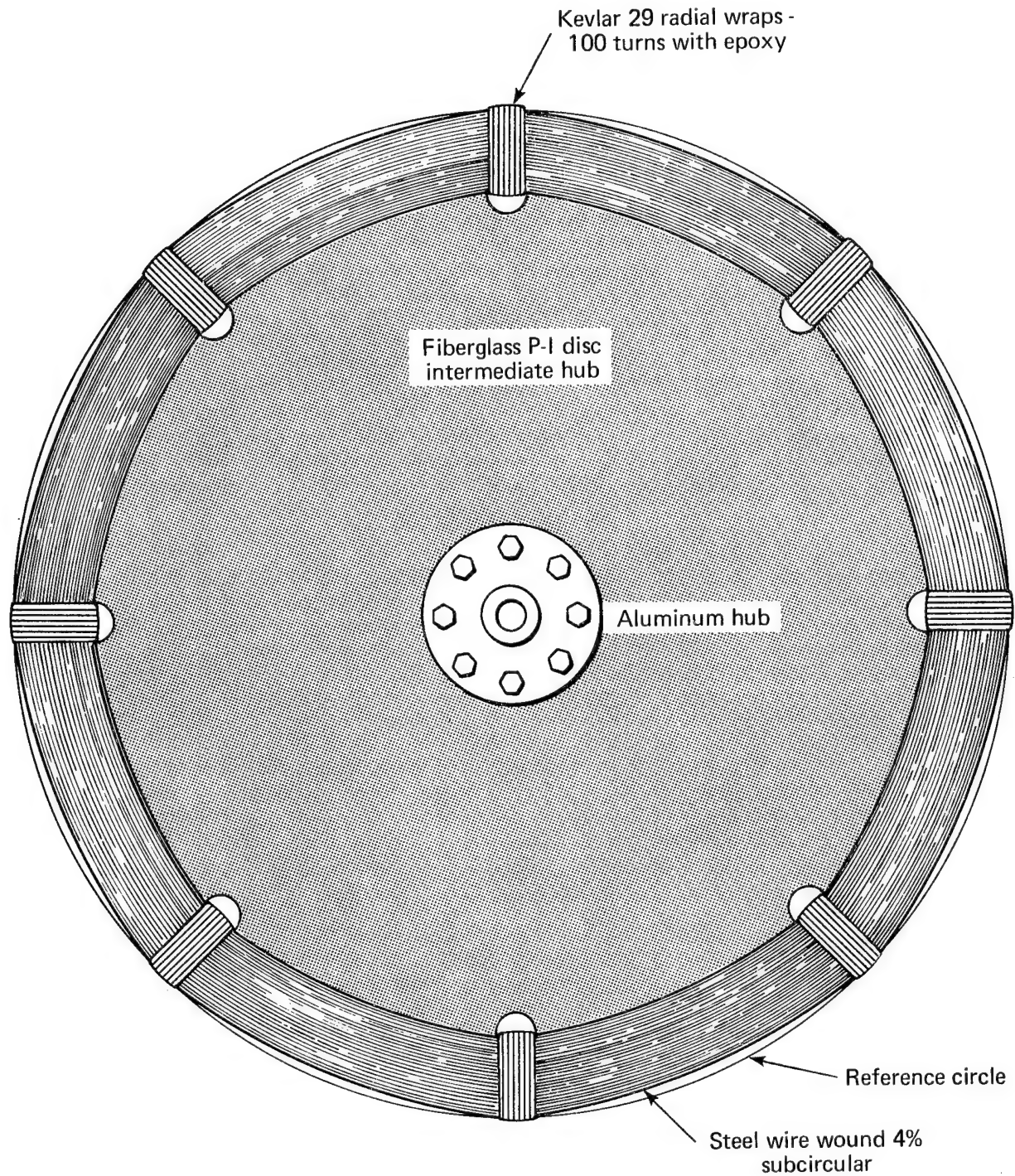
Fig. 52   Segment details of 30-kWh flywheel.

Steel hub

Intermediate
fiberglass hub

Steel backup plate

A–A
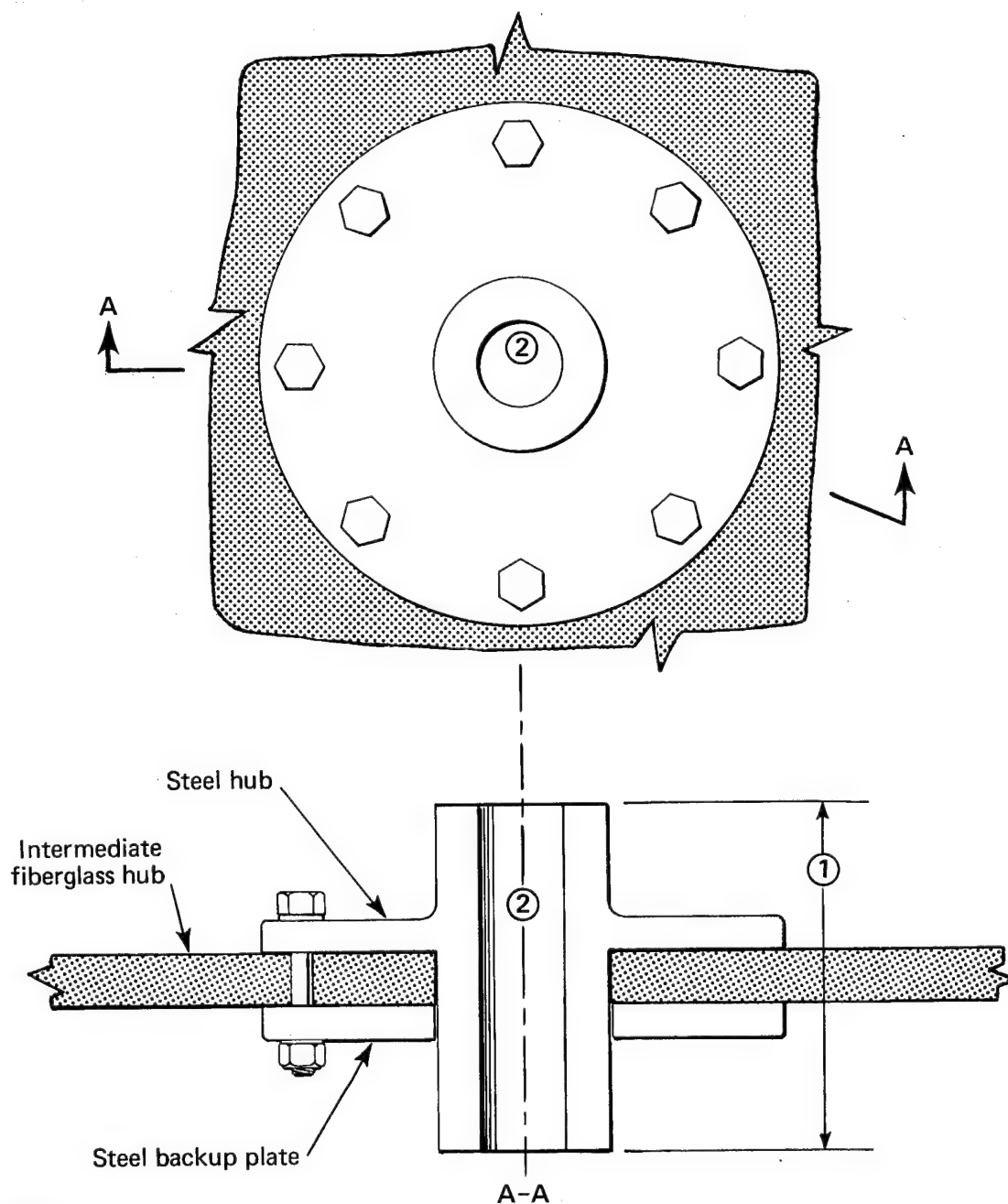
Notes:

① Dimension equals the flywheel axial thickness

② Center hole is for main rotor shaft, which is also
used to tie all segments together

Fig. 53   Hub details of the 30-kWh flywheel.

- Flywheel is 48" OD X 40" axial

- Weight is 9460 lb

- Energy stored is 113,516 Wh

- Four segments with
  inside wound radius
  = 56% of outside
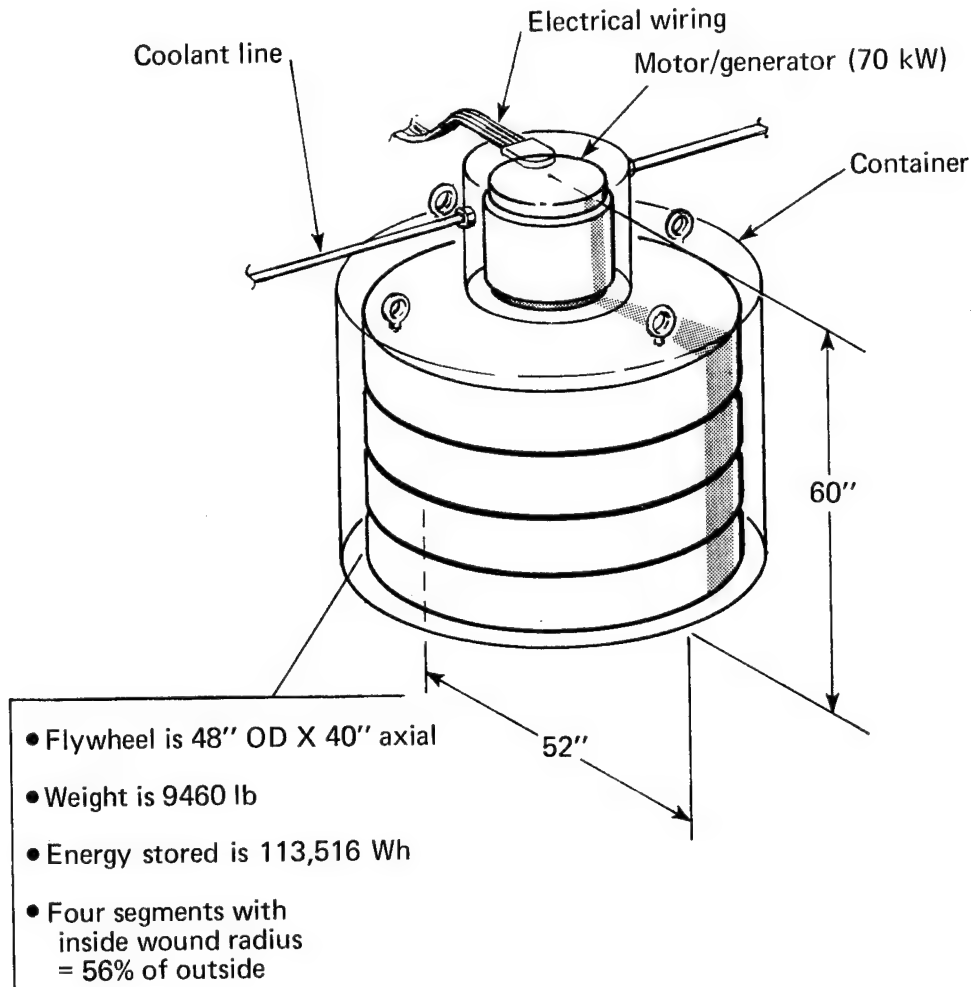
Fig. 54   113-kWh flywheel module.

ment of the flywheel silos is illustrated in Fig. 55. This ar-
rangement would allow an energy storage of 4.5 MWh per silo. Thus
the optimum arrangement for a 160-MWh energy-storage system would
be 36 silos located on a 6 x 6 grid in an underground location,
as illustrated in Fig. 55. The physical characteristics of such a
large scale system are listed in Table 12.

An attempt was made to estimate the cost of such a large scale
multi-flywheel array by looking at the various components and tasks
required in the preparation and assembly of the system. In addi-
tion to costs of the flywheel modules, estimates were made for the
necessary earth removal, concrete silo preparation, steel fram-
ing, etc. The total system cost thus obtained was then compared
to the cost of a single flywheel system, using similar methods.

- 78 -

Table 11

Characteristics of 113-kWh flywheel

1.	Outside diameter (in.)	48
2.	Inside diameter (in.)	28 (58% O.D.)
3.	Axial length of each segment (in.)	10
4.	Number of segments	4
5.	Total axial length (in.)	40
6.	Energy in wound rings (Wh)	113, 516
7.	Weight of wound rings (1b)	9460
8.	Maximum design rotational speed (rpm)	7200
9.	Material	Steel wire
10.	Energy density (Wh/lb)	12

Table 12

General characteristics of 160-MWh flywheel array

1.	Flywheel characteristics	see Table 10
2.	Number of flywheels per floor	5
3.	Number of floors per silo	8
4.	Number of silos in array	36
5.	Number of flywheels per array (160 MWh)	1440
6.	Installed area (including 8-ft. road matrix)	0.5 acre
7.	Energy per square foot of installed area	≈8 kWh
8.	Energy per square foot of silo area	22.6 kWh

Flywheel
module

Coolant &
electrical
connections

16'

7-ft dia. service area
at center of silo

36 silos
1/2 acre including
roadways

2'

Total flywheel array

1440 flywheels
160 MWh
100 MW peak
Est. cost = $154.00/kWh
for 30-year life cycle

48'

- Five flywheels per floor
- 8 Floors per silo
- 4.54 MWh per silo
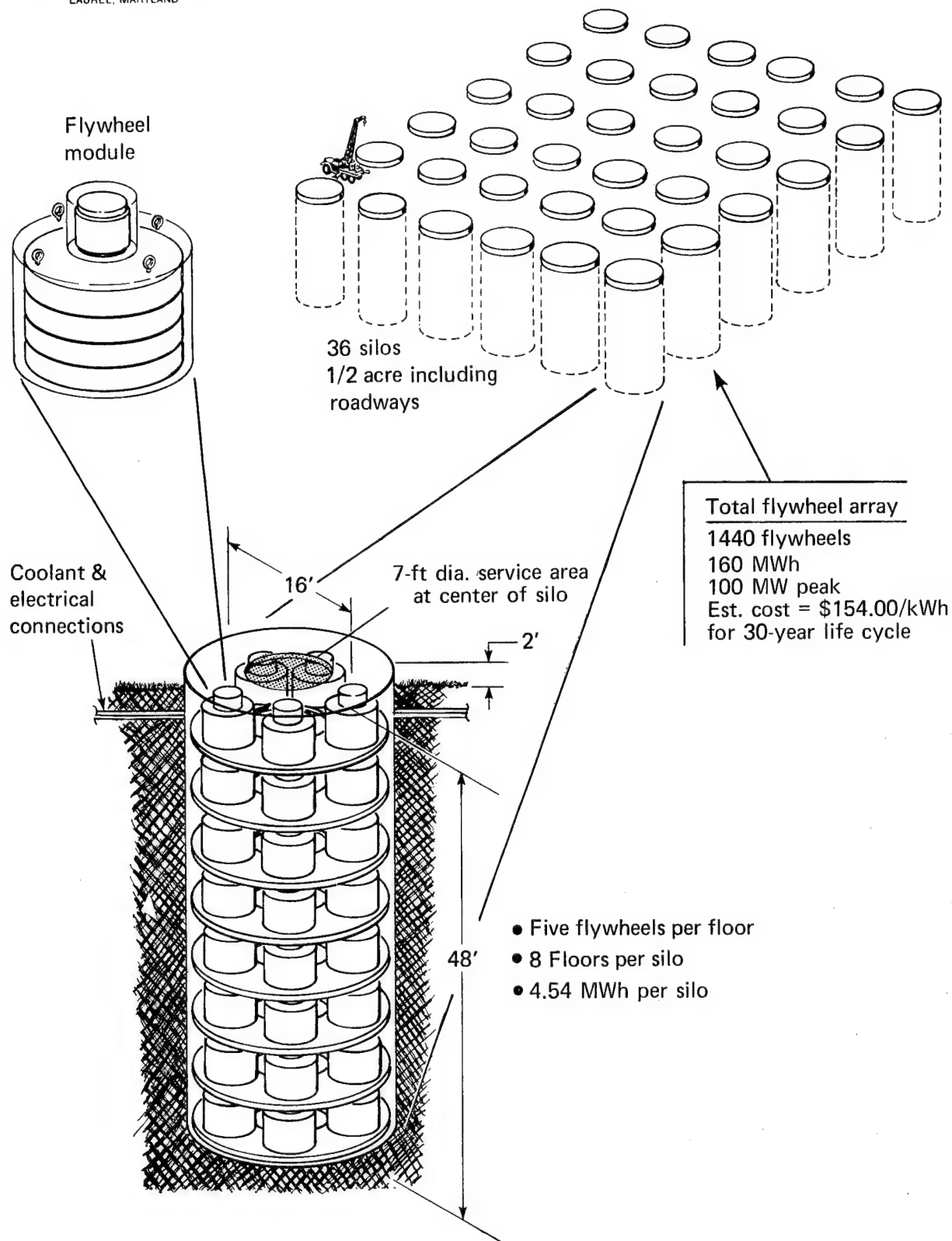
Fig. 55   Large-scale, modular flywheel array (160 MWh, 100 MW).

The apparent result from this exercise was that the cost of
the single unit system may be about 27% less than the apparent cost
of the large scale system with multiple flywheels. However, it is
important to note that the gross difference involved was probably
several times less than the estimated development costs for the
large flywheel systems. In addition, there are significant advan-
tages to the system comprised of a large number of small flywheels.
First, it is believed that the technology for building the small
flywheel system has already been demonstrated. Secondly, the re-
liability of the multi-flywheel system can be orders of magnitude
greater than the reliability with a single system (or one having
a small number of flywheels) because the failure of one flywheel
represents only 0.07% of the total system. Also, the failure of
several modules in the system would still not change the output
voltage or frequency because all of the generators in the system
would be operating at the same voltage and frequency.

9. CONCLUSIONS AND RECOMMENDATIONS

The following conclusions have been drawn from the program:

1. Although a production flywheel cost of $50/kWh is marginal with the materials used in this program, it appears that there are several materials that could be available in the near future, that would permit achieving this goal. On this basis, it is believed that the program objective of demonstrating the feasibility of a $50/kWh flywheel has been satisfactorily achieved.

2. The bare-filament steel-wire flywheel configuration has exhibited good effeciency of material use and low fabrication cost, and permits the use of a variety of configurations of low-cost materials (such as filaments, wires, tapes and flat strips). Therefore this configuration is believed to be one of the best available for the low-cost application.

3. Load-relieved mechanical bearings look very promising for the low-cost, long-life stationary flywheel system and other possible applications. Losses for the load-relieved system may be quite competitive with magnetic suspension. However, additional work will be required to validate the predicted long-life capability.

4. In general, the feasibility of home energy storage in a flywheel system appears to have been established. However, additional tests are needed to validate the predictions of possible improved electrical efficiency and reduced aerodynamic losses.

5. The feasibility of using an electronically controlled variable speed motor/generator was substantiated, in part, by its intrinsic simplicity and the availability of components. It is possible that a system utilizing a constant speed motor/generator controlled by a variable speed transmission may be economically competitive with the present variable-speed system.

The results of the work accomplished in the program suggest that there should be additional work in several areas, as defined in the following recommendations:

1. The success of the bare-filament steel-wire flywheel configuration appears to warrant initiating an immediate program to develop full-scale flywheels for the home storage application.

- 83 -

2. Although the feasibility of the low-cost flywheel system
    (flywheel, suspension, bearings, etc.) appears to have
    been established, the feasibility of a complete low-cost
    energy-storage system remains to be established. As
    stated in the foregoing, additional work is required to
    optimize the cost and operating efficiency of the electri-
    cal and electronic equipment. A program addressing these
    problems appears to be warranted.

3. In-depth studies should be conducted to compare the life-
    time cost-effectiveness of the variable-speed and constant-
    speed motor/generator systems.

4. The present and projected capabilities for Metglas amor-
    phous metal ribbon make this new material expecially at-
    tractive for future flywheel energy storage systems that
    require moderately low cost, low weight, and low volume
    for vehicular as well as stationary applications. Con-
    tinued research and development on full-scale Metglas rib-
    bon flywheels is recommended.

5. The aerodynamic losses are the predominant component of
    the total coasting losses of the flywheel system. Means
    for reducing these losses should be investigated, in-
    cluding:

    a. Refinement of flywheel aerodynamic surface
        shape,

    b. Efficient means for reducing container pressure
        below 10^{-3} Torr, and

    c. Use of container gas having lower density and
        viscosity.

6. A detailed analysis of the large-array utility-size
    flywheel system should be conducted and, if warranted,
    should include a hardware demonstration of at least one
    flywheel system module.

10. SUMMARY OF SUBCONTRACT WORK

There are three modest subcontracts in support of this program. The first was issued to the Jobmaster Corporation of Randallstown, Maryland, as reported in Section 6 and described in Ref. 14. The principal output of this contract was the passive magnet-bearing load-relief unit used in the APL flywheel suspension system. The work under this subcontract involved detailed studies in the areas of performance and availability of magnetic materials and magnetic circuits. The work also included detail designs for two different units, as well as fabrication and testing of the units. Studies were also made of the estimated production costs for the various configurations studied.

The second subcontract was issued to the University of Minnesota, as indicated in Section 3, and is reported in detail in Ref. 6. This work included extensive analysis and testing of wood and wood products in terms of strength versus a number of variables, such as moisture content, vacuum, duration of load, orientation of fibers, etc. It also involved discussions of state-of-the-art processes at a number of plywood and paper products mills in Wisconsin and Minnesota. The studies included the subjects of wood bonding techniques and veneering processes, as well as detailed review of the paper industry and its various processes.

Extensive references on wood and wood products were searched in regard to structural behavior, and especially in regard to factors affecting the cost of these products in relation to the possible flywheel applications. These results are catalogued in detail in Ref. 6.

The third subcontract was awarded to the Lord Corporation of Erie, Pennsylvania. As in the previous APL flywheel program (Ref. 8), the Lord Corporation contributed a valuable and convenient service by providing various energy-absorbing elastomeric components for evaluating bonded flywheel-hub attachments, laminated P-I disc structures, and flywheel suspension-system components. After the Lord Corporation had demonstrated the importance of these elastomeric components in providing resonance-free flywheel suspension, it was commissioned to perform extensive life-cycle testing of representative elastomeric components to demonstrate their possible applicability to real flywheel systems (vs. APL experimental systems). These tests, which are described in detail in Ref. 15, involved the design and fabrication of special equipment capable of automatic testing of the components to 10^9 stress cycles, and beyond. These important tests, which were conducted over a period of several months, established the basic applicability of elastomeric materials to flywheel applications, including possible vehicular applications, where the number of stress

cycles may be 10^4 times greater than in stationary flywheel energy-storage systems.

Appendix A

FLYWHEEL FABRICATION LOG

Thirty-two flywheels were fabricated at APL during this program. Detailed descriptions of each one are contained in the daily log books at the Flywheel Testing Laboratory. The following flywheel designation code was set up to permit easy identification of the flywheel configuration, material, hub type, etc.:

Flywheel Identification Code

Number in series		Number of tests of
(1 to 10)		same flywheel

— 4-1S2 —

Flywheel hub type   └─ Rim or flywheel material

```
3 = spoked hub, 20 in. dia.        S = steel wire
4 = 12-in. dia. plywood,           M = Metglas ribbon
    3% subcircular                 G = vinyl-glass
5 = 12-in. dia. Kevlar, spoked    SR = rubber-bonded steel wire
TAS = 24-in. full-scale flywheel  PI = pseudo-isotropic disc
    (Type Approval System)
```
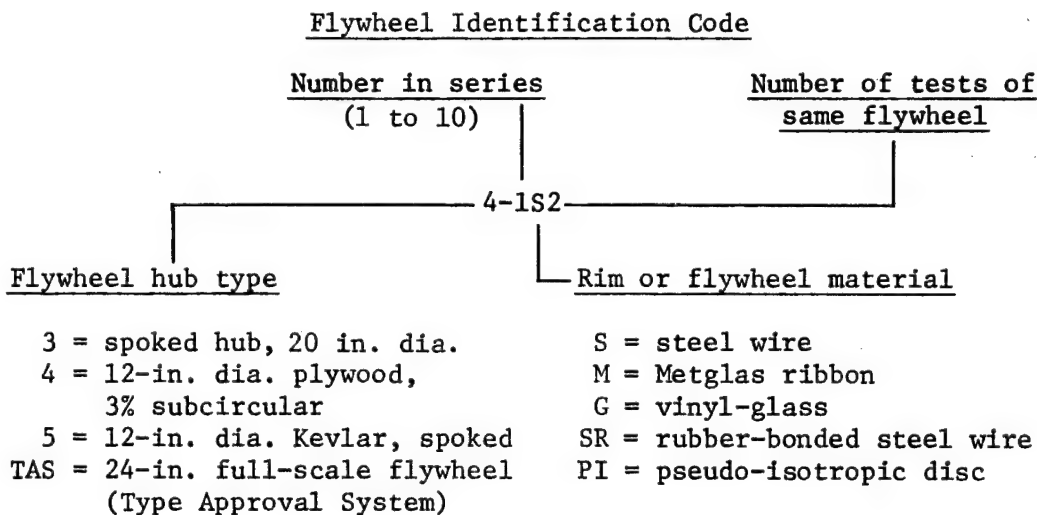
The following list uses this code and provides a brief summary of the characteristics of the flywheels that were made during the program. It should be noted that the dates are the date of fabrication. The test dates are covered in Appendix B.

Date	Identification	Remarks
Mar 9, 1978	4-1S	Not spun
Mar 10, 1978	4-2S	Not spun
Mar 15, 1978	4-2G	Not spun
Mar 22, 1978	4-3G	3 spin tests
Mar 22, 1978	4-3S	4 spin tests
May 8, 1978	4-4S	Spun to destruction
May 15, 1978	4-5S	Spun to 27,000 rpm and retired
May 23, 1978	4-6S	Spun to destruction
May 24, 1978	4-7S	Spun to destruction
Jun 8, 1978	5-1S	Spun to destruction
Jun 12, 1978	5-2S	Spun to destruction
Jun 15, 1978	4-8S	Shaft whip
Jun 20, 1978	5-3S	2 tests, destruct
Jun 23, 1978	4-9S	3 tests, undamaged after 30,140 rpm

Date	Identification	Remarks
Jul 20, 1978	4-4G	Bond failure, rewound
Aug 3, 1978	4-4G2	Bond failure
Sep 7, 1978	4-1M	Hub bond failure, destruct
Sep 18, 1978	4-5G	Hub bond failure, destruct
Oct 23, 1978	4-10S	85 pound rotor, did not spin
Nov 9, 1978	4-3M	Spun to destruction
Nov 11, 1978	4-6G	Spun to destruction
Nov 27, 1978	4-4M	Spun to destruction
Nov 28, 1978	4-7G	Spun to destruction
Nov 29, 1978	4-8G	Spun to destruction
Mar 27, 1979	TAS_2-1(S)*	Did not spin, fabrication problems
Apr 3, 1979	TAS_2-2(S)	Did not spin, fabrication problems
Apr 5, 1979	TAS_2-A(S)	8 pounds, spun to destruction
Apr 11, 1979	TAS_3-B(S)	18 pounds, did not spin, bond problems
Apr 17, 1979	TAS_3-B(S)	18 pounds, did not spin, winding problems
May 9, 1979	TAS-III-1S	Final tooling, hub failure, destruct
May 11, 1979	TAS-III-2S	1/2 inch axial thickness, winding check
May 22, 1979	TAS-III-3S	Final flywheel, life cycle tests

- continuing -

* Subscripts refer to modifications to basic TAS design

Appendix B

FLYWHEEL AND MATERIALS TEST LOG

Sixty-two spin tests of flywheels and materials were conducted as follows:

Vinyl-glass flywheel tests	10
Metglas ribbon flywheel tests	4
Steel wire flywheel tests	20
Suspension diagnostic spin tests	7
Vendor flywheel spin tests	4
Wood disc spin tests	2
Materials spin tests	15

The following list briefly summarizes the results of each test. The flywheel identification code is the same as that described in Appendix A. Details of each test are contained in the respective log books on file at the Flywheel Testing Laboratory.

Test date	Identification	Abbreviated Test Results
Sep 28, 1977	Vinyl-glass, 9 3/4-in. dia.	Shaft broke @ 28,200 rpm
Oct 11, 1977	Pirelli 0.38mm wire	Strand broke @ 22,170 rpm
Oct 12, 1977	Pirelli 0.38mm wire	Strand broke @ 20,040 rpm
Oct 12, 1977	Pirelli 0.38mm wire	Strand broke @ 21,710 rpm
Oct 12, 1977	Pirelli 0.38mm wire	Strand broke @ 21,350 rpm
Mar 27, 1978	4-3S flywheel 13-in. dia.	Shaft broke @ 710 rpm
Apr 10, 1978	4-3S flywheel	Bearing mount broke @ 11,750 rpm
Apr 13, 1978	4-3S flywheel	Shaft bent @ 13,200 rpm
Apr 14, 1978	4-3S flywheel	Hub broke @ 16,930
Apr 28, 1978	Pull test CPE	Ribbon broke @ 38.23 pounds
May 12, 1978	4-4S flywheel	Hub shattered @ 17,610 rpm
May 15, 1978	Pull test - Pirelli wire	Broke @ 56.84 lb (321,648 psi @ 0.38mm)
May 22, 1978	4-5S flywheel	Wheel survived 27,050 rpm
May 23, 1978	Pull test, std. wire	Broke @ 41.6 lb (367,824 psi @ 0.012-in. dia.)
Jun 1, 1978	4-6S flywheel	Hub shattered @ 23,230 rpm
Jun 6, 1978	4-7S flywheel	High speed photos at failure @ 27,040
Jun 12, 1978	5-1S	Spokes broke @ 16,650 rpm
Jun 14, 1978	5-2S	Spokes broke @ 18,400 rpm
Jun 15, 1978	L^3 simulator run	Accel. to 8660 rpm, OK
Jun 20, 1978	4-8S	Shaft whip @ $\approx$21,000 rpm
Jun 22, 1978	Suspension test 1	17g vibration @ 19,920 rpm
Jun 22, 1978	Suspension test 2	19g vibration @ 19,409 rpm

Test date	Identification	Abbreviated Test Results
Jun 22, 1978	Suspension test 3	18g vibration @ 19,244 to 34,330 rpm
Jun 26, 1978	Suspension test 4	12g vibration @ 18,690 rpm
Jun 26, 1978	Suspension test 5	5g @ 17,000-20,000 rpm; 7 g @ 37,850 rpm
Jun 26, 1978	Suspension test 6	6g @ 15-19,000 rpm; whip failure @ 43,170 rpm
Jun 29, 1978	Suspension test 7	15g @ 17-26,000 rpm; reached 51,370 rpm
Jul 3, 1978	4-9S flywheel	Braked to stop from 21,830 rpm
Jul 3, 1978	4-9S flywheel	Braked to stop from 21,020 rpm
Jul 3, 1978	4-9S flywheel	Lost radials @ 30,140 rpm - flywheel OK
Jul 5, 1978	5-3S flywheel	10-lb. Lord mount failure @ 12,000 rpm
Jul 5, 1978	5-3S flywheel	Solid mount, reached 29,531 rpm
Jul 17, 1978	L^3 simulator	Critical speed check to 6800 rpm, OK
Jul 18, 1978	L^3 flywheel	Failed @ 36,000 rpm, test OK
Aug 16, 1978	30-in. Metglas ribbon	Broke @ 16,680 rpm (230,966 psi)
Aug 16, 1978	30-in. Metglas ribbon	Broke @ 17,700 rpm (260,077 psi)
Aug 22, 1978	10-in. dia. tapered bird disc	Smooth run, broke @ 32,120 rpm
Aug 23, 1978	4-1SR-Pirelli FW	Flung off rubber from flywheel @ 19,760 rpm
Aug 24, 1978	4-4G flywheel	Tapered wood hub separated @ 16,490 rpm
Sep 9, 1978	4-1M flywheel	Hub epoxy failure @ 10,900 rpm
Sep 21, 1978	4-5G flywheel	Hub epoxy failure @ 10,900 rpm
Sep 22, 1978	4-5G flywheel	Bolted hub, glass unwound @ 22,900 rpm
Sep 22, 1978	Aluminum slab FW	Up to 6000 rpm, trouble shooting system 1
Oct 11, 1978	4-2M flywheel	Metglas ribbon unwound partly @ 16,820 rpm
Oct 17, 1978	4-3G flywheel	Lost bearing housing @ 5700 rpm
Nov 10, 1978	4-3G2 flywheel	Glass unwound @ 25,220 rpm

Test date	Identification	Abbreviated Test Results
Nov 15, 1978	4-3M flywheel	Partial failure @ 19,820 rpm
Nov 16, 1978	4-3G3 flywheel	23g vibration, broke shaft @ 19,275 rpm
Nov 22, 1978	4-6G flywheel	Wood hub burst @ 23,830 rpm
Dec 4, 1978	4-8G extra wide	Smooth, clean burst @ 28,855 rpm
Jan 8, 1978	4-4M	Partial failure @ 23,100 rpm
Jan 11, 1978	Tapered ply disc 16-in. dia.	Clean burst @ 22,100 rpm
Jan 19, 1978	4-7g flywheel	Clean break @ 26,515 rpm
Feb 26, 1979	Vinyl-glass pull tests	6 tests averaged 40.25 lb @ break
Mar 5, 1979	Vinyl-glass density test	50/50 v/g = 0.0452 lb/in^3
Mar 5, 1979	Vinyl-glass density test	Different type = 0.0463 lb/in^3
Mar 6, 1979	Vinyl-glass density test	Wound rim = 0.0557 lb/in^3
Apr 17, 1979	TAS_2-A	8 lb, 17.5-in. dia., broke @ 16 210 rpm
Apr 19, 1979	24" P-I disc	Hi speed TV test, shaft whip @ 22,670 rpm
May 14, 1979	TAS III-1S	24 lb, wood hub failed @ 15,010 rpm
May 17, 1979	4-5S demo run	DOE sponsor dem., terminated @ 21,000 rpm
Jul 1979	TAS III-3S	Final flywheel, many tests @ design conditions – still continuing

REFERENCES

1. D. W. Rabenhorst, "Flywheel Testing Laboratory of The Johns Hopkins University Applied Physics Laboratory," APL/JHU Report, 24 Apr 1979.

2. N. V. Gulia, <u>Inertial Energy Accumulators</u>, Voronezh University Press, Published in Russia, 1973.

3. J. R. Strife and K. M. Prewo, "Evaluation of Amorphous Ribbon Reinforced Resin Matrix Composites," R79-914389-6, United Technologies Research Center, Second Quarterly Report, Contract F33615-78-C-5063, 15 Feb 1979.

4. W. C. Emmens and A. L. Mulder, "Non-Conventional Materials in Flywheel Technology," State University of Utrecht, Department of Technical Physics, Sorbonnelaan 4, Utrecht 2506, The Netherlands.

5. D. W. Rabenhorst, "The Applicability of Wood Technology to Kinetic Energy Storage," <u>APL Tech. Dig.</u>, Vol. 11, No. 5, May–Jun 1972.

6. A. G. Erdman and D. L. Hagen, "Costs for Energy Stored in Cellulose Rotors," University of Minnesota, Final Report prepared for APL/JHU under Contract No. APL 600854, May 1979.

7. D. W. Rabenhorst, et al., "Pseudo-isotropic Filament Disk Structures," U.S. Patent #3,788,162, 29 Jan 1974.

8. D. W. Rabenhorst and T. R. Small, "Composite Flywheel Development Program: Final Report," APL/JHU SDO-4616A, Apr 1977.

9. R. C. Clerk, "The Utilization of Flywheel Energy," ASME Paper No. 711A, Jun 1963.

10. D. Raskin, "Energy Storage Propulsion System for Rapid Transit Cars: Test Results and System Evaluation," UMTA-NY-06-0006-78-1, Final Report, Metropolitan Transportation Authority, New York, NY, Oct 1978.

11. "Barden Precision Miniature and Instrument Ball Bearings," Catalogue No. M6, The Barden Corp., Danbury, Connecticut.

12. J. E. Notti, A. Cormack III, and W. C. Schmill, "Integrated Power/Attitude Control System (IPACS) Study, Vol. 1, Feasibility Studies," NASA CR-2383, Apr 1974.

13. D. B. Eisenhaure and E. P. Kingsbury, "Final Report on the Development of an Advanced Flywheel Bearing Performance Model," SAND79-7003, Sandia Laboratories, Mar 1979.

14. C. A. Castronovo, "Magnetic Thrust Bearings in Low Cost Flywheel Systems," Report on APL/JHU Subcontract #600820, Jobmaster Corporation, Applied Magnetics Laboratory, 14 Nov 1978.

15. A. J. Hannibal, "Flywheel Engineering Study for Johns Hopkins University - APL," K/TR79-011, Lord Corporation, 7 May 1979.

INITIAL DISTRIBUTION EXTERNAL TO THE APPLIED PHYSICS LABORATORY

Department of Energy
600 E Street, N.W.
Washington, DC 20545
Attn: Dr. Eberhart Reimers,
    Program Manager   50

U.S. Department of Energy
Operations, Division of Pro-
  curement
400 First Street, N.W.,
Room 208
Washington, DC 20545
Attn: Contracting Officer
    Ms. Eula L. Irick   1

Patent Office
Assistant General Counsel for
  Patents
Office of General Counsel
Department of Energy
Washington, DC 20545   1

U.S. Department of Energy
Washington, DC 20545
Attn: Mr. Douglas Harvey   1

University of Wisconsin
1513 University Avenue
Madison, WI 53706
Attn: Prof. Norman Beachley   1

U.S. Dept. of Transportation
2100 Second Street, S.W.
Washington, DC 20590
Attn: Mr. James Campbell
    Program Manager, Energy
    Propulsion Technician   1

Sandia Laboratories
Division 5743
P. O. Box 5800
Albuquerque, NM 87185
Attn: Mr. Henry M. Dodd
    Division Supervisor   1

Rocketdyne Division
Rockwell International
6633 Canoga Avenue
Canoga Park, CA 91304
Attn: Dr. Donald E. Davis
    Program Manager   1

Charles Stark Draper Lab.
555 Technology Square
Cambridge, MA 02139
Attn: Mr. David Eisenhaure
    Mail Station 37   1

University of Minnesota
Mechanical Engineering Dept.
Minneapolis, MN 55455
Attn: Prof. Arthur G. Erdman   1

University of Wisconsin
Department of Electrical and
  Computer Engineering
Madison, WI 53706
Attn: Prof. Andrew Frank   1

Kelsey Hayes
2500 Green Road
Ann Arbor, MI 48105
Attn: Mr. Dick Glaser   1

University of Minneosta
111 Church Street, S.E.
Minneapolis, MN 55455
Attn: Mr. David Hagen
    Research Associate   1

Kelsey Hayes
38481 Hurron River Drive
Romulus, MI 48174
Attn: Mr. Edward Hayes, V.P.   1

Lawrence Livermore Laboratory
P. O. Box 808, L-338
Livermore, CA 94550
Attn: Dr. S. V. Kulkarni   1

General Electric Co.
1 River Road
Schenectady, NY 12345
Attn: Mr. E. L. Lustenader
       Manager
	1	William M. Brobeck & Associates
		1235 10th Street
		Berkeley, CA 94710
		Attn: Mr. Francis C. Younger
		       President
			1

Kinergy Research & Development P. O. Box 1128 Wake Forest, NC 27587 Attn: Mr. H. K. Marshall President	1	University of Oklahoma School of AMNE, 865 Asp Avenue Norman, OK 73019 Attn: Dr. Charles W. Bert	1
Massachusetts Inst. of Tech. Lincoln Laboratory P. O. Box 73 Lexington, MA 02173 Attn: Dr. Alan Millner	1	Brunswick Corp. 4300 Industrial Ave. Lincoln, NB 68504 Attn: Mr. William E. Dick	1
Garrett AiResearch Corp. 2525 West 190th Street Torrance, CA 90505 Attn: Mr. Theodore W. Place Project Engineer	1	Hercules, Inc. P. O. Box 210 Cumberland, MD 21502 Attn: Mr. P. Ward Hill	1
Garrett AiResearch Corp. 2525 West 190th Street Torrance, CA 90505 Attn: Mr. Arthur E. Raynard Sr. Project Engineer	1	Lord Kinematics 1635 W. 12th St. Erie, PA 16512 Attn: Mr. Dennis P. McGuire	1
Lawrence Livermore Laboratory P. O. Box 808 L-338 Livermore, CA 94550 Attn: Mr. J. R. Rinde	1	Brunswick Corp. 4300 Industrial Avenue Lincoln, NB 68504 Attn: Mr. Norman L. Newhouse	1
Garrett AiResearch Corp. 2525 West 190th Street Torrance, CA 90505 Attn: Mr. David L. Satchwell Sr. Dev. Engineer	1	Lawrence Livermore Laboratory P. O. Box 808 Livermore, CA 94550 Attn: Mr. L. G. O'Connell	1
Sandia Laboratories Division 4715 Albuquerque, NM 87185 Attn: Dr. Robert O. Woods	1	3M Company 3M Center, Bldg. 230-1F St. Paul, MN 55101 Attn; Mr. Joe Schurb	1
		U.S. Flywheels, Inc. 1882 McGaw Avenue Irvine, CA 92714 Attn: Mr. B. E. Swartout	1

Lawrence Livermore Laboratory
P. O. Box 808
Livermore, CA 94550
Attn; Mr. Neil Frank   1

Applied Magnetics Laboratory
Jobmaster Corporation
9006 Liberty Road
Randallstown, MD 21133
Attn; Mr. Charles A. Castronovo
      Director   1

Popular Science
380 Madison Avenue
New York, NY 10017
Attn; Ms. Susan Renner-Smith
      Assoc. Editor   1

Analyst International Corp.
7615 Metrol Blvd.
Minneapolis, MN 55435
Attn: Dr. John Radford   1

Metallurgy & Materials Science
Division
Associates Universities, Inc.
Brookhaven National Lab.
Upton, NY 11973
Attn: Mr. David O. Welch   1

University Patents, Inc.
P. O. Box 6080
Norwalk, CT 06852
Attn: Mr. L. W. Miles, President   1

University Patents, Inc.
P. O. Box 6080
Norwalk, CT 06852
Attn: Mr. David Koffsky   1

National-Standard Company
Niles, MI 49120
Attn; Mr. Joe Wooldridge   1

Mr. D. A. Rabenhorst
12 D Summit Avenue
Southfields, NY 10975   1

Potomac Electric Power Co.
1900 Pennsylvania Avenue
Washington, DC 20006
Attn; Mr. James S. Potts   1

Lord Corporation
2000 West Grandview Blvd.
Erie, PA 16512
Attn: Dr. Armand Lewis   1

PPG Industries, Inc.
300 N. Lee Street
Room 302
Alexandria, VA 22314
Attn: Mr. Richard E. Harmon   1

Owens-Corning Fiberglas Corp.
997 Old Eagle School Road
Suite 215
Wayne, PA 19087
Attn; Mr. Steve Walling   1

E. I. DuPont de Nemours Co.
Wilmington, DE 19898
Attn: Mr. Robert Hunter
      Marketing Manager
      KEVLAR   1

Department of Energy
4800 Forbes Avenue
Pittsburgh, PA 15213
Attn: Mr. Thomas Zemo   1

Mr. Dan Haley
Waddington, NY 13694   1

Power Generators, Inc.
94 Stokes Avenue
Trenton, NJ 08638
Attn; Mr. A. J. Larrecq,
      President   1

Union Carbide
Y-12 Plant
Oak Ridge, TN 37830
Attn: Mr. Robert Steele   1

Commander
Naval Surface Weapons Center
White Oak
Silver Spring, MD 20910
Attn: Mr. Winsor Furr
      Department U-13   1

Electric Power Research Inst.
P. O. Box 10412
Palo Alto, CA 94303
Attn: Mr. Fritz R. Kalhammer   1

Foreign Distribution for APL/JHU Department of Energy Contract

Final Report on Flywheel Program

Dr. Hans Asper
Energy Conversion Study Group
Microwave Laboratories ETHZ
Voltastr. 24
CH-8044 Zurich, Switzerland   3

Max W. Grobly
Schweizerische   (Gwerbenstrasse, 8952 Schlieren)
Wagons-Und Aufzugefabrik A.G.
Schlieren-Zurich
Switzerland   1

Pierre Poubeau
Aerospatiale
Route de Verneuil
Les Mureaux 78 230 France   1

Dr. Giancarlo Genta
Politecnico di Torino
10100 Torino-Corso Duca
Degli Abruzzi 24, Italy   1

Dr. Giorgio Tangorra
Centro Studi Speciali - 0006
Industrie Pirelli S.p.A.
Viale Sarca, 202
20100 Milano, Italy   1

Dr. Giampiero Brusaglino
Fiat Motor Company   (Strada del Drosso, 145)
Turin, Italy   (Casella Postale 202 Ferr)
    (10135 Torino, Italy)   1

Prof. Dr.-Ing. Hubertus Christ
Daimler-Benz AG
7000 Stuttgart 60
Germany   1

Herr Gwinner
Daimler-Benz AG
7000 Stuttgart 60
Germany   1

Mr. Maarten van Zanten
ECN Netherlands Energy Research Foundation
Research Centre
3 Westerduinweg
Petten, (NH) The Netherlands 1755 LE   1

Dr. A. J. Pennings
Lab.voor Polymeerchemie
Universiteitscomplex Paddepoel
Groningen
The Netherlands   1

IR. W. C. Emmens
Fysisch Laboratorium
Rijksuniversiteit Utrecht
Sorbonnelaan 4
Utrecht 2506
The Netherlands   1

Mr. A. L. Mulder
Rijksuniversiteit
Technisch-Fysische Laboratoria
Universiteitscomplex Paddepoehl
Groningen, Netherlands   1

Mr. R. Anahara
Fuji Electric Co., Ltd.
New Yurakucho Bldg.
12-1, Yurakucho 1-chome, Chiyoda-ku
Tokyo, 100 Japan   1

Mr. Tadao Sugita
Planning Manager
Technical Planning Center
Fuji Electric Company, Ltd.
New Yurakucho Building
11, Yurakucho 1-chome
Chiyoda-ku, Tokyo 100, Japan   1

Mr. Gordon L. Bredenkamp
University of Pretoria
Hatfield
Pretoria, Republic of South Africa   0002   1

Mr. S. Ohashi, Deputy Director, General Manager
Products Planning & Marketing Dept.
Mitsui Engineering & Shipbuilding Co., Ltd.
6-4, Tsukiji 5-chome,
Chuo-ku, Tokyo 104, Japan   1

Mr. S. Nakamura, Chief
Products Planning & Marketing Dept.,
Products Development H.Q.
Mitsui Engineering & Shipbuilding Co., Ltd.
6-4, Tsukiji 5-chome
Chuo-ku, Tokyo 104, Japan   1

Mr. M. Okada
Mitsui Shipbuilding & Engineering Co., Ltd.
Suite #2029, One World Trade Center
New York, NY 10048   1

Dr. Tsuneji Yada
Head, Vehicle Control Section
Mechanical Engineering Laboratory
12-1 Igusa 4-chome,
Suginami-ku, Tokyo, Japan   1

Mr. Kozo Kitoh
Japan Automobile Research Institute, inc.
Yatabe-cho
Tsukuba-gun
Ibaraki 300-21, Japan   1

Dr. N. V. Gulia
USSR National Committee on Theoretical
      and Applied Mechanics
Moscow 117526
Vernadskogo Avenue 101
U.S.S.R.   1

Mr. Robert C. Clerk
20 Whitehill Road
Whitehill Ind. Estate
Glenrothes, Fife
Scotland   1

Mr. Arne Jonason
Volvo Car Corporation S-405 08
Goteborg, Sweden   1

Office International de documentation et Librairie
48, Rue Gay-Lussac F 75240
Paris Cedex 5, France   1

Dr. Hans Weber
Depto, Engenharia Mecanica
Universidade Estadual de Campinas
Cidade Universitaria
Barao Geraldo
Campinas, SP Brazil   1

Messrs. Ebbe Lundgren and Christer Nilsson
The Lund Institute of Technology
Division of Mechanics
Fack 725 S-220 07
Lund 7, Sweden